MEDICAL UNIVERSITY – PLEVEN

Faculty of Medicine

Department of Cardiology, Pulmonology and Endocrinology

A B S T R A C T

Dr. Victoria Tsvetanova Tsvetkova

Changes in Pancreatic Beta-Cell Function in COVID-19

Dissertation

for awarding the educational and scientific degree

“DOCTOR” (PhD)

Scientific Supervisor: Assoc. Prof. Katya Todorova, MD, PhD

Pleven, 2026

The dissertation comprises 505 typewritten pages and is illustrated with 165 figures and 144 tables. The bibliography includes 463 references, of which 4 are in Cyrillic and 459 in Latin script.

The public defense of the dissertation will take place on 19 May 2026 at 13:00 in the "Ambroise Paré" Hall at Medical University – Pleven. The defense materials are available on the website of Medical University – Pleven: www.mu-pleven.bg.

TABLE OF CONTENTS

List of Abbreviations

8-epi-PGF2α – 8-epi-prostaglandin F2α

ALAT – Alanine aminotransferase

ARDS – Acute respiratory distress syndrome

ASAT – Aspartate aminotransferase

BMI – Body mass index

CD4 – Cluster of differentiation 4

CD8 – Cluster of differentiation 8

CRP – C-reactive protein

DM – Diabetes mellitus

GGT – Gamma-glutamyl transferase

GLM (Gamma, log link) – Generalized linear model with gamma distribution and log link function

GLP-1 – Glucagon-like peptide-1

GP-73 – Golgi protein 73

HbA1c – Glycated hemoglobin

HCF-D – Human complement factor D

HDL-C – High-density lipoprotein cholesterol

HIF-1α – Hypoxia-inducible factor 1 alpha

HOMA-B – Homeostasis model assessment of beta-cell function

HOMA-IR – Homeostasis model assessment of insulin resistance

IFG – Impaired fasting glucose

IFN-γ – Interferon gamma

IGT – Impaired glucose tolerance

IL – Interleukin

IR – Insulin resistance

LADA – Latent autoimmune diabetes in adults

LDL-C – Low-density lipoprotein cholesterol

MAFLD – Metabolic-associated fatty liver disease

MetS – Metabolic syndrome

METS-IR – Metabolic score for insulin resistance

NFE2L2 – Nuclear factor erythroid 2–related factor 2

OGTT – Oral glucose tolerance test

PCR – Polymerase chain reaction

QUICKI – Quantitative insulin sensitivity check index

TG – Triglycerides

TNF-α – Tumor necrosis factor alpha

TyG index – Triglyceride-glucose index

INTRODUCTION

Coronavirus disease 2019 (COVID-19), caused by SARS-CoV-2, was initially regarded as an acute respiratory infection; however, accumulating clinical and experimental evidence over recent years has demonstrated its pronounced systemic nature, with profound and long-lasting effects on metabolic and endocrine homeostasis. Particular attention has been drawn to the increasing reports of hyperglycemia, insulin resistance (IR), and newly developed disturbances in carbohydrate metabolism observed both during the acute phase of infection and in the post-COVID period.

Emerging data suggest that SARS-CoV-2 infection may impair pancreatic β-cell function through a complex interplay of direct and indirect mechanisms, including virus-mediated cellular injury, immune-mediated inflammation, oxidative stress, cellular hypoxia, and disruption of insulin signaling pathways. Experimental and histopathological studies have demonstrated alterations in insulin secretion, impaired proteolytic processing of proinsulin, and morphological features of β-cell stress, supporting the hypothesis of direct viral involvement in the dysregulation of glucose homeostasis.

In parallel, IR has been identified as a predominant metabolic defect in the course of COVID-19, including in individuals without pre-existing diabetes mellitus (DM). Acute inflammatory and metabolic stress, combined with adipocyte dysfunction, alterations in lipid metabolism, and activation of cell-mediated immune responses, creates conditions for the development of transient or persistent metabolic disturbances. Within this context, COVID-19 has been conceptualized as an immunometabolic trigger capable of initiating or accelerating pathological processes leading to DM and other disorders of carbohydrate metabolism.

Despite the growing body of international evidence, the mechanisms, temporal dynamics, and clinical significance of these disturbances remain incompletely understood, particularly with regard to phase-dependent differences between the acute infection and the post-COVID period. Moreover, there is a lack of studies simultaneously evaluating β-cell function, insulin sensitivity, and immunometabolic interactions within the same cohort using an integrated clinical, biochemical, and immunological approach.

Against this background, the present dissertation aims to provide a comprehensive assessment of the relationship between SARS-CoV-2 infection, β-cell function, and IR by analyzing changes in glucose homeostasis during the acute and post-COVID phases and comparing them with a reference group of individuals with metabolic syndrome (MetS). This approach enables

a more precise distinction between infection-induced metabolic alterations and those associated with chronic metabolic risk, thereby contributing to a deeper understanding of the immunometabolic continuum associated with COVID-19.

AIM OF THE STUDY

The aim of the study is to evaluate the impact of SARS-CoV-2 infection on β-cell function and insulin sensitivity during the acute and post-COVID phases, in the context of immunometabolic interactions associated with disturbances in carbohydrate metabolism.

OBJECTIVES OF THE STUDY

1. To perform a general clinical and metabolic characterization of the studied population.
2. To investigate the lipid profile and other key metabolic parameters, as well as the status of liver function, in the different phases of infection.
3. To analyze inflammatory and immune status, including the involvement of pro- and anti-inflammatory cytokines and other markers of immune inflammation in the acute and post-COVID phases, and their role in metabolic dysregulation.
4. To examine the role of oxidative stress, antioxidant defense, and virus-induced cellular hypoxia in the pathophysiology of disturbances in glucose metabolism and β-cell function.
5. To assess glucose homeostasis in the acute phase of COVID-19 and in the asymptomatic post-COVID period through analysis of pancreatic α- and β-cell function, insulin secretion, and insulin sensitivity.
6. To evaluate the involvement of adipocytokines and other hormonally active molecules in the pathogenesis of COVID-19–associated dysglycemia.
7. To analyze risk factors associated with the development of newly diagnosed DM in the context of SARS-CoV-2 infection.
8. To assess quality of life in individuals who have recovered from COVID-19 using a validated questionnaire (SF-36).

SCIENTIFIC CONCEPT / WORKING HYPOTHESIS

SARS-CoV-2 infection may act as an immunometabolic trigger which, through complex inflammatory, hypoxic, and metabolic mechanisms, contributes to the development of disturbances in glucose homeostasis and newly diagnosed DM.

MATERIALS AND METHODS

Study Design

The present study represents a comprehensive clinical and laboratory investigation conducted in the period 2021–2023, aimed at evaluating changes in glucose homeostasis, β-cell function, and insulin sensitivity in patients with SARS-CoV-2 infection during the acute and post-COVID phases, in comparison with a reference group of individuals with MetS.

Study Population

A total of 235 individuals were included in the study and allocated into the following groups:

Main study population:

Group 1 – individuals with active SARS-CoV-2 infection, diagnosed by PCR testing, examined during the acute phase of the disease (n = 32);

Group 2 – individuals who had recovered from COVID-19 and presented with newly developed disturbances in carbohydrate metabolism, diagnosed during the asymptomatic post-COVID period (n = 35);

Group 3 – individuals without prior SARS-CoV-2 infection, meeting the criteria for MetS, included as a reference group (n = 33).

Additional study population:

Group 4 – hospitalized patients with active SARS-CoV-2 infection (n = 135), dynamically (longitudinally) followed during hospitalization. In this group, clinical severity of infection, inflammatory and coagulation parameters, as well as the dynamics of glycemic control (including variations in blood glucose levels and the need for insulin therapy) were analyzed. This cohort allows assessment of glycemic dynamics and metabolic changes during the course of acute infection. In addition to intragroup analysis, data from Group 4 were also used in intergroup comparisons for selected parameters (e.g., lipid profile, uric acid, and inflammatory markers), when methodologically justified.

The use of a reference group with MetS enables differentiation of infection-induced immunometabolic changes from pre-existing chronic metabolic disturbances.

Inclusion and Exclusion Criteria and Stratification

Participant selection was performed based on predefined inclusion and exclusion criteria, described in detail in the dissertation.

Inclusion Criteria:

- Age ≥ 18 years;
- Active SARS-CoV-2 infection confirmed by PCR testing (Groups 1 and 4);
- History of PCR-confirmed SARS-CoV-2 infection with a period ≥ 6 months after the acute phase (Group 2);
- Newly developed disturbances in carbohydrate metabolism following SARS-CoV-2 infection, with documented normal glycemia prior to the disease (Group 2);
- Individuals with MetS, defined according to harmonized criteria (presence of ≥ 3 out of 5 components), with a negative PCR test for SARS-CoV-2 and no anamnestic, clinical, or serological evidence (when available) of prior infection (Group 3).

Exclusion Criteria:

- Age under 18 years or over 90 years;
- Pregnancy or breastfeeding;
- Individuals with type 1 or type 2 DM diagnosed prior to COVID-19 (for Group 2);
- Previous immunization against SARS-CoV-2 (for Group 1 and 3);
- Known autoimmune diseases;
- Presence of severe decompensated cardiovascular, respiratory, gastrointestinal, renal, or active oncological diseases;
- Use of biological therapy, immunosuppressive agents, cytostatics, or systemic glucocorticoids in clinically significant doses within the preceding 12 months, including treatment with ≥ 0.5–1.0 mg/kg/day methylprednisolone (or equivalent) for > 10 days.

Classification of disturbances in carbohydrate metabolism was performed according to WHO and ADA criteria, based on fasting glucose levels, HbA1c, and data from an oral glucose tolerance test (OGTT), when applicable. Individuals in Groups 2 and 3 were further stratified into subgroups according to the type of diagnosed disturbance (T1DM, T2DM, impaired fasting glucose (IFG), impaired glucose tolerance (IGT), and IR with normoglycemia).

Methods

Clinical, anthropometric, and laboratory investigations were performed, including:

- parameters of glucose homeostasis and lipid profile;
- hormonal markers of pancreatic α- and β-cell function (insulin, C-peptide, proinsulin, glucagon);
- inflammatory and immunological markers, including pro- and anti-inflammatory cytokines (TNF-α, IFN-γ, IL-7, IL-10, IL-17A), markers of cell-mediated immunity (CD4, CD8), and components of the complement system (HCF-D);
- markers of oxidative stress (8-epi-PGF2α), antioxidant defense (NFE2L2), and cellular hypoxia (HIF-1α);
- adipokines (leptin, adiponectin), incretin hormones (GLP-1), and other biomolecules with glucoregulatory function (GP-73).

Specialized hormonal, immunological, and oxidative stress parameters were determined using validated immunoanalytical methods – electrochemiluminescence immunoassay (ECLIA) and enzyme-linked immunosorbent assay (ELISA), in accordance with the methodology of the respective assays.

Venous blood samples for metabolic and immunological analysis were collected at hospital admission and prior to the initiation of treatment with glucocorticosteroids, antibiotics, anticoagulants, and oxygen therapy, whenever the clinical condition permitted. Due to disease severity, body mass index (BMI) was not assessed in individuals with active infection (Groups 1 and 4), which limits the evaluation of nutritional status in these groups.

Assessment of β-Cell Function

For a comprehensive evaluation of β-cell functional status, complementary surrogate indices were used, reflecting different aspects of β-cell adaptation and dysfunction:

- **HOMA-B** – an index assessing the secretory capacity of β-cells;
- **C-peptide/glucose ratio** – a marker of insulin secretion efficiency relative to the glycemic load;
- **Insulin/Proinsulin** ratio – an indicator of the efficiency of proinsulin proteolytic processing;
- **Proinsulin/C-peptide ratio** – a marker of β-cell stress and impaired insulin processing.

The combined use of these indices allows differentiation between compensatory hypersecretion, impaired hormonal processing, and pronounced insulinopenia.

Assessment of Insulin Resistance and Adipose Tissue Functional Status

IR was assessed using both insulin-based and non–insulin-based surrogate indices, including **HOMA-IR, QUICKI, TyG index, TG/HDL-C ratio,** and **METS-IR**, in order to provide a more precise characterization of different aspects of peripheral and hepatic IR.

The functional status of adipose tissue and adipokine balance were evaluated using the **Adiponectin/Leptin ratio**, applied as an integrative index of adipocyte function and insulin sensitivity.

Assessment of Quality of Life

Quality of life in individuals who had recovered from COVID-19 was assessed using the official Bulgarian version of the validated SF-36 questionnaire, which includes physical and psycho-emotional domains.

Statistical Analysis

Statistical analysis of the results was performed at the Medical Center for Health Information using the statistical package SPSS Statistics for Windows, version 25.0 (IBM Corp., Armonk, NY, USA).

Quantitative variables were described by mean and standard deviation (SD), as well as by median and interquartile range (IQR).

Normality of distribution of quantitative variables was assessed using the Kolmogorov–Smirnov and Shapiro–Wilk tests. Due to deviation from normal distribution in at least one of the groups for each analyzed variable, non-parametric statistical methods were used for intergroup comparisons.

For comparison among three or more independent groups, the Kruskal–Wallis test was applied. When a statistically significant difference was identified, post-hoc analysis was performed using the Mann–Whitney U test with Bonferroni correction. Differences were considered statistically significant at $p < 0.05$. For comparisons among three groups, statistical significance was accepted at $p < 0.0167$ (0.05/3).

Given the pronounced asymmetry and right-skewed distribution of the analyzed variables, intergroup differences were additionally evaluated using Generalized Linear Models (GLM) with a Gamma distribution and log link function, appropriate for positively defined and asymmetrically distributed variables. The models were adjusted for age and sex, with the COVID-negative MetS group used as the reference category. Due to the lack of reliable BMI data in patients with active SARS-CoV-2 infection, BMI was not included as a covariate in the regression models.

Additional comparative analyses by sex and by diabetes status were performed within each group. Statistical significance was accepted at $p < 0.05$.

An additional inter-subgroup analysis was conducted, including comparisons between diabetic and non-diabetic individuals across the three main groups, with Bonferroni correction applied in this case as well ($p < 0.0167$).

Individuals in Group 2 were further stratified into subgroups according to the type of carbohydrate metabolism disturbance (T1DM, T2DM, IFG, IGT, and IR with normoglycemia). Differences among subgroups were analyzed using the Kruskal–Wallis test, followed by the Mann–Whitney U test with Bonferroni correction, with statistical significance accepted at $p < 0.0083$ (0.05/6). Due to the small number of individuals in the IFG and IGT subgroups, these were combined into a single "prediabetes" subgroup for inter-subgroup comparisons, in order to increase the statistical reliability of the analysis.

Correlation analysis was performed using Spearman's non-parametric correlation coefficient to evaluate associations between metabolic, biochemical, and immunological parameters, with correlations considered statistically significant at $p < 0.05$.

Additionally, Receiver Operating Characteristic (ROC) analysis was performed to assess the discriminatory capacity of the studied parameters and indices and to determine cut-off values associated with increased risk of DM in the context of SARS-CoV-2 infection.

Ethical Considerations

The study was conducted in accordance with the ethical principles of the Declaration of Helsinki. All participants were enrolled voluntarily after providing written informed consent, following detailed explanation of the aims and nature of the study.

Participants in Groups 1–3 were prospectively enrolled within the framework of research project No. D6/2023, approved by the Ethics Committee of the Medical University – Pleven (Protocol No. 72/05.06.2023). Individuals in Group 4 were prospectively followed based on extended informed consent for the use of clinical and laboratory data from hospital records for research purposes, without performing additional research interventions beyond routine clinical practice. Full confidentiality and use of anonymized data without the possibility of individual identification were ensured.

RESULTS

1. General Clinical and Metabolic Characteristics of the Studied Population

1.1. General Clinical Characteristics of the Studied Population

The mean age of the participants differed significantly among the groups (Kruskal–Wallis H(2) = 29.880; $p < 0.001$), with patients with active SARS-CoV-2 infection (Group 1) being significantly older compared to recovered individuals (Group 2; Mann–Whitney U = 153.5; $p < 0.01$) and the reference MetS group (Group 3; Mann–Whitney U = 175.5; $p < 0.01$) (Fig. 1).

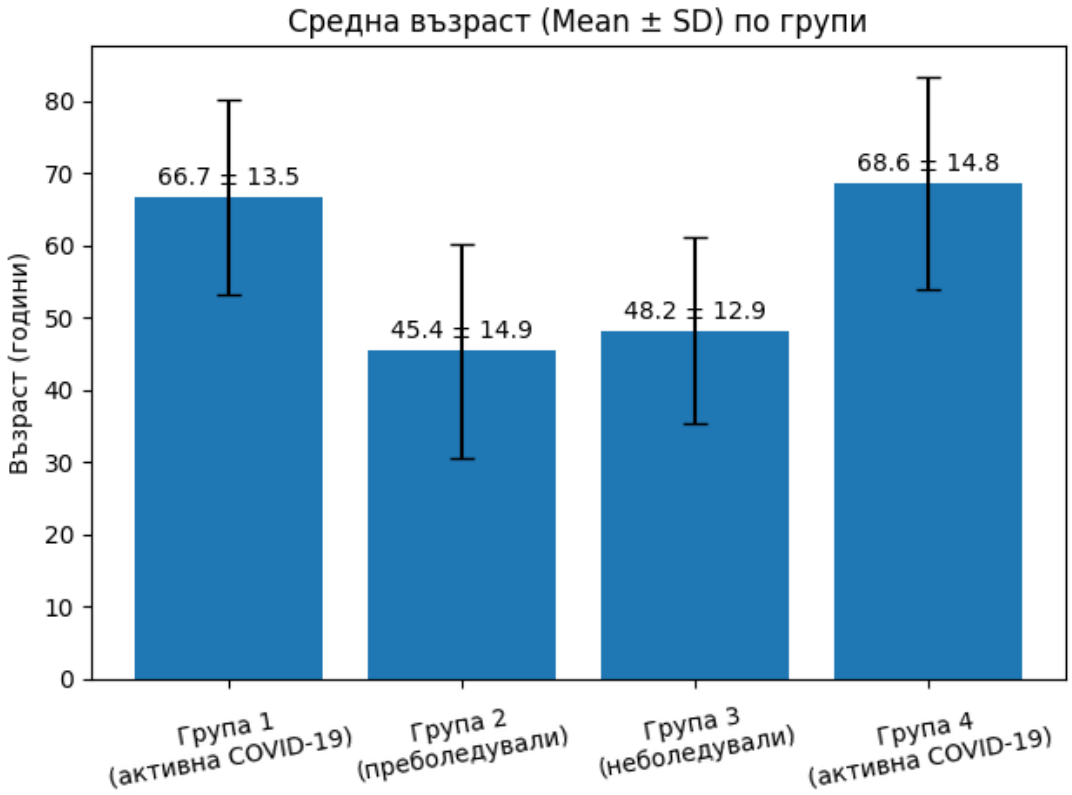

Figure 1. Mean age of individuals in the studied groups – Group 1 (n = 32); Group 2 (n = 35); Group 3 (reference group; n = 33); and Group 4 (n = 135).

The longitudinally followed cohort with active infection (Group 4) demonstrated a similar age to Group 1 ($p > 0.05$), but was significantly older compared to Groups 2 and 3 (Kruskal–Wallis $H(2) = 73.39$; $p < 0.001$). Correlation analysis revealed statistically significant associations between age and HIF-1α in all three groups (Group 1: $r_s = 0.521$; $p = 0.004$; Group 2: $r_s = 0.433$; $p = 0.001$; Group 3: $r_s = 0.640$; $p < 0.001$).

In the overall study population (n = 235), females predominated (60.85% vs. 39.15% males) (Fig. 2). In the main study cohort (n = 100), females accounted for 66% and males for 34%. By group, female predominance was observed among recovered individuals (Group 2 – 62.85%), non-infected individuals with MetS (Group 3 – 90.90%), and the longitudinally followed active infection cohort (Group 4 – 57%), whereas in individuals with active infection (Group 1) a relatively higher proportion of males was observed (56.25%).

The sex distribution among groups was statistically significant ($\chi^2 = 16.64$; $p < 0.001$).

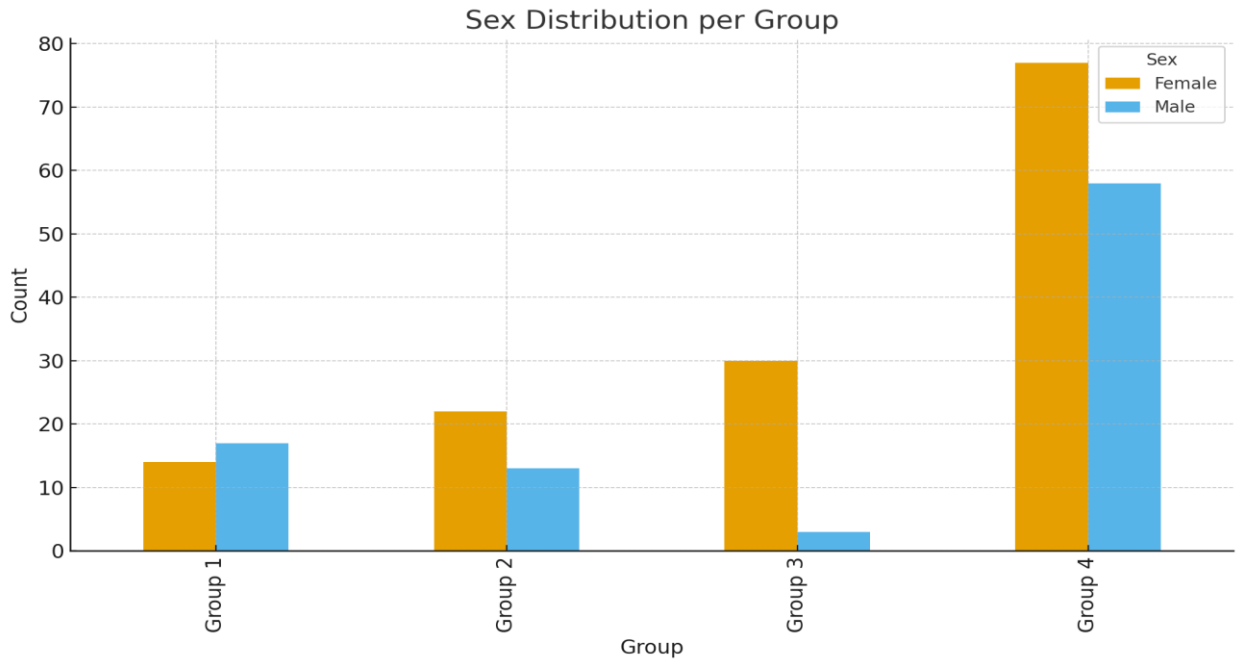

Figure 2. Sex distribution of patients in each study group.

A family history of DM was identified in 33.62% of all examined individuals, with higher prevalence among recovered individuals with newly developed disturbances in carbohydrate metabolism (40%) and among non-infected individuals with MetS (45.45%), compared to individuals with active infection (Group 1 – 21.88% and Group 4 – 31.85%).

With regard to demographic status, urban residence predominated (70.2%), with similar distribution across groups and no substantial differences. The proportion of active smokers in the main study population was 25%, with no significant differences observed between groups.

1.2. Metabolic Characteristics of the Studied Population

BMI was analyzed in recovered individuals with newly developed disturbances in carbohydrate metabolism (Group 2) and in non-infected individuals with MetS (Group 3).

The mean BMI in Group 2 was 31.91 ± 2.57 kg/m² (Med = 32.0; IQR = 10.0), with 54.3% of individuals classified as obese. In Group 3, the mean BMI was higher – 35.67 ± 7.89 kg/m² (Med = 35.0; IQR = 11.0), and the prevalence of obesity reached 75.7%, including 33.3% with morbid obesity (Fig. 3). Despite these differences, no statistically significant difference was observed between the two groups (Mann–Whitney U = 407.0; p = 0.0539).

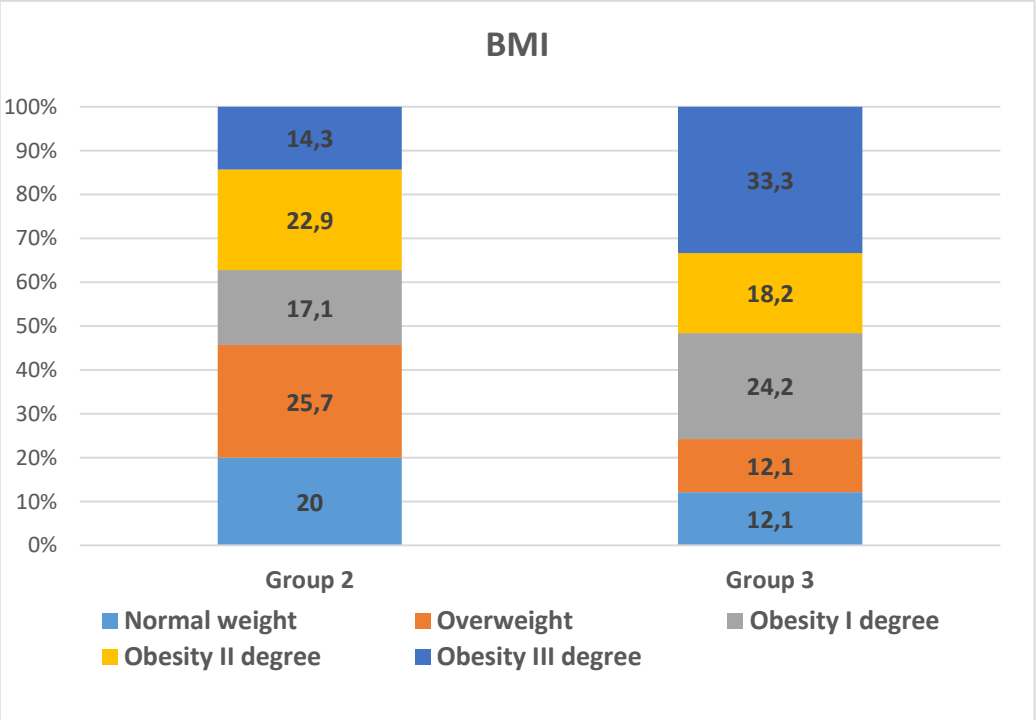

Figure 3. Percentage distribution of individuals in the two groups according to BMI.

Subgroup analysis revealed that diabetic individuals in Group 3 had a significantly higher BMI compared to diabetic individuals in Group 2 (Mann–Whitney U = 55.0; p = 0.035), whereas no statistically significant differences were observed between diabetic and non-diabetic individuals within each group (p > 0.05) (Fig. 4).

BMI showed a positive correlation with METS-IR (Group 2: $r_s = 0.781$; $p < 0.001$; Group 3: $r_s = 0.942$; $p < 0.001$) and a negative correlation with the adiponectin/leptin ratio (Group 2: $r_s = -0.434$; $p = 0.012$; Group 3: $r_s = -0.709$; $p = 0.026$).

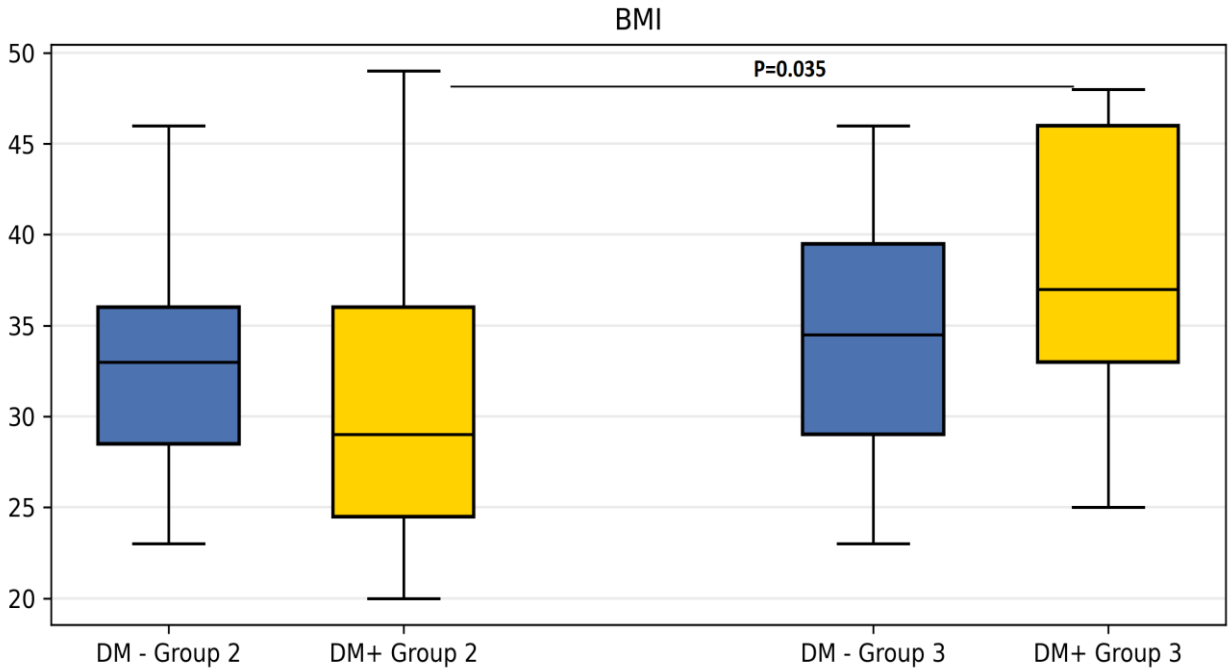

Figure 4. BMI values [kg/m²] in individuals with diabetes (DM+) and without diabetes (DM−) from Groups 2 and 3; a significant difference was observed between diabetic individuals in the two groups (p = 0.035).

1.3. Metabolic Profile of the Studied Individuals

The metabolic profile of individuals with active SARS-CoV-2 infection (**Group** 1) demonstrated a high prevalence of DM (50%), with 21.88% of patients newly diagnosed during hospitalization, while 28.12% had pre-existing T2DM. Among patients with pre-existing diabetes, only 11.11% were receiving insulin therapy at the time of admission, whereas the remainder were treated with non-insulin oral antidiabetic therapy.

Among recovered individuals with newly developed disturbances in carbohydrate metabolism (**Group 2**), 54.28% had newly diagnosed DM, including 22.85% with T1DM (including LADA) and 31.43% with T2DM. Prediabetic states were identified in 20.0% of individuals, including 11.43% with IFG and 8.57% with IGT. In the remaining 25.72%, normoglycemia was observed, accompanied by basal and/or stimulated hyperinsulinemia and IR (Fig. 5).

Elevated median BMI values within the obesity range were observed in all subgroups except for individuals with T1DM, in whom BMI remained within the normal body weight range (24 kg/m²).

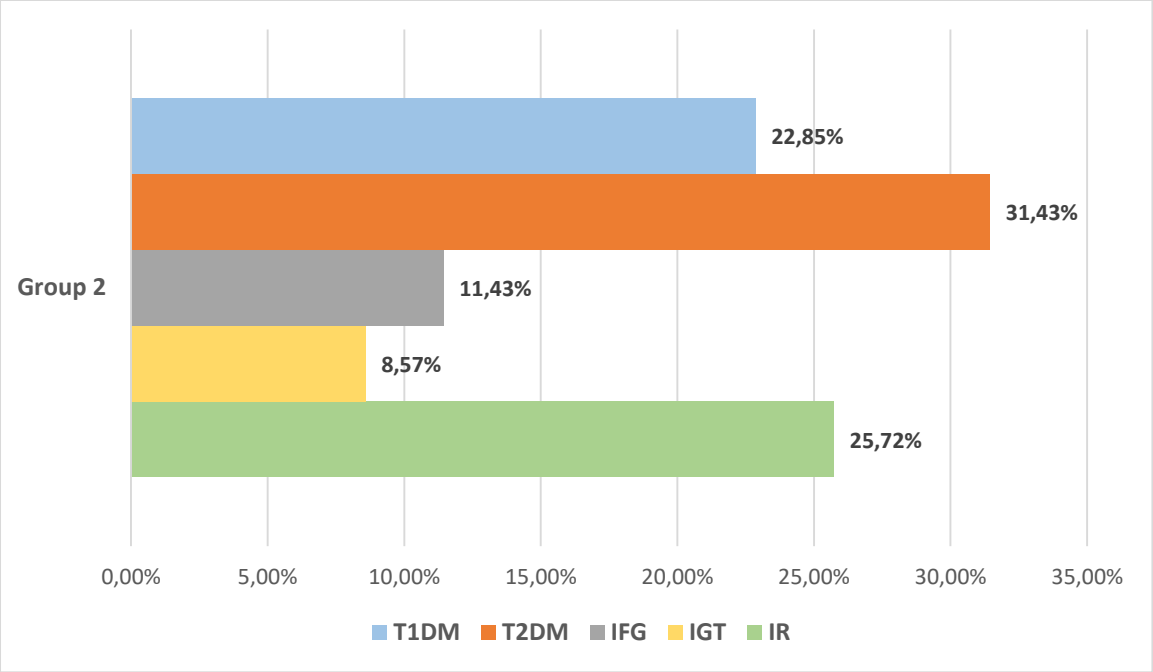

Figure 5. Percentage distribution of individuals in Group 2 according to the type of identified carbohydrate disturbances.

Among non-infected individuals with MetS (**Group 3**), 33.33% had T2DM, with 6.06% newly diagnosed. Prediabetic states were identified in 21.21% of individuals, including 9.09% with IFG and 12.12% with IGT, while the remaining 45.45% exhibited normoglycemia accompanied by pronounced IR and hyperinsulinemia (Fig. 6). In all subgroups, median BMI values were within the obesity range.

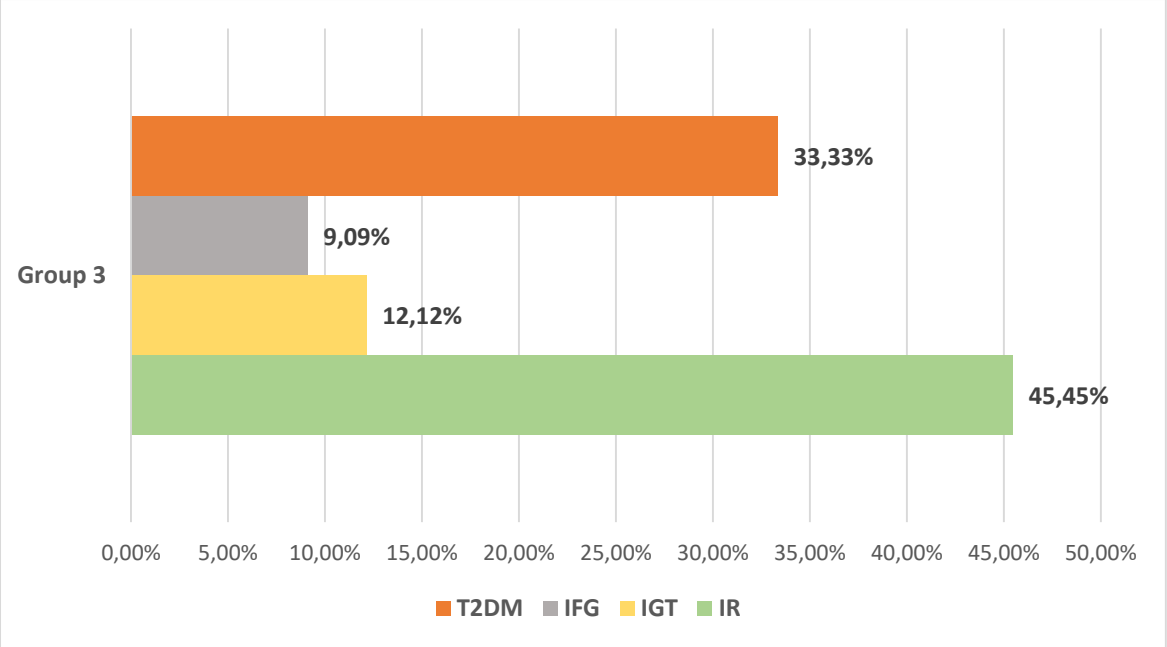

Figure 6. Percentage distribution of individuals in Group 3 according to the type of carbohydrate disturbances.

Among hospitalized individuals with active SARS-CoV-2 infection from the baseline cohort (**Group 4**), 31.11% had DM, with 9.63% newly diagnosed during hospitalization and 21.47% with pre-existing T2DM. Among individuals with known diabetes, 27.6% were receiving insulin therapy, whereas 72.4% were treated with non-insulin antidiabetic therapy, including injectable agents.

1.4. Lipid Profile and Uric Acid Levels

Analysis of the lipid profile and uric acid levels revealed substantial differences among the studied groups (Table 1). In individuals with active SARS-CoV-2 infection (Group 4), the most unfavorable lipid profile was observed, characterized by the highest triglycerides (TG) levels and markedly reduced HDL-cholesterol (HDL-C). Hypertriglyceridemia was most frequent in this group, and decreased HDL-C levels were observed in almost all patients. LDL-cholesterol (LDL-C) levels were comparable to those in the other groups.

In recovered individuals with newly developed disturbances in carbohydrate metabolism (Group 2), the lipid profile was moderately unfavorable, with elevated TG and low HDL-C levels, but with a lower prevalence of hypertriglyceridemia compared to the active infection group.

In the reference group with MetS (Group 3), a typical atherogenic lipid profile was observed, with a high prevalence of hypertriglyceridemia and nearly universally reduced HDL-C levels.

Uric acid levels were highest in the MetS group, followed by the recovered individuals, and lowest in the active infection group.

Table 1. Lipid Profile and Uric Acid Levels in the Studied Groups

Parameter	Active COVID-19 (n = 68)	Post-COVID with carbohydrate disturbances (n = 29)	COVID –negative with MetS (n = 33)
Total Cholesterol [mmol/L]	4.00 ± 1.11 Med 3.8 (3.2–10.4) >5.2 mmol/L:**16.18%**	4.87 ± 1.64 Med 4.8 (3.2–10.4) >5.2 mmol/L: **17.14%**	4.88 ± 1.14 Med 4.7 (2.30–10.40) >5.2 mmol/L: **33.33%**
Triglycerides (mmol/L)	2.05 ± 0.86 Med 1.97 (0.86–6.2) ≥1.7 mmol/L: **59.42%**	1.88 ± 0.84 Med 1.57 (0.9–3.67) ≥1.7 mmol/L: **31.45%**	1.90 ± 0.82 Med 1.64 (0.85–4.16) ≥1.7 mmol/L: **45.46%**
HDL-C [mmol/L]	0.72 ± 0.24 Med 0.68 (0.2–1.14) ↓: ♂ 100%, ♀ 88.89%	0.96 ± 0.38 Med 0.94 (0.1–2.06) ↓: ♂ 61.5%, ♀ 68%	0.87 ± 0.23 Med 0.81 (0.51–1.55) ↓: ♂ 100%, ♀ 96.6%
LDL-C [mmol/L]	3.23 ± 0.93 Med 3.23 (1.67–5.5) >3.4 mmol/L: **33.33%**	3.09 ± 1.37 Med 2.97 (1.51–8.14) >3.4 mmol/L: **25.7%**	3.16 ± 0.96 Med 3.2 (1.02–5.12) >3.4 mmol/L: **33.33%**
Uric Acid [µmol/L]	367.67 ± 159.0 Med 341 (117–739) ↑: ♂ 26.19%, ♀ 55%	398.23 ± 101.58 Med 378.5 (193–625) ↑: ♂ 60%, ♀ 62.5%	415.04 ± 101.37 Med 391 (298–718) ↑: ♂ 33.33%, ♀83.33%

Note: Data are presented as Mean ± SD; Median (range). Decreased HDL-C levels and elevated values of the remaining parameters are defined according to generally accepted reference ranges. *n reflects the number of participants with available data for the respective parameter and may vary between analyses.

2. Assessment of Key Lipid Parameters and Other Major Metabolic Indicators, as well as Liver Function Status, Across Different Phases of Infection

2.1. Main Lipid and Other Metabolic Parameters

Analysis of the lipid profile in Groups 2 (post-COVID with newly developed disturbances in carbohydrate metabolism), 3 (COVID-negative individuals with MetS), and 4 (active COVID-19) revealed a phase-dependent pattern of changes (Fig. 7).

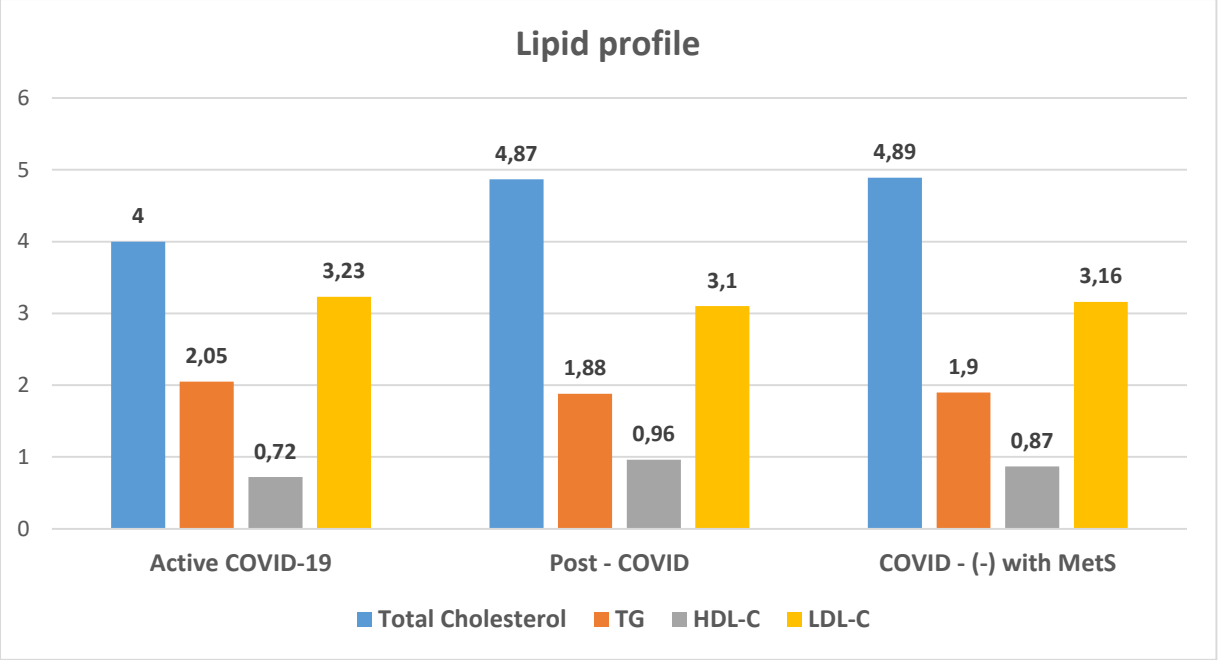

Figure 7. Mean values [mmol/L] of main lipid profile parameters among individuals in the three groups – active COVID, post-COVID, and non-infected individuals with MetS.

Total Cholesterol. Statistically significant differences in total cholesterol levels were observed among the three groups (Kruskal–Wallis H(2) = 20.74; $p < 0.001$). In active SARS-CoV-2 infection, values were significantly lower compared to Group 2 (Mann–Whitney U = 1411.5; $p = 0.001$) and Group 3 (Mann–Whitney U = 1667.0; $p < 0.001$), with no difference between Groups 2 and 3 (Mann–Whitney U = 434.0; $p = 0.530$).

After adjustment for age and sex (GLM, gamma), active infection remained independently associated with lower total cholesterol compared to Group 3 ($\beta = -0.239$; $e^{\beta} = 0.79$; 95% CI 0.68–0.91; $p = 0.001$) and Group 2 ($\beta = -0.230$; $e^{\beta} = 0.79$; 95% CI 0.69–0.92; $p = 0.002$), with no difference between Groups 2 and 3 ($\beta = -0.009$; $p = 0.899$). No intragroup differences were observed by sex or diabetes status ($p > 0.05$). Among non-diabetic individuals, active infection was associated with significantly lower cholesterol compared to post-COVID (Mann–Whitney U = 460.5; $p = 0.014$) and the reference MetS group (Mann–Whitney U = 832.5; $p < 0.001$), whereas no significant differences were observed among diabetic individuals ($p > 0.05$).

TG. TG levels differed significantly among the groups (Kruskal–Wallis H(2) = 16.617; $p < 0.001$), with the highest values observed during active infection, significantly higher compared to Group 3 (Mann–Whitney U = 187.0; $p = 0.017$) and Group 2 (Mann–Whitney U = 103.0; $p < 0.001$), with no difference between Groups 2 and 3 ($p > 0.05$).

After adjustment for age and sex (GLM, gamma), no independent differences were identified between the post-COVID and reference groups (β = −0.039; p = 0.724), between active and reference groups (β = 0.021; p = 0.855), or between the active and post-COVID phases (β = 0.060; p = 0.607). No significant intragroup differences by sex were observed (p > 0.05). With regard to diabetes status, a statistically significant difference was observed only in Group 3, where diabetic individuals had higher TG levels compared to non-diabetics (Mann–Whitney U = 180.0; p = 0.025); no differences were found in the other groups (p > 0.05).

HDL-C. No statistically significant differences in HDL-C were observed among the three groups (Kruskal–Wallis H(2) = 6.19; p > 0.05), despite a trend toward lower values during active SARS-CoV-2 infection.

After adjustment for age and sex (GLM, gamma log-link), no differences were observed between the post-COVID and reference groups (β = 0.156; p = 0.058), nor between the active and reference groups (β = −0.153; p = 0.145). Direct comparison showed significantly lower HDL-C levels during active infection compared to the post-COVID phase (β = −0.309; e^{β} = 0.73; 95% CI 0.58–0.93; p = 0.039). Female sex was independently associated with higher HDL-C levels (e^{β} = 1.31; 95% CI 1.11–1.55; p = 0.0015). A statistically significant intragroup sex difference was observed only in active SARS-CoV-2 infection (Mann–Whitney U = 24.0; p = 0.003). In the non-infected MetS group, diabetic individuals had significantly lower HDL-C levels compared to non-diabetics (Mann–Whitney U = 69.0; p = 0.049).

LDL-C. LDL-C levels did not differ significantly among the groups (Kruskal–Wallis H(2) = 0.818; p = 0.664). After adjustment for age and sex using GLM with gamma distribution, no independent differences were observed between the post-COVID and reference groups (β = −0.054; p = 0.572), between active infection and the reference group (β = −0.039; p = 0.770), or between the active and post-COVID phases (β = 0.015; p = 0.911). A statistically significant intragroup sex difference was observed only in individuals with active SARS-CoV-2 infection, where males had higher LDL-C levels (Mann–Whitney U = 37.0; p = 0.021). No significant differences were observed between diabetic and non-diabetic individuals (p > 0.05).

Uric Acid. Statistically significant differences among the three groups were observed in the non-parametric analysis (Kruskal–Wallis H(2) = 6.105; p = 0.047), despite a clear trend toward the lowest values during active SARS-CoV-2 infection. However, subsequent post-hoc analysis did not confirm statistically significant differences in pairwise comparisons. After adjustment for age and sex using a generalized linear model (GLM, gamma, log-link),

recovered patients did not differ significantly from non-infected individuals with MetS (β = 0.002; p = 0.981). In contrast, active SARS-CoV-2 infection was associated with significantly lower uric acid levels compared to both the reference MetS group (β = −0.332; e^{β} = 0.72; 95% CI 0.59–0.87; p < 0.001) and the post-COVID group (β = −0.334; e^{β} = 0.72; 95% CI 0.59–0.87; p < 0.001).

No statistically significant intragroup differences by sex were observed (p > 0.05). Regarding diabetes status, a significant difference was observed only in active infection, where diabetic individuals demonstrated higher uric acid levels compared to non-diabetics (Mann–Whitney U = 793.5; p = 0.013). No differences were observed in the remaining groups (p > 0.05).

Correlation Analysis

Correlation analysis identified statistically significant associations between clinical and biochemical parameters. TG levels correlated positively with the TyG index and the TG/HDL-C ratio in all groups (p < 0.001), whereas HDL-C showed a negative correlation with these indices in Groups 2 and 3. Total cholesterol correlated positively with LDL-C in all groups (r_s = 0.791–0.919; p < 0.001). Uric acid showed a positive correlation with METS-IR (r_s = 0.612; p = 0.002) in post-COVID patients and with age during active infection (r_s = 0.354; p < 0.001).

2.2. Assessment of Hepatobiliary Function

Liver enzymes demonstrated phase-dependent differences among the studied groups, with the most pronounced deviations observed during active SARS-CoV-2 infection.

Table 2. Descriptive statistics (Mean ± SD; Median (IQR)) and intergroup comparisons of serum ASAT and ALAT levels [IU/L].

Parameter	Group 1 – Active COVID (n = 25*)	Group 2 – Post-COVID (n = 35*)	Group 3 – COVID(-) with MetS (n = 33*)	Kruskal–Wallis Test
ASAT	37.72 ± 30.52 29.0 (29.0)	20.13 ± 13.73 17.0 (11.75)	24.50 ± 19.35 19.5 (9.25)	*H = 10.573* *p = 0.005*
ALAT	34.77 ± 26.54 28.0 (27.0)	34.34 ± 45.74 23.5 (17.75)	26.09 ± 20.81 17.5 (16.75)	*H = 2.599* *p = 0.272*

n – the number of examined individuals may vary between groups due to missing or incomplete data for some of the analyzed parameters.

ASAT. Statistically significant intergroup differences were observed (Kruskal–Wallis H(2) = 10.573; p = 0.005), with the highest values recorded during active infection (Table 2). Post-hoc analysis demonstrated a significant difference only between Groups 1 and 2 (Mann–Whitney U = 491.5; p = 0.002). After adjustment for age and sex (GLM, Gamma, log-link),

active infection remained independently associated with higher ASAT levels compared to the reference group ($\beta = 0.34$; $e^{\beta} = 1.40$; 95% CI 1.05–1.87; $p = 0.021$) and compared to the post-COVID group ($\beta = 0.24$; $e^{\beta} = 1.27$; 95% CI 1.09–1.49; $p = 0.003$). A trend toward higher ASAT levels in males compared to females was observed across groups, with the most pronounced difference in patients with active COVID-19 infection. With regard to diabetes status, no substantial intragroup differences were identified, except for significantly higher ASAT levels in diabetic individuals with active infection (Group 1) compared to recovered diabetic individuals (Group 2) (Mann–Whitney $U = 187.5$; $p = 0.008$).

ALAT. No statistically significant intergroup differences were observed (Kruskal–Wallis $H(2) = 2.599$; $p = 0.272$), although the highest mean and median values were recorded during active infection (Table 2). After adjustment for age and sex (GLM, Gamma, log-link), no independent differences among groups were demonstrated—both active COVID-19 and post-COVID status showed a non-significant trend toward higher levels compared to the reference group. A trend toward higher values in males and in non-diabetic individuals was observed, without statistical significance.

Liver Enzymes in Active SARS-CoV-2 Infection – Comparative Analysis

When comparing the two groups with active SARS-CoV-2 infection (Table 3), the baseline cohort (Group 4) demonstrated statistically significantly higher ASAT levels compared to Group 1 (Mann–Whitney $U = 2231.5$; $p = 0.011$), with a higher prevalence of elevated values (> 40 U/L) (40% vs. 21.88%). Regarding ALAT, a trend toward higher levels was observed in Group 4, although without statistical significance ($p = 0.178$), with a greater relative proportion of pathological values (31.11% vs. 21.88%). GGT levels did not differ substantially between the groups ($p = 0.885$), despite a markedly higher frequency of elevated values (> 35 U/L) in Group 4 (63.7% vs. 28%).

Table 3. Descriptive statistics (Mean ± SD; Median (IQR)) and intergroup comparisons of serum ASAT, ALAT, and GGT levels [IU/L]

Parameter	Group 1 (n = 25*)	Group 4 (n = 135*)	Mann–Whitney U Test
ASAT	37.72 ± 30.52 29.0 (29.0)	61.77 ± 92.02 43.0 (31.16)	*U = 2231.5* *p = 0.011*
ALAT	34.77 ± 26.54 28.0 (27.0)	47.93 ± 50.07 33.38 (28.65)	*U = 1975.0* *p = 0.178*
GGT	106.78 ± 121.31 49.0 (108.04)	106.1 ± 199.04 47.51 (106.06)	*U = 1028.5* *p = 0.885*

** n – the number of examined individuals may vary between groups due to missing or incomplete data for some of the analyzed parameters.*

Correlation analysis in individuals with active infection (Group 1) demonstrated a strong positive association between ALAT and ASAT ($r_s = 0.788$; $p < 0.001$), as well as a moderate correlation between ALAT and GGT ($r_s = 0.607$; $p = 0.016$).

In the baseline cohort with active COVID-19 (Group 4), ALAT correlated positively with GGT ($r_s = 0.456$; $p < 0.001$) and LDH ($r_s = 0.419$; $p < 0.001$). In the same group, a strong correlation was observed between ASAT and ALAT ($r_s = 0.767$; $p < 0.001$), along with a positive association between ASAT and LDH ($r_s = 0.536$; $p < 0.001$).

During active infection, correlations were also identified between liver enzymes and inflammatory mediators, including ALAT and IL-17A ($r_s = 0.514$; $p = 0.008$), ASAT and IL-17A ($r_s = 0.397$; $p = 0.049$), as well as GGT with IL-10 ($r_s = 0.786$; $p < 0.001$) and HIF-1α ($r_s = 0.468$; $p = 0.012$). In the post-COVID group (Group 2), ALAT showed a positive correlation with IL-10 ($r_s = 0.418$; $p = 0.033$).

3. Assessment of Inflammatory Status, the Involvement of Pro- and Anti-Inflammatory Cytokines, and Other Markers of Immune Inflammation

3.1. Inflammatory Status and Infection Severity

Infection Severity. Among patients with active SARS-CoV-2 infection (Group 1; n = 32), severe forms accounted for 50%, while critical disease was observed in 9.38% (Fig. 8). A mortality rate of 6.25% was registered, and the mean length of hospital stay was 10.45 days.

In the longitudinally followed cohort with active COVID-19 (Group 4; n = 135), severe and critical forms accounted for 66.7% and 18.5%, respectively, with a mortality rate of 3.7% and a mean hospital stay of 10.39 days.

In Group 1, no substantial differences in disease severity were observed between diabetic and non-diabetic individuals, whereas in Group 4, individuals with DM demonstrated a more severe clinical course and less favorable outcomes.

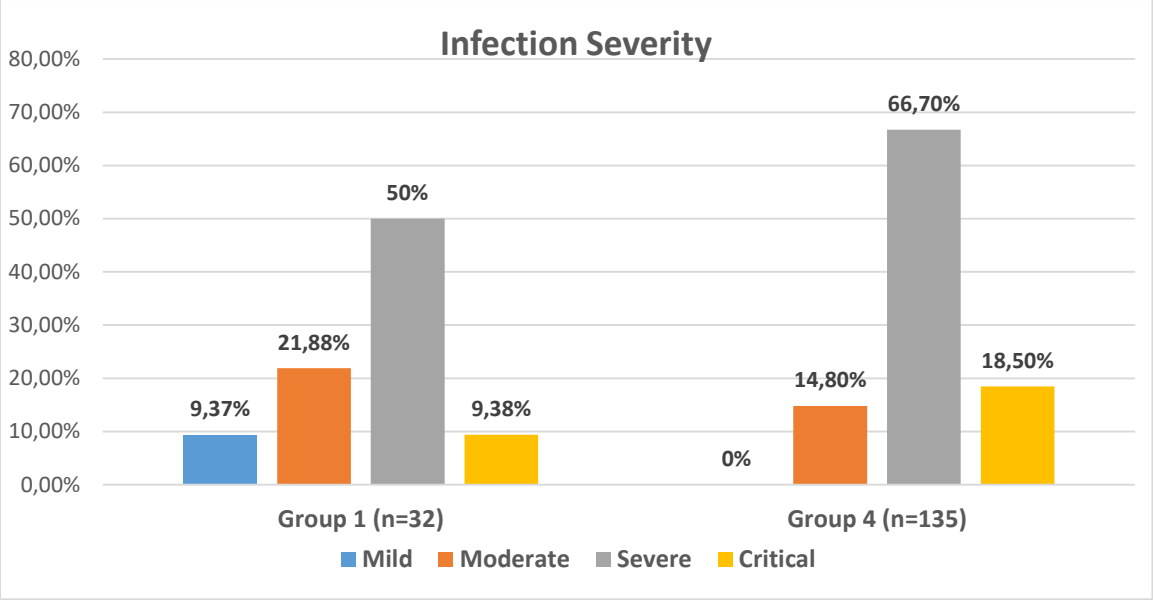

Figure 8. Percentage distribution of individuals according to COVID-19 severity in the two groups with active SARS-CoV-2 infection – Group 1 and Group 4

Inflammatory and Tissue Markers

CRP and **LDH** levels were elevated in both cohorts (Table 4), with significantly higher values observed in Group 4 (CRP: p = 0.018; LDH: p = 0.025). In the baseline cohort, LDH correlated with disease severity (r_s = 0.304; p < 0.001).

Table 4. Descriptive statistics (Mean ± SD; Median (IQR)) and intergroup comparison of inflammatory and tissue markers in patients with active SARS-CoV-2 infection (Group 1 and Group 4)

Parameter	Group 1 (n = 32)	Group 4 (n = 135)	Mann–Whitney Test
CRP (mg/L)	64.15 ± 73.90 36.15 (52.75)	93.17 ± 69.54 81.04 (91.01)	*U = 1017.5* *p = 0.018*
LDH (IU/L)	645.56 ± 383.54 566.0 (414.52)	765.42 ± 389.0 721.0 (389.0)	*U = 985.0* *p = 0.025*
Fibrinogen (g/L)	5.08 ± 1.02 5.0 (1.21)	4.88 ± 1.13 4.91 (1.45)	*U = 1330.0* *p = 0.590*
D-dimer (µg/mL)	5.01 ± 8.38 0.91 (4.52)	1.73 ± 2.06 0.95 (1.72)	*U = 1487.5* *p = 0.261*

Fibrinogen levels were at the upper limit of the reference range and were similar between groups, without statistically significant difference (p = 0.59). **D-dimer** levels were elevated in both cohorts, with no statistically significant difference between them (p = 0.261). In Group 1, D-dimer showed a positive correlation with LDH (r_s = 0.526; p = 0.021) and with GP-73 (r_s = 0.460; p = 0.048).

3.2. Pro- and Anti-Inflammatory Cytokines

3.2.1. Pro-Inflammatory Cytokines

Table 5. Descriptive statistics (Mean ± SD; Median (IQR)) and intergroup comparisons of serum TNF-α, IL-17A, and IFN-γ levels [pg/mL]

Parameter	Group 1 – Active COVID (n = 32*)	Group 2 – Post-COVID (n = 35*)	Group 3 – COVID(-) with MetS (n = 33*)	Kruskal–Wallis Test
TNF-α	117.09 ± 77.71 110.60 (95.39)	129.09 ± 116.95 89.92 (136.37)	85.36 ± 71.60 59.67 (106.17)	*H = 4.142* *p = 0.126*
IL-17A	29.44 ± 4.90 28.07 (3.86)	30.26 ± 14.76 26.14 (3.86)	40.45 ± 35.01 29.04 (7.71)	*H = 12.148* *p = 0.002*
IFN-γ	12.23 ± 3.33 11.17 (4.75)	5.90 ± 4.25 4.53 (4.13)	14.90 ± 5.79 13.12 (8.60)	*H = 40.288* *p < 0.001*

** n – the number of examined individuals may vary between groups due to missing or incomplete data for some of the analyzed parameters.*

TNF-α. No statistically significant differences in serum TNF-α levels were observed among the three groups in the unadjusted analysis (Kruskal–Wallis H(2) = 4.142; p = 0.126), despite a trend toward higher values in recovered patients with newly developed disturbances in carbohydrate metabolism and in individuals with active infection compared to COVID-negative individuals with MetS (Table 5).

After adjustment for age and sex (GLM, Gamma, log-link), a statistically significant increase in TNF-α was observed in the post-COVID group compared to the control group (β = 0.43; e^{β} = 1.53; 95% CI 1.01–2.31; p = 0.045), whereas active infection showed a non-significant trend toward elevation (β = 0.26; p = 0.352), with no difference between the two COVID phases (β = −0.16; p = 0.537). No significant intergroup differences were identified by sex or diabetes status (p > 0.05).

Correlation analysis demonstrated strong positive associations between TNF-α and CD4 and CD8 T-lymphocyte markers in all groups (p < 0.001), as well as a moderate negative correlation with HbA1c during active infection (r_s = −0.472; p = 0.047).

IL-17A. Statistically significant intergroup differences in serum IL-17A levels were observed (Kruskal–Wallis H(2) = 12.148; p = 0.002). Post-hoc analysis showed no difference between the active and post-COVID phases (p = 0.230), significantly higher levels in COVID-negative individuals with MetS compared to recovered patients (Mann–Whitney U = 281.0; p = 0.001), and a non-significant difference between active infection and controls (Mann–Whitney U = 349.5; p = 0.142) (Table 5).

After adjustment for age and sex (GLM, Gamma, log-link), a trend toward lower levels was observed during active infection compared to controls ($\beta = -0.37$; $p = 0.065$), and a statistically significant reduction was found in the post-COVID period ($\beta = -0.34$; $e^{\beta} = 0.71$; 95% CI 0.52–0.96; $p = 0.028$), with no difference between the two COVID phases ($\beta = -0.03$; $p = 0.858$).

Intragroup analysis by sex and diabetes status did not reveal significant differences; however, a statistically significant difference was observed between diabetic individuals in Groups 2 and 3 (Mann–Whitney U = 39.5; $p = 0.011$), as well as between non-diabetics in the same groups (Mann–Whitney U = 88.5; $p = 0.015$).

Correlation analysis demonstrated significant associations with immune, metabolic, and oxidative markers: during active infection—with ALAT ($r_s = 0.514$; $p = 0.008$), ASAT ($r_s = 0.397$; $p = 0.049$), and IFN-γ ($r_s = 0.378$; $p = 0.047$); in the post-COVID group—with CD8 ($r_s = 0.456$; $p = 0.007$), NFE2L2 ($r_s = 0.367$; $p = 0.038$), total cholesterol ($r_s = 0.407$; $p = 0.035$), LDL-C ($r_s = 0.394$; $p = 0.042$), and the TyG index ($r_s = 0.384$; $p = 0.047$); and in the MetS control group—with IL-7 ($r_s = 0.457$; $p = 0.008$) and NFE2L2 ($r_s = 0.431$; $p = 0.015$).

IFN-γ. Analysis of serum IFN-γ levels revealed pronounced and statistically significant intergroup differences (Kruskal–Wallis H(2) = 40.288; $p < 0.001$). Pairwise comparisons demonstrated significantly lower levels in recovered individuals with newly developed carbohydrate disturbances compared to both active infection (Mann–Whitney U = 113.0; $p < 0.001$) and COVID-negative MetS controls (Mann–Whitney U = 100.5; $p < 0.001$), with no difference between active infection and the control group ($p = 0.142$) (Table 5).

After adjustment for age and sex (GLM, Gamma, log-link), active infection was not associated with a significant change compared to the control group ($\beta = -0.16$; $p = 0.360$), whereas the post-COVID group demonstrated a marked reduction ($\beta = -0.94$; $e^{\beta} = 0.39$; 95% CI 0.30–0.50; $p < 0.001$). Direct comparison between the active and post-COVID groups showed significantly higher levels during active infection ($\beta = 0.79$; $e^{\beta} = 2.20$; 95% CI 1.58–3.06; $p < 0.001$).

Intragroup analysis by sex and diabetes status did not reveal significant differences ($p > 0.05$); however, in intergroup comparisons, diabetic individuals in the post-COVID group had significantly lower levels compared to diabetics with active infection (Mann–Whitney U = 246.0; $p < 0.001$) and compared to the control group (Mann–Whitney U = 20.5; $p < 0.001$). A similar pattern was observed among non-diabetics (Group 1 vs. 2: Mann–Whitney U = 161.0; $p < 0.001$; Group 2 vs. 3: Mann–Whitney U = 31.5; $p < 0.001$).

Correlation analysis revealed significant associations: during active infection—with IL-7 (r_s = 0.462; p = 0.013) and IL-17A (r_s = 0.378; p = 0.047); in the post-COVID group—with IL-7 (r_s = 0.609; p < 0.001), HCF-D (r_s = 0.394; p = 0.023), proinsulin (r_s = 0.534; p = 0.001), GP-73 (r_s = −0.623; p < 0.001), the Insulin/Proinsulin ratio (r_s = −0.488; p = 0.007), and the TG/HDL-C ratio (r_s = 0.411; p = 0.037); and in the reference group—with NFE2L2 (r_s = 0.416; p = 0.019) and GP-73 (r_s = 0.488; p = 0.007).

3.2.2. Anti-Inflammatory and Immunoregulatory Cytokines

IL-7. Statistically significant intergroup differences in serum IL-7 levels were observed (Kruskal–Wallis H(2) = 28.072; p < 0.001). Post-hoc analysis demonstrated significantly higher values in COVID-negative individuals with MetS compared to both the active infection group (Mann–Whitney U = 224.5; p = 0.001) and the post-COVID group (Mann–Whitney U = 160.5; p < 0.001), with no difference between the active and post-COVID phases (p > 0.05) (Table 6).

Table 6. Descriptive statistics (Mean ± SD; Median (IQR)) and intergroup comparisons of serum IL-7 and IL-10 levels [pg/mL]

Parameter	Group 1 – Active COVID (n = 32*)	Group 2 – Post-COVID (n = 35*)	Group 3 – COVID(-) with MetS (n = 33*)	Kruskal–Wallis Test
IL-7	36.70 ± 10.84 36.76 (12.91)	34.38 ± 33.01 28.18 (7.80)	55.22 ± 29.19 51.42 (25.83)	*H = 28.07* *p < 0.001*
IL-10	4.54 ± 4.75 3.09 (2.27)	3.45 ± 4.30 2.35 (0.89)	2.99 ± 1.26 2.81 (0.79)	*H = 4.73* *p = 0.094*

** n – the number of examined individuals may vary between groups due to missing or incomplete data for some of the analyzed parameters.*

After adjustment for age and sex (GLM, Gamma, log-link), IL-7 remained significantly reduced both during active infection (β = −0.62; e^{β} = 0.54; 95% CI 0.36–0.81; p = 0.003) and in the post-COVID period (β = −0.56; e^{β} = 0.57; 95% CI 0.42–0.78; p < 0.001) compared to controls, with no significant difference between the two COVID phases (β = −0.06; p = 0.747).

Intragroup analysis by sex and diabetes status did not reveal significant differences (p > 0.05). However, in intergroup comparisons, diabetic individuals in the MetS control group demonstrated higher IL-7 levels compared to diabetics with active infection (Mann–Whitney U = 38.5; p = 0.015) and compared to the post-COVID group (Mann–Whitney U = 34.0; p = 0.005). Among non-diabetics, IL-7 levels were higher in the control group compared to the post-COVID group (Mann–Whitney U = 42.5; p < 0.001).

Correlation analysis revealed: during active infection—positive associations with IFN-γ (r_s = 0.462; p = 0.013), HCF-D (r_s = 0.436; p = 0.020), and NFE2L2 (r_s = 0.439; p = 0.019); in the post-COVID group—positive correlations with CD4 (r_s = 0.351; p = 0.045), CD8 (r_s = 0.365; p = 0.036), BMI (r_s = 0.475; p = 0.006), and METS-IR (r_s = 0.425; p = 0.030), as well as a negative association with GP-73 (r_s = −0.398; p = 0.021); and in the MetS reference group—positive correlations with IL-10 (r_s = 0.694; p < 0.001), IL-17A (r_s = 0.457; p = 0.008), and NFE2L2 (r_s = 0.433; p = 0.014).

IL-10. A trend toward higher serum IL-10 levels was observed in individuals with active SARS-CoV-2 infection compared to the post-COVID group with newly developed carbohydrate disturbances and the MetS controls (Table 6); however, intergroup differences did not reach statistical significance (Kruskal–Wallis H(2) = 4.733; p = 0.094).

After adjustment for age and sex (GLM, Gamma, log-link), no independent group effect on IL-10 levels was observed: active infection vs. controls (β = 0.05; p = 0.860), post-COVID vs. controls (β = −0.07; p = 0.746), and active vs. post-COVID (β = 0.12; p = 0.655).

No significant intragroup differences by sex or diabetes status were identified (p > 0.05). However, in intergroup comparisons, significantly higher IL-10 levels were observed in non-diabetics from the control group (Group 3) compared to non-diabetics from the post-COVID group (Group 2) (Mann–Whitney U = 42.5; p < 0.001).

Correlation analysis demonstrated: during active infection - a positive correlation with HIF-1α (r_s = 0.425; p = 0.024); in the post-COVID group - positive associations with glucose (r_s = 0.369; p = 0.034), HbA1c (r_s = 0.510; p = 0.013), and ALAT (r_s = 0.418; p = 0.033), a negative association with HOMA-B (r_s = −0.458; p = 0.011), as well as positive correlations with IR indices – TyG index (r_s = 0.481; p = 0.008), TG/HDL-C ratio (r_s = 0.435; p = 0.021), and METS-IR (r_s = 0.437; p = 0.020); and in the MetS reference group - positive correlations with IL-7 (r_s = 0.694; p < 0.001) and NFE2L2 (r_s = 0.381; p = 0.034).

Immunological Profile in Subgroups with Newly Developed Carbohydrate Disturbances (Group 2)

Comparison of serum IL-7, IL-10, IL-17A, IFN-γ, and TNF-α levels among the subgroups with newly developed disturbances in carbohydrate metabolism during the post-COVID period did not reveal statistically significant differences (p > 0.05 for all parameters, Fig. 9).

Descriptive analysis demonstrated variability in the distribution of values across the different forms of dysglycemia. Individuals with T1DM/LADA exhibited a wider range of TNF-α, IL-7, and IL-17A values. The subgroup with IGT showed relatively higher levels of IL-10, IL-17A, and IFN-γ, whereas individuals with IFG demonstrated higher median TNF-α values. The subgroups with T2DM and IR displayed similar distributions of the analyzed cytokines.

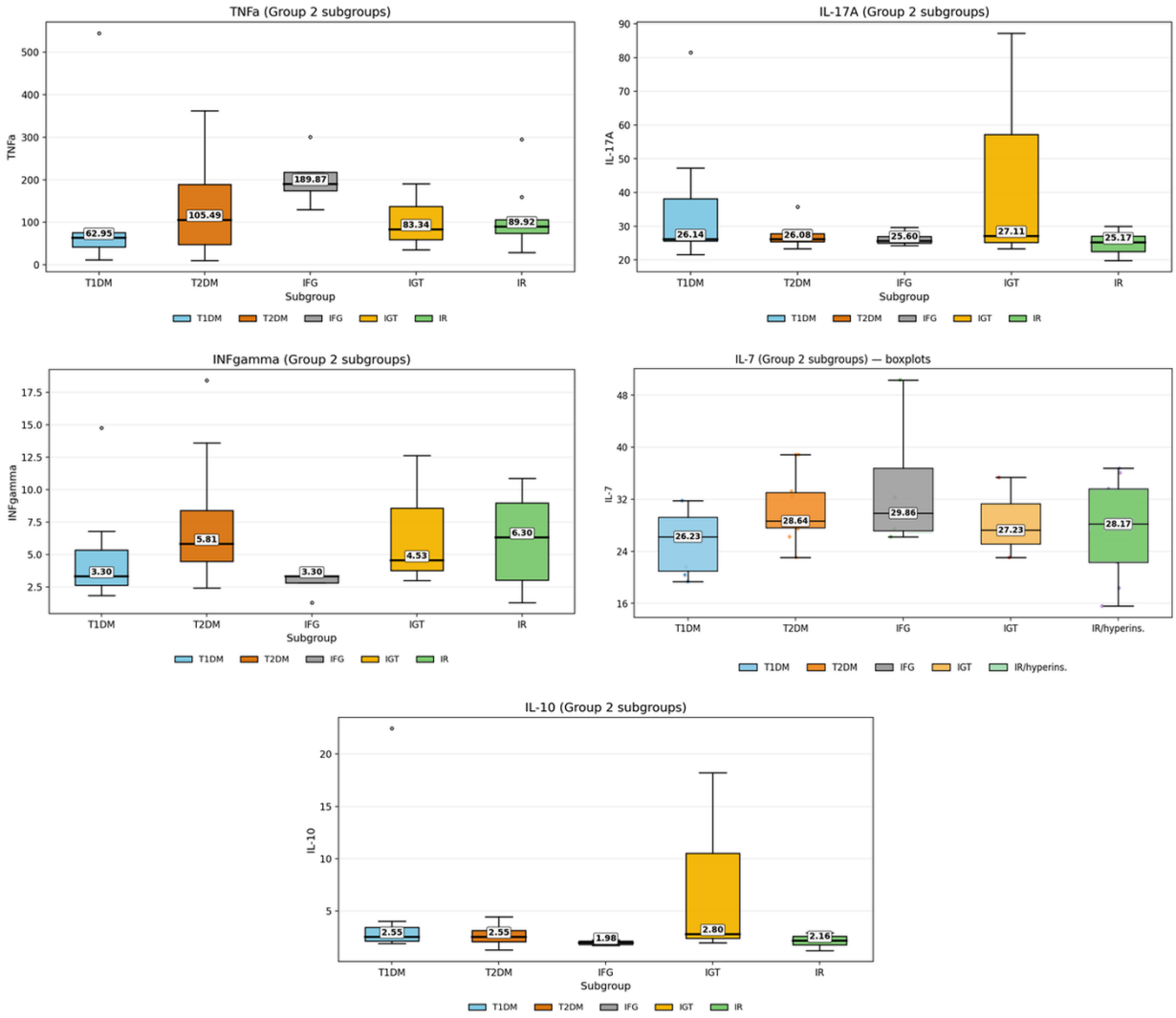

Figure 9. Distribution (Median; IQR) of pro- and anti-inflammatory cytokines across the subgroups of Group 2 – T1DM/LADA, T2DM, IFG, IGT, and IR.

3.3. Markers of Cell-Mediated Immune Response and the Complement System

Comparison of serum levels of markers of cell-mediated immune response (CD4, CD8) and the complement factor HCF-D among the three groups (Group 1 – active SARS-CoV-2 infection; Group 2 – post-COVID with newly developed disturbances in carbohydrate metabolism; Group 3 – COVID-negative individuals with MetS) revealed pronounced and statistically significant intergroup differences (Table 8).

Table 8. Descriptive statistics (Mean ± SD; Median (IQR)) and intergroup comparisons of serum CD4, CD8, and HCF-D levels [ng/mL]

Parameter	Group 1 – Active COVID (n = 32*)	Group 2 – Post-COVID (n = 35*)	Group 3 – COVID(-) with MetS (n = 33*)	Kruskal–Wallis Test
CD4	8.65 ± 2.07 7.90 (8.78)	8.24 ± 3.18 4.89 (7.80)	4.41 ± 1.30 3.59 (4.70)	*H = 10.24* *p = 0.005*
CD8	18.70 ± 4.21 15.55 (11.82)	24.45 ± 8.27 16.01 (22.62)	31.08 ± 7.73 26.90 (31.96)	*H = 4.41* *p = 0.110*
HCF-D	8027.77 ± 13354.29 1 175.52 (9149.46)	966.18 ± 2038.86 318.02 (516.26)	34 611.23 ± 27 011.75 36 012.55 (35 344.65)	*H = 49.27* *p < 0.001*

** n – the number of examined individuals may vary between groups due to missing or incomplete data for some of the analyzed parameters.*

CD4. Serum CD4 levels demonstrated statistically significant intergroup differences (Kruskal–Wallis H(2) = 10.239; p = 0.005). Post-hoc analysis revealed significantly higher values in individuals with active SARS-CoV-2 infection compared to COVID-negative individuals with MetS (Mann–Whitney U = 237.5; p = 0.001), with no significant differences between the active and post-COVID phases or between the post-COVID group and controls (p > 0.05) (Table 8).

After adjustment for age and sex (GLM, Gamma, log-link), a statistically significant increase in CD4 was observed in the post-COVID group compared to the reference group ($\beta = 0.61$; $e^{\beta} = 1.84$; 95% CI 1.19–2.83; p = 0.006), whereas active infection showed a non-significant trend toward elevation ($\beta = 0.46$; p = 0.104). No significant difference was identified between the active and post-COVID phases ($\beta = -0.15$; p = 0.596). Intragroup analysis by sex and diabetes status did not reveal statistically significant differences (p > 0.05).

Correlation analysis demonstrated a strong positive association between CD4 and CD8 in all groups (Group 1: $r_s = 0.899$; p < 0.001; Group 2: $r_s = 0.789$; p < 0.001; Group 3: $r_s = 0.799$; p < 0.001), as well as between CD4 and TNF-α (Group 1: $r_s = 0.971$; p < 0.001; Group 2: $r_s = 0.825$; p < 0.001; Group 3: $r_s = 0.798$; p < 0.001).

Additionally, in the post-COVID group, a positive correlation with IL-7 was observed ($r_s = 0.351$; p = 0.045), while in the control group positive associations were found with NFE2L2 ($r_s = 0.375$; p = 0.037) and 8-epi-PGF2α ($r_s = 0.544$; p = 0.023). In the active infection group, a negative correlation was observed between CD4 and the C-peptide/Glucose ratio ($r_s = -0.458$; p = 0.018).

CD8. CD8 levels showed a gradient distribution among groups, with the lowest values observed during active infection, intermediate values in the post-COVID group, and the highest levels in COVID-negative individuals with MetS (Table 8). However, no statistically significant intergroup differences were detected (Kruskal–Wallis $H(2) = 4.409$; $p = 0.110$).

After adjustment for age and sex (GLM, Gamma, log-link), a statistically significant reduction in CD8 was observed in active SARS-CoV-2 infection compared to the control group ($\beta = -0.69$; $e^{\beta} = 0.50$; 95% CI 0.30–0.82; $p = 0.006$), whereas post-COVID patients showed a non-significant trend toward lower values ($\beta = -0.31$; $p = 0.110$). Direct comparison between the active and post-COVID phases did not demonstrate a statistically significant difference ($\beta = -0.40$; $p = 0.102$). Intragroup analysis by sex and diabetes status also revealed no statistically significant differences ($p > 0.05$).

Correlation analysis demonstrated strong positive associations between CD8 and CD4 in all groups (Group 1: $r_s = 0.899$; $p < 0.001$; Group 2: $r_s = 0.789$; $p < 0.001$; Group 3: $r_s = 0.799$; $p < 0.001$), as well as between CD8 and TNF-α (Group 1: $r_s = 0.907$; $p < 0.001$; Group 2: $r_s = 0.699$; $p < 0.001$; Group 3: $r_s = 0.958$; $p < 0.001$).

During active infection, moderate negative correlations were observed between CD8 and C-peptide ($r_s = -0.429$; $p = 0.023$), as well as between CD8 and the C-peptide/Glucose ratio ($r_s = -0.454$; $p = 0.009$). In the post-COVID group, positive correlations were identified between CD8 and IL-7 ($r_s = 0.365$; $p = 0.036$) and IL-17A ($r_s = 0.456$; $p = 0.008$).

HCF-D. Complement factor D (HCF-D) demonstrated the most pronounced intergroup differences, with the lowest levels observed in the post-COVID group, intermediate levels during active infection, and markedly higher levels in COVID-negative individuals with MetS (Kruskal–Wallis $H(2) = 49.274$; $p < 0.001$). Post-hoc analysis revealed significant differences between active infection and the post-COVID group (Mann–Whitney $U = 222.0$; $p < 0.001$), between active infection and MetS controls (Mann–Whitney $U = 136.5$; $p < 0.001$), and between the post-COVID group and controls (Mann–Whitney $U = 40.0$; $p < 0.001$) (Table 8).

After adjustment for age and sex (GLM, Gamma, log-link), HCF-D remained significantly reduced both during active SARS-CoV-2 infection compared to controls ($\beta = -1.32$; $e^{\beta} = 0.27$; 95% CI 0.09–0.80; $p = 0.018$) and in the post-COVID period ($\beta = -3.53$; $e^{\beta} = 0.03$; 95% CI 0.01–0.07; $p < 0.001$). Direct comparison between the active and post-COVID phases demonstrated significantly higher levels during active infection ($\beta = 2.20$; $e^{\beta} = 9.06$; 95% CI 3.24–25.31; $p < 0.001$).

Intragroup analysis by sex and diabetes status did not reveal significant differences ($p > 0.05$). However, in intergroup comparisons, diabetic individuals in the post-COVID group exhibited lower HCF-D levels compared to diabetics with active infection (Mann–Whitney U = 242.0; $p = 0.003$) and compared to diabetics in the MetS control group (Mann–Whitney U = 2.0; $p < 0.001$). Similarly, among non-diabetics, HCF-D was lower in the post-COVID group compared to non-diabetics with active infection (Mann–Whitney U = 32.0; $p = 0.001$) and compared to non-diabetics in the control group (Mann–Whitney U = 13.0; $p < 0.001$).

Correlation analysis showed that during active infection HCF-D was positively associated with IL-7 ($r_s = 0.436$; $p = 0.021$), IL-17A ($r_s = 0.489$; $p = 0.008$), and NFE2L2 ($r_s = 0.415$; $p = 0.028$). In the post-COVID group, positive correlations were identified with IFN-γ ($r_s = 0.394$; $p = 0.023$) and the TyG index ($r_s = 0.387$; $p = 0.038$). In the MetS control group, HCF-D correlated positively with NFE2L2 ($r_s = 0.415$; $p = 0.023$), LDL-C ($r_s = 0.458$; $p = 0.011$), the C-peptide/Glucose ratio ($r_s = 0.455$; $p = 0.033$), and the Adiponectin/Leptin ratio ($r_s = 0.361$; $p = 0.038$), and negatively with HbA1c ($r_s = −0.609$; $p = 0.047$).

Markers of Cell-Mediated Immunity and the Complement System in Subgroups with Newly Developed Carbohydrate Disturbances (Group 2)

Analysis of markers of the cell-mediated immune response (CD4, CD8) and complement factor HCF-D across the individual subgroups with newly developed carbohydrate disturbances within the post-COVID group did not reveal statistically significant differences among them ($p > 0.05$) (Fig. 10).

Nevertheless, descriptive data indicate variability in the levels of the analyzed parameters. Individuals with T1DM exhibited higher mean values of CD4 and CD8, whereas those with T2DM showed higher mean HCF-D levels. The subgroups with IFG, IGT, and IR demonstrated intermediate values with substantial overlap of ranges, reflecting heterogeneity of the immune profile within the post-COVID group.

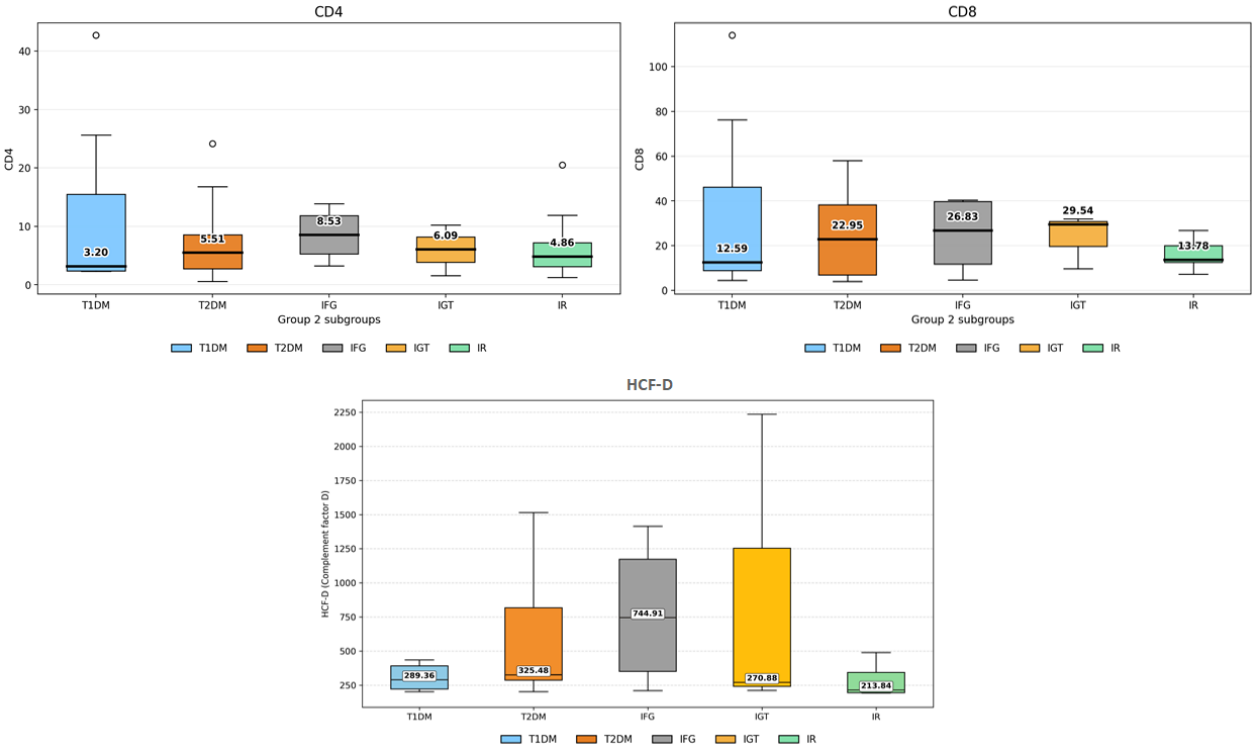

Figure 10. Distribution (Median; IQR) of CD4, CD8, and HCF-D across the subgroups of Group 2 – T1DM/LADA, T2DM, IFG, IGT, and IR

4. Markers of Oxidative Stress, Antioxidant Defense, and Virus-Induced Cellular Hypoxia

Monitoring of markers of oxidative stress, antioxidant defense, and virus-induced cellular hypoxia revealed a heterogeneous profile across the three groups (Table 9).

Table 9. Descriptive statistics (Mean ± SD; Median (IQR)) and intergroup comparisons of serum levels of oxidative stress (8-epi-PGF₂α), antioxidant defense (NFE2L2), and cellular hypoxia (HIF-1α) markers [pg/mL]

Parameter	Group 1 – Active COVID (n = 32*)	Group 2 – Post-COVID (n = 35*)	Group 3 – COVID(-) with MetS (n = 33*)	Kruskal–Wallis Test
8-epi-PGF2α	46.74 ± 3.91 44.17 (3.86)	62.64 ± 8.47 58.06 (12.92)	85.81 ± 28.41 69.96 (21.30)	*H = 32.444* *p < 0.001*
NFE2L2	229.21 ± 69.04 227.00 (77.05)	244.86 ± 330.49 172.00 (100.42)	220.53 ± 104.53 214.00 (153.11)	*H = 3.584* *p = 0.167*
HIF-1α	1321.51 ± 1224.92 1035.67 (796.09)	358.76 ± 478.73 212.22 (220.37)	558.87 ± 458.98 373.97 (558.87)	*H = 32.974* *p < 0.001*

** n – the number of examined individuals may vary between groups due to missing or incomplete data for some of the analyzed parameters.*

Oxidative Stress (8-epi-PGF₂α). Statistically significant intergroup differences in serum 8-epi-PGF₂α levels were observed (Kruskal–Wallis H(2) = 32.444; p < 0.001). Post-hoc analysis

demonstrated significantly lower values in individuals with active infection compared to the post-COVID group (Mann–Whitney U = 66.0; $p < 0.001$) and to COVID-negative individuals with MetS (Mann–Whitney U = 17.0; $p < 0.001$). Additionally, a significant difference was found between the post-COVID group and MetS controls (Mann–Whitney U = 89.5; $p = 0.004$), with the highest values recorded in the control group (Table 9).

After adjustment for age and sex (GLM, Gamma, log-link), 8-epi-$PGF_{2}\alpha$ remained significantly reduced both in active infection compared to controls ($\beta = -0.60$; $e^{\beta} = 0.55$; 95% CI 0.38–0.78; $p < 0.001$) and in the post-COVID group ($\beta = -0.29$; $e^{\beta} = 0.75$; 95% CI 0.57–0.98; $p = 0.036$). Comparison between the active and post-COVID phases demonstrated borderline statistical significance ($\beta = -0.32$; $e^{\beta} = 0.73$; 95% CI 0.54–1.00; $p = 0.051$).

Intragroup analysis by sex and diabetes status did not reveal significant differences in Group 1 ($p > 0.05$). In Group 2, significantly higher levels were observed in females compared to males (Mann–Whitney U = 38.0; $p = 0.012$), with no difference by diabetes status ($p > 0.05$). In Group 3, a significant difference was identified between diabetic and non-diabetic individuals (Mann–Whitney U = 3.0; $p = 0.027$).

In intergroup comparisons, diabetic individuals in the post-COVID group had higher levels compared to diabetics with active infection (Mann–Whitney U = 17.0; $p = 0.003$). Similarly, non-diabetics in the post-COVID group differed significantly from non-diabetics with active infection (Mann–Whitney U = 15.0; $p = 0.003$) and from non-diabetics in the control group (Mann–Whitney U = 3.0; $p < 0.001$).

Correlation analysis demonstrated a positive association between 8-epi-$PGF_{2}\alpha$ and fasting glucose in the post-COVID group ($r_s = 0.480$; $p = 0.028$). In the MetS control group, positive correlations were observed with LDL-C ($r_s = 0.536$; $p = 0.027$), CD4 ($r_s = 0.544$; $p = 0.023$), and the Insulin/Proinsulin ratio ($r_s = 0.525$; $p = 0.044$).

Antioxidant Defense (NFE2L2). Similar serum NFE2L2 levels were observed across the three groups, without statistically significant intergroup differences (Kruskal–Wallis $H(2) = 3.584$; $p = 0.167$). Post-hoc analysis likewise did not reveal significant differences between individual group pairs ($p > 0.05$) (Table 9).

After adjustment for age and sex (GLM, Gamma, log-link), no significant difference was identified for active infection compared to MetS controls ($\beta = -0.13$; $p = 0.632$), for post-COVID compared to controls ($\beta = 0.00$; $p = 0.991$), or between the active and post-COVID

phases (β = −0.13; p = 0.607). Intragroup analysis by sex and diabetes status also revealed no statistically significant differences in any of the three groups (p > 0.05).

Correlation analysis demonstrated that during active infection (Group 1), NFE2L2 showed positive associations with IL-7 (r_s = 0.439; p = 0.019), HCF-D (r_s = 0.415; p = 0.023), ASAT (r_s = 0.541; p = 0.005), and ALAT (r_s = 0.541; p = 0.005). In the post-COVID group (Group 2), NFE2L2 correlated positively with IL-17A (rs = 0.367; p = 0.038) and negatively with insulin (r_s = −0.401; p = 0.025). In the MetS control group (Group 3), positive correlations were observed with CD4 (r_s = 0.375; p = 0.037), IL-10 (r_s = 0.381; p = 0.034), IFN-γ (r_s = 0.416; p = 0.019), IL-17A (r_s = 0.431; p = 0.015), and HCF-D (r_s = 0.415; p = 0.023).

Cellular Hypoxia (HIF-1α). The highest serum HIF-1α levels were recorded in the acute phase (Group 1), the lowest in the post-COVID group (Group 2), and intermediate levels in COVID-negative individuals with MetS (Group 3) (Table 9).

Statistically significant intergroup differences were observed (Kruskal–Wallis H(2) = 32.974; p < 0.001). Post-hoc analysis demonstrated significant differences between all group pairs—between Group 1 and Group 2 (Mann–Whitney U = 123.0; p < 0.001), between Group 1 and Group 3 (Mann–Whitney U = 199.0; p < 0.001), and between Group 2 and Group 3 (Mann–Whitney U = 273.5; p = 0.001).

After adjustment for age and sex (GLM, Gamma, log-link), however, HIF-1α did not differ significantly in active infection compared to controls (β = −0.03; p = 0.929), whereas in the post-COVID period it was significantly reduced compared to controls (β = −0.54; e^{β} = 0.58; 95% CI 0.36–0.94; p = 0.026). Direct comparison between the active and post-COVID phases showed a non-significant trend toward higher levels during active infection (β = 0.52; p = 0.089).

Intragroup analysis by sex and diabetes status did not reveal significant differences in Groups 1 and 2 (p > 0.05), whereas in Group 3 diabetic individuals had significantly higher levels compared to non-diabetics (Mann–Whitney U = 163.0; p = 0.030). In intergroup comparisons by diabetes status, diabetic individuals in Group 1 differed significantly from those in Group 2 (Mann–Whitney U = 284.0; p < 0.001), and diabetics in Group 2 differed from those in Group 3 (Mann–Whitney U = 41.0; p = 0.007). Among non-diabetics, a significant difference was observed between Groups 1 and 2 (Mann–Whitney U = 152.0; p = 0.010).

Correlation analysis demonstrated a positive association between age and HIF-1α in all three groups (Group 1: $r_s = 0.521$; $p = 0.004$; Group 2: $r_s = 0.433$; $p = 0.01$; Group 3: $r_s = 0.640$; $p < 0.001$). During active infection (Group 1), HIF-1α correlated positively with IL-10 ($r_s = 0.425$; $p = 0.024$). In the post-COVID group (Group 2), HIF-1α showed positive correlations with glucose ($r_s = 0.347$; $p = 0.048$), HbA1c ($r_s = 0.426$; $p = 0.043$), glucagon ($r_s = 0.467$; $p = 0.005$), and HOMA-IR ($r_s = 0.415$; $p = 0.023$), as well as a negative correlation with QUICKI ($r_s = -0.415$; $p = 0.023$).

In the MetS reference group (Group 3), significant correlations were identified between HIF-1α and BMI ($r_s = 0.417$; $p = 0.020$), TG ($r_s = 0.357$; $p = 0.048$), uric acid ($r_s = 0.592$; $p = 0.002$), HDL-C ($r_s = -0.433$; $p = 0.015$), the TyG index ($r_s = 0.489$; $p = 0.005$), the TG/HDL-C ratio ($r_s = 0.453$; $p = 0.011$), METS-IR ($r_s = 0.490$; $p = 0.005$), glucagon ($r_s = 0.542$; $p = 0.011$), GP-73 ($r_s = 0.514$; $p = 0.024$), and adiponectin ($r_s = -0.460$; $p = 0.041$).

Subgroup Analysis of Oxidative Stress, Antioxidant Defense, and Hypoxic Response Markers in the Post-COVID Group

In the subgroup analysis within the post-COVID group (Group 2), no statistically significant differences were observed in 8-Epi-PGF-2α levels across the individual subgroups according to the type of newly developed carbohydrate disturbance (Kruskal–Wallis, $p > 0.05$), despite descriptive variability in distribution (Fig. 11).

In contrast, NFE2L2 levels differed significantly between subgroups (Kruskal–Wallis $H(3) = 11.0137$; $p = 0.026$). Post-hoc analysis demonstrated a statistically significant difference exclusively between the T1DM/LADA subgroup and the combined prediabetes subgroup (IFG + IGT) (Mann–Whitney $U = 44.0$; $p = 0.008$).

Similarly, statistically significant differences in HIF-1α levels were identified within the same group (Kruskal–Wallis $H(3) = 12.30$; $p = 0.015$). Post-hoc analysis revealed a significant difference between the IR subgroup and the combined prediabetes subgroup (IFG + IGT) (Mann–Whitney $U = 5.0$; $p = 0.003$).

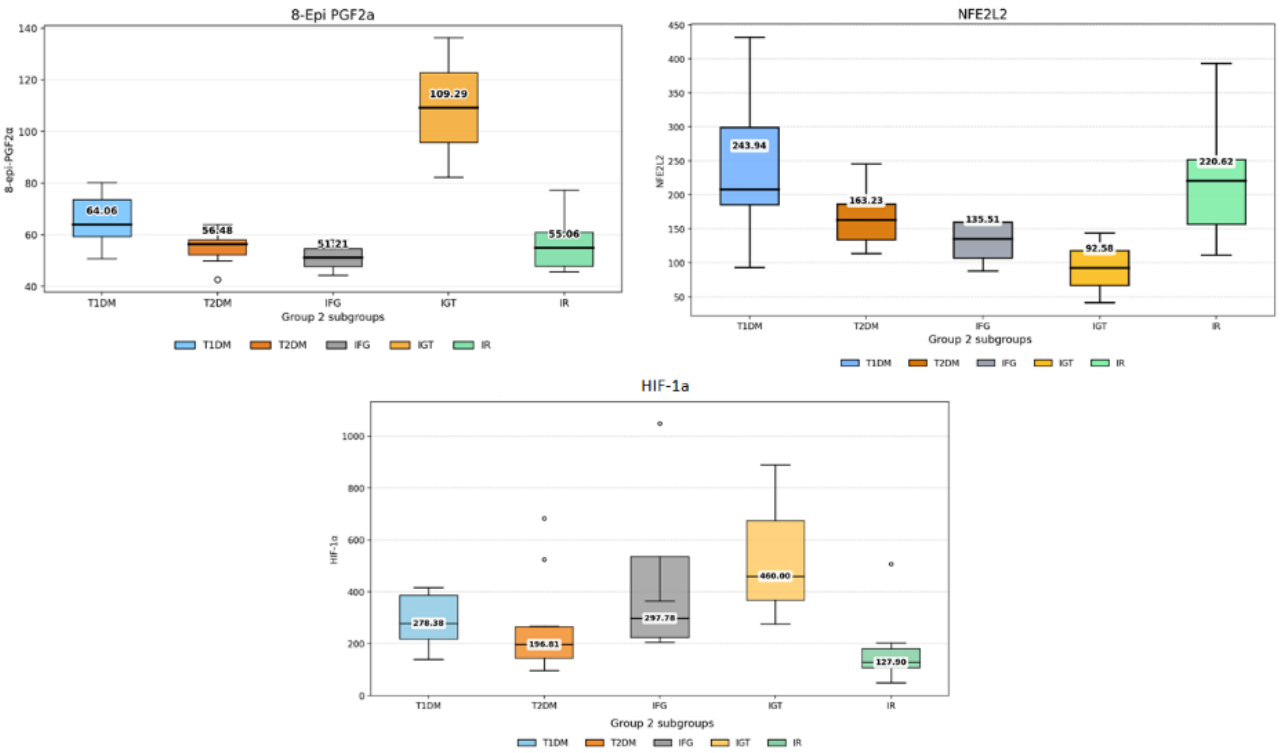

Figure 11. Distribution (Median; IQR) of oxidative stress (8-Epi-PGF-2α), antioxidant defense (NFE2L2), and hypoxia (HIF-1α) markers across the subgroups of Group 2 – T1DM/LADA, T2DM, IFG, IGT, and IR.

5. Assessment of Glucose Homeostasis in the Acute Phase of COVID-19 and in the Asymptomatic Post-COVID Period Through Analysis of Pancreatic α- and β-Cell Function, Insulin Secretion, and Insulin Sensitivity

5.1. Main Parameters of Glucose Homeostasis

Fasting Plasma Glucose (FPG)

Fasting plasma glucose levels were assessed in individuals from the three main groups. In patients with active coronavirus infection (Group 1), measurements were performed prior to the initiation of glucocorticosteroid (GCS) therapy.

The highest mean values were observed in recovered individuals with newly developed carbohydrate disturbances (Group 2: 7.64 ± 3.69 mmol/L), followed by those with active infection (Group 1: 7.37 ± 1.81 mmol/L), while the lowest values were recorded in COVID-negative individuals with MetS (Group 3: 5.69 ± 1.76 mmol/L). Median analysis confirmed the same trend, with the greatest variability (IQR = 4.1 mmol/L) observed in the post-COVID group (Group 2).

Non-parametric analysis revealed statistically significant differences between the three groups (Kruskal–Wallis $H(2) = 17.96$; $p < 0.001$). Post-hoc comparisons demonstrated significant differences between Group 1 and Group 3 (Mann–Whitney $U = 840.0$; $p < 0.001$), as well as between Group 2 and Group 3 (Mann–Whitney $U = 745.5$; $p = 0.010$), whereas the difference between Group 1 and Group 2 did not reach statistical significance ($p > 0.05$).

Results from the generalized linear model (GLM, Gamma, log-link), adjusted for age and sex, showed that during active infection fasting glucose levels did not differ significantly from those of individuals with MetS ($\beta = 0.11$; $p = 0.589$). In contrast, recovered individuals demonstrated significantly higher levels compared to the control group ($\beta = 0.21$; $e^{\beta} = 1.23$; 95% CI: 1.08–1.51; $p = 0.004$), corresponding to approximately a 23% increase. Comparison between the active and post-COVID groups demonstrated a borderline trend toward lower values during active infection ($\beta = -0.10$; $e^{\beta} = 0.90$; 95% CI: 0.68–1.01; $p = 0.061$).

In intragroup analysis by sex, no statistically significant differences were observed in any group ($p > 0.05$). Regarding diabetes status, in Group 2 diabetic individuals demonstrated significantly higher fasting glucose levels compared to non-diabetics (Mann–Whitney $U = 238.0$; $p < 0.001$), and a similar association was observed in Group 3 (Mann–Whitney $U = 199.5$; $p = 0.003$). In Group 1, the difference between diabetics and non-diabetics did not reach statistical significance ($p > 0.05$).

In Group 1, 43.75% of individuals exhibited values ≥ 7.0 mmol/L, and 6.25% had values ≥ 11.1 mmol/L, with stress-induced hyperglycemia identified in 12.5% of patients. In Group 2, 31.43% had FBG ≥ 7.0 mmol/L and 14.28% ≥ 11.1 mmol/L, whereas in Group 3 these proportions were 12.12% and 3.03%, respectively.

Correlation analysis revealed in the post-COVID group a moderate positive correlation between FPG and IL-10 ($r_s = 0.369$; $p = 0.034$). In the MetS reference group, FPG correlated positively with BMI ($r_s = 0.444$; $p = 0.010$), basal insulin ($r_s = 0.531$; $p = 0.006$), and leptin ($r_s = 0.512$; $p = 0.025$), as well as with IR indices—HOMA-IR ($r_s = 0.707$; $p < 0.001$), TyG index ($r_s = 0.754$; $p < 0.001$), TG/HDL-C ratio ($r_s = 0.465$; $p = 0.006$), and METS-IR ($r_s = 0.537$; $p = 0.001$) and negatively with QUICKI ($r_s = -0.707$; $p < 0.001$) and the Adiponectin/Leptin ratio ($r_s = -0.549$; $p = 0.022$).

In individuals from Group 4, dynamic monitoring of the glycemic profile was performed during hospitalization, including glucose at admission, mean, maximum, minimum values, and glycemic variability (ΔFBG = max–min glucose) (Table 10).

Table 10. Parameters Reflecting the Glycemic Profile in Group 4 (Hospitalized Individuals with Active Coronavirus Infection, n = 135)

Parameter	Mean ± SD	Median	Range (min–max)
Glucose at admission [mmol/L]	8.39 ± 4.41	7.05	4.17 – 32.73
Mean glucose [mmol/L]	8.43 ± 3.01	7.56	4.52 – 18.89
Maximum glucose [mmol/L]	11.78 ± 6.24	9.60	4.69 – 36.40
Minimum glucose [mmol/L]	5.59 ± 1.45	5.50	2.70 – 12.10
ΔGlucose (max–min) [mmol/L]	6.25 ± 6.40	4.06	0 – 29.10

Note: *ΔGlucose = difference between the maximum and minimum measured blood glucose values during hospitalization.*

Glucose at admission was elevated in a substantial proportion of patients, with values above 10.0 mmol/L recorded in 15.5% of cases. Diabetic individuals demonstrated significantly higher admission glucose levels compared to non-diabetics (Mann–Whitney U = 801.5; $p < 0.001$). Admission glucose correlated positively with CRP ($r_s = 0.282$; $p = 0.001$) and with the TyG index ($r_s = 0.604$; $p < 0.001$).

Mean glucose levels during hospitalization correlated with infection severity ($r_s = 0.327$; $p = 0.001$) and with the TyG index ($r_s = 0.416$; $p = 0.001$).

Maximum glycemic values were significantly higher in diabetic patients (Mann–Whitney U = 186.0; $p < 0.001$) and also correlated with infection severity ($r_s = 0.326$; $p = 0.001$) and the TyG index ($r_s = 0.390$; $p = 0.001$).

Minimum glucose values did not differ significantly by sex or diabetes status ($p > 0.05$).

Glycemic variability (ΔGlucose) was significantly more pronounced in diabetics compared to non-diabetics (Mann–Whitney U = 221.0; $p < 0.001$) and correlated both with infection severity ($r_s = 0.326$; $p = 0.001$) and with the TyG index ($r_s = 0.379$; $p = 0.001$).

When comparing individuals with previously known versus newly diagnosed diabetes, no statistically significant differences were observed in the main indicators of glycemic variability ($p > 0.05$), despite a trend toward greater instability in newly diagnosed cases (Fig. 12).

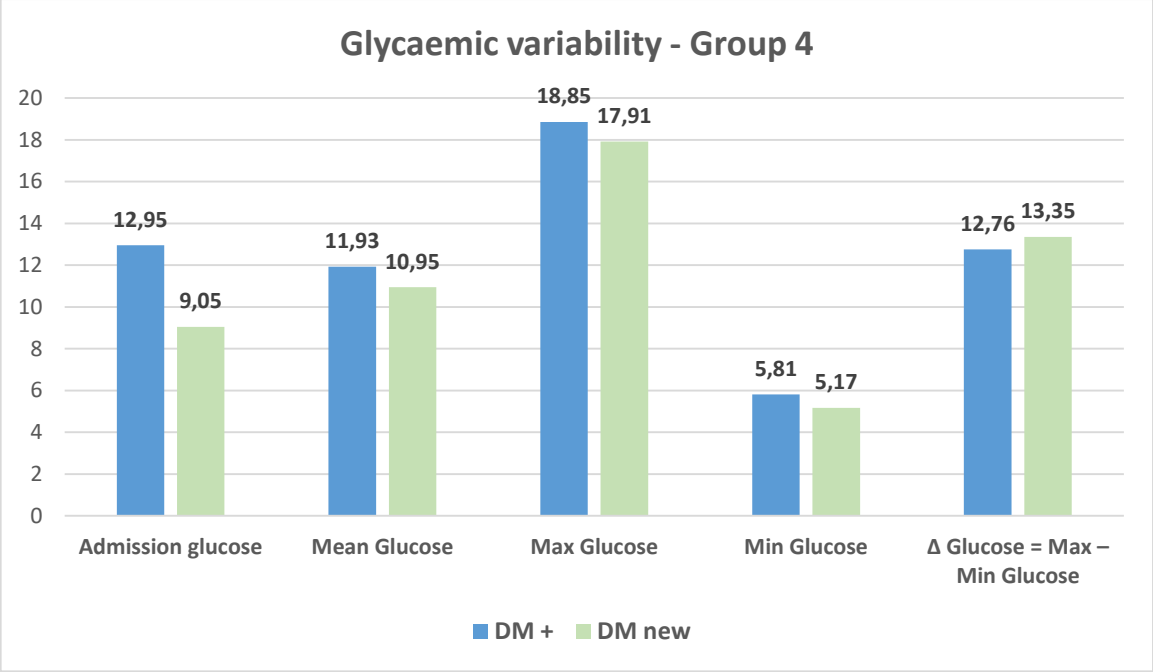

Figure 12. Monitoring of variations in mean glycaemic levels in individuals with previously known diabetes (DM+) and those with newly diagnosed diabetes (DM new) from Group 4 (baseline cohort of individuals with active coronavirus infection, n = 42).

HbA1c. No statistically significant intergroup differences in HbA1c levels were observed (Kruskal–Wallis H(2) = 3.64; p = 0.162), despite a tendency toward higher values in recovered individuals with newly developed carbohydrate disturbances (Table 11).

Table 11. Serum HbA1c levels [%] in the studied groups (Mean ± SD; Median (IQR))

Parameter	Group 1 – Active COVID (n = 18*)	Group 2 – Post-COVID (n = 23*)	Group 3 – COVID(-) with MetS (n = 18*)	Kruskal–Wallis Test
HbA1c [%]	6.33 ± 0.83 6.23 (1.57)	8.00 ± 2.69 7.20 (5.10)	7.04 ± 1.40 6.61 (2.57)	*H = 3.64* *p = 0.162*

** n – the number of examined individuals varies due to missing laboratory data.*

Results from the generalized linear model (GLM, Gamma, log-link), adjusted for age and sex, showed no significant difference between individuals with active infection and the MetS control group (β = −0.11; p = 0.087), nor between recovered individuals and the control group (β = 0.19; p = 0.284).

Direct comparison between the active and post-COVID phases demonstrated significantly lower values during active infection (β = −0.21; e^{β} = 0.81; 95% CI 0.60–0.93; p = 0.008).

Intragroup analysis revealed significantly higher HbA1c levels in diabetics compared to non-diabetics in Group 1 (Mann–Whitney U = 48.5; p = 0.033) and in Group 2 (Mann–Whitney U = 112.0; p < 0.001), without reaching significance in Group 3 (p > 0.05). In intergroup

comparison, diabetics from Group 2 demonstrated significantly higher values compared to diabetics from Group 1 (Mann–Whitney U = 32.0; $p < 0.001$).

Subgroup analysis within the post-COVID group (Group 2) revealed statistically significant differences in HbA1c levels between the different types of newly developed carbohydrate disturbances (Kruskal–Wallis H(3) = 19.6238; $p < 0.001$) (Table 12).

Post-hoc analysis demonstrated that statistically significant differences were present only between the T1DM and T2DM subgroups (Mann–Whitney U = 1.0; $p = 0.001$), between T2DM and IR (Mann–Whitney U = 40.0; $p = 0.004$), and between T1DM and IR (Mann–Whitney U = 40.0; $p = 0.004$). No statistically significant differences were observed between the remaining subgroups ($p > 0.05$).

Table 12. HbA1c levels (Mean ± SD; Median IQR)) in the individual subgroups of Group 2

Parameter	**T1DM (n = 8)**	**T2DM (n = 8)**	**IFG (n = 1)**	**IGT (n = 1)**	**IR (n = 5)**	**Kruskal–Wallis Test**
HbA1c [%]	11.11 ± 1.85 11.26 (5.64)	7.21 ± 0.69 7.06 (2.06)	5.70 5.70 (0)	5.80 5.80 (0)	5.19 ± 0.58 5.29 (0.60)	*H = 19.62* *p < 0.001*

Correlation analysis revealed that in Group 1, HbA1c correlated positively with proinsulin ($r_s = 0.499$; $p = 0.035$) and fasting glucose ($r_s = 0.426$; $p = 0.043$). In Group 2, positive correlations were observed between HbA1c and IL-10 ($r_s = 0.510$; $p = 0.012$), as well as between HbA1c and HIF-1α ($r_s = 0.426$; $p = 0.043$). In the same group, a strong negative correlation was identified between HbA1c and HOMA-B ($r_s = -0.818$; $p < 0.001$), along with a positive correlation with the TyG index ($r_s = 0.528$; $p = 0.012$). In the subgroup with normoglycemia and IR/hyperinsulinemia, a strong positive correlation was observed between HbA1c and IL-10 ($r_s = 0.946$; $p < 0.001$).

Frequency of Newly Diagnosed Diabetes during Active COVID-19

Newly diagnosed diabetes was identified in 11.98% of patients with active infection (21.87% in Group 1 and 9.63% in Group 4).

5.1. Analysis of Pancreatic α- and β-Cell Function

5.1.1. Alpha (α)-Cell Function – Glucagon

Analysis of glucagon levels across the three studied groups revealed pronounced intergroup differences (Table 13). The highest values were recorded in COVID-negative individuals with MetS (Group 3), the lowest in recovered individuals with newly developed carbohydrate

disturbances (Group 2), while individuals with active coronavirus infection (Group 1) demonstrated intermediate values.

Table 13. Descriptive statistics (Mean ± SD; Median (IQR)) and intergroup comparisons of serum levels of Glucagon [pg/mL], Insulin [μU/mL], C-peptide [ng/mL], and Proinsulin [pg/mL]

Parameter	Group 1 – Active COVID (n = 32*)	Group 2 – Post-COVID (n = 35*)	Group 3 – COVID(-) with MetS (n = 33*)	Kruskal–Wallis Test
Glucagon	6456.68 ± 2391.16 5782.69 (3725.04)	5403.88 ± 1999.43 4893.64 (2350.28)	8152.59 ± 1492.96 7847.44 (2593.63)	*H = 21.91* *p < 0.001*
Insulin	26.19 ± 16.52 25.90 (27.19)	20.11 ± 19.50 14.54 (9.27)	31.86 ± 62.38 14.53 (19.07)	*H = 3.67* *p = 0.159*
C-peptide	1.21 ± 1.21 0.70 (1.39)	1.54 ± 1.30 1.32 (1.92)	0.42 ± 0.61 0.24 (0.38)	*H = 19.65* *p < 0.001*
Proinsulin	56.03 ± 34.14 50.21 (62.27)	41.55 ± 39.98 29.81 (24.98)	54.22 ± 52.37 34.08 (52.86)	*H = 3.84* *p = 0.147*

** n – the number of examined individuals may vary between groups due to missing or incomplete data for some of the analyzed parameters.*

Non-parametric analysis demonstrated statistically significant differences among the three groups (Kruskal–Wallis H(2) = 21.909; $p < 0.001$). Post-hoc analysis did not reveal a significant difference between Groups 1 and 2 (Mann–Whitney U = 306.0; $p = 0.068$). In contrast, statistically significant differences were identified both between Groups 1 and 3 (Mann–Whitney U = 126.5; $p = 0.003$) and between Groups 2 and 3 (Mann–Whitney U = 95.0; $p < 0.001$).

Results from the generalized linear model (GLM, Gamma, log-link), adjusted for age and sex, demonstrated that glucagon levels were significantly lower both in individuals with active infection ($\beta = -0.40$; $e^{\beta} = 0.67$; 95% CI: 0.49–0.92; $p = 0.014$) and in recovered individuals with newly developed carbohydrate disturbances ($\beta = -0.39$; $e^{\beta} = 0.68$; 95% CI: 0.51–0.90; $p = 0.008$) compared to the MetS reference group. Direct comparison between the active and post-COVID phases did not reveal a statistically significant difference ($\beta = -0.01$; $e^{\beta} = 0.99$; 95% CI: 0.74–1.32; $p = 0.913$).

Intragroup analysis did not identify statistically significant differences in glucagon levels according to sex or diabetes status within any of the three groups ($p > 0.05$). In intergroup comparison by diabetes status, diabetic individuals from Group 3 exhibited significantly higher glucagon levels compared to diabetics from Group 2 (Mann–Whitney U = 16.0; $p = 0.001$). Similarly, among non-diabetic individuals, glucagon levels in Group 3 were significantly higher than those in Group 2 (Mann–Whitney U = 32.5; $p < 0.001$).

Subgroup analysis within the post-COVID group (Fig. 13) did not demonstrate statistically significant differences in glucagon levels among the individual phenotypic subgroups according to the type of carbohydrate disturbance (Kruskal–Wallis H(3) = 3.68; p > 0.05).

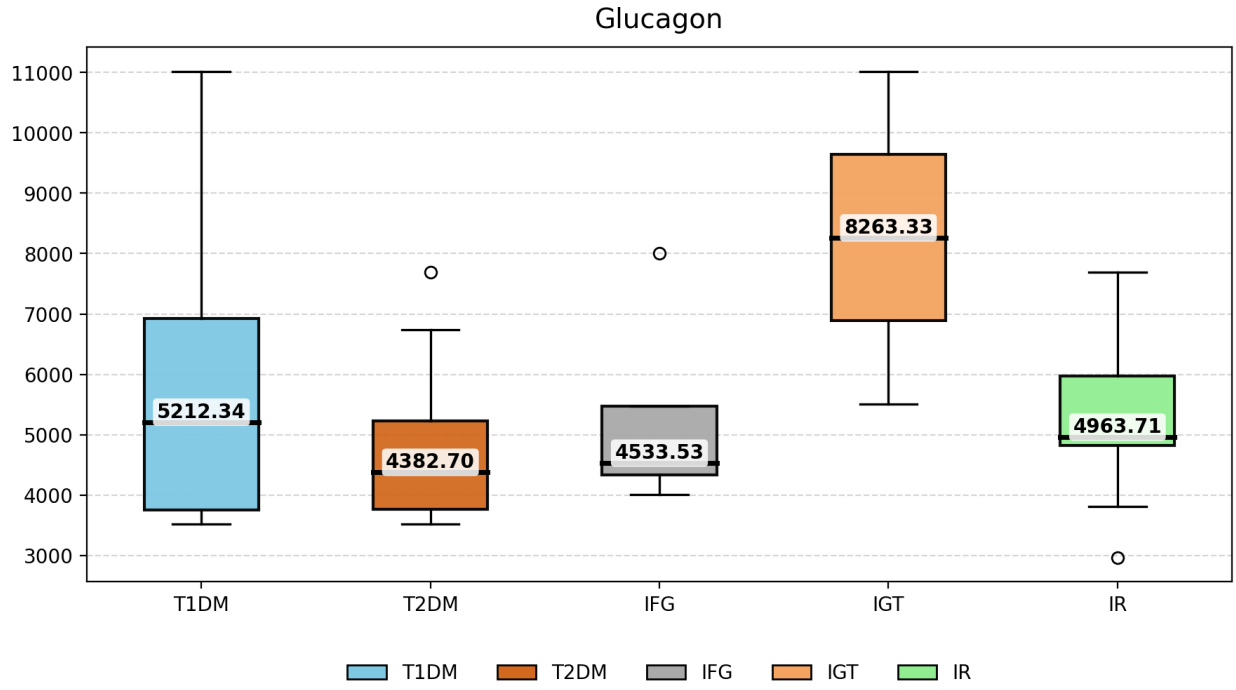

Figure 13. Distribution (Median; IQR) of serum glucagon levels across the subgroups of Group 2 – T1DM/LADA, T2DM, IFG, IGT, and IR.

Correlation analysis revealed statistically significant positive correlations between glucagon and CD4 in Group 1 (r_s = 0.399; p = 0.023) and Group 2 (r_s = 0.387; p = 0.028). In Group 2, a positive correlation was also observed between glucagon and HIF-1α (r_s = 0.467; p = 0.005), as well as with adiponectin (r_s = 0.398; p = 0.020). In Group 3, glucagon correlated positively with HIF-1α (r_s = 0.542; p = 0.011) and GP-73 (r_s = 0.599; p = 0.011).

5.1.2. Beta (β)-Cell Function

Insulin. Analysis of basal insulin levels across the three studied groups showed that the highest mean values were observed in the reference group with MetS (Group 3), the lowest in recovered COVID-19 individuals with newly developed carbohydrate disturbances (Group 2), while individuals with active coronavirus infection (Group 1) demonstrated intermediate values. Median analysis revealed a different distribution pattern, with the highest median levels recorded during active infection (Table 13).

Non-parametric analysis did not demonstrate statistically significant differences among the three groups (Kruskal–Wallis $H(2) = 3.67$; $p = 0.159$).

However, results from the generalized linear model (GLM, Gamma, log-link), adjusted for age and sex, showed that insulin levels were significantly lower both in individuals with active coronavirus infection ($\beta = -0.48$; $e^{\beta} = 0.62$; 95% CI: 0.39–0.99; $p = 0.045$) and in recovered individuals ($\beta = -0.52$; $e^{\beta} = 0.59$; 95% CI: 0.37–0.94; $p = 0.027$) compared to the MetS control group. Direct comparison between the active and post-COVID groups did not reveal a statistically significant difference ($\beta = 0.04$; $e^{\beta} = 1.04$; 95% CI: 0.49–2.20; $p = 0.913$).

Intragroup analysis did not identify statistically significant differences in insulin levels according to sex or diabetes status within any of the three groups ($p > 0.05$). Intergroup comparison of the respective subgroups likewise did not reveal statistically significant differences ($p > 0.05$).

Subgroup analysis within the post-COVID group (Group 2) demonstrated a statistically significant difference between the T1DM subgroup and the combined prediabetes subgroup (IFG + IGT) (Mann–Whitney $U = 0$; $p = 0.0025$), while no statistically significant differences were observed between the remaining subgroups ($p > 0.05$) (Fig. 14).

Correlation analysis showed that in Group 1 insulin correlated positively with HOMA-B ($r_s = 0.866$; $p < 0.001$), HOMA-IR ($r_s = 0.960$; $p < 0.001$), and the Insulin/Proinsulin ratio ($r_s = 0.756$; $p < 0.001$), and negatively with QUICKI ($r_s = -0.953$; $p < 0.001$).

In Group 2, positive correlations were observed with HOMA-B ($r_s = 0.697$; $p < 0.001$), HOMA-IR ($r_s = 0.697$; $p < 0.001$), and the Insulin/Proinsulin ratio ($rs = 0.521$; $p = 0.003$), along with a negative correlation with QUICKI ($r_s = -0.697$; $p < 0.001$). A moderate negative correlation was also identified between insulin and NFE2L2 ($r_s = -0.401$; $p = 0.025$).

In Group 3, insulin correlated positively with BMI ($r_s = 0.552$; $p = 0.004$), FPG ($r_s = 0.531$; $p = 0.006$), proinsulin ($r_s = 0.860$; $p < 0.001$), GLP-1 ($r_s = 0.794$; $p < 0.001$), leptin ($r_s = 0.745$; $p < 0.001$), HOMA-B ($r_s = 0.746$; $p < 0.001$), HOMA-IR ($r_s = 0.969$; $p < 0.001$), the Insulin/Proinsulin ratio ($r_s = 0.637$; $p = 0.003$), the Proinsulin/C-peptide ratio ($r_s = 0.600$; $p = 0.018$), TyG index ($r_s = 0.476$; $p = 0.016$), and METS-IR ($r_s = 0.500$; $p = 0.011$), and negatively with QUICKI ($r_s = -0.969$; $p < 0.001$) and the Adiponectin/Leptin ratio ($r_s = -0.739$; $p = 0.002$).

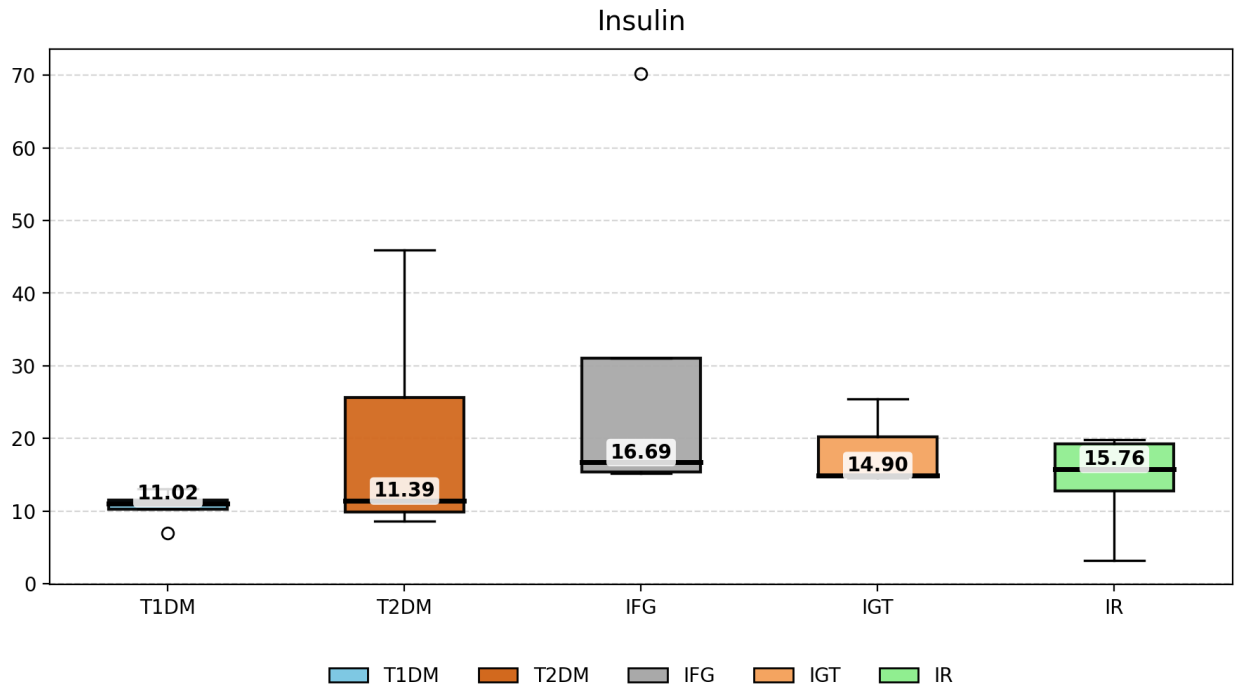

Figure 14. Distribution (Median; IQR) of serum insulin levels across the subgroups of Group 2 – T1DM/LADA, T2DM, IFG, IGT, and IR.

C-peptide. Basal C-peptide levels were assessed in the three studied groups. The highest mean and median values were observed in recovered individuals with newly developed carbohydrate disturbances (Group 2), followed by individuals with active coronavirus infection (Group 1), whereas the lowest levels were recorded in COVID-negative individuals with MetS (Group 3) (Table 13).

Non-parametric analysis demonstrated statistically significant differences among the three groups (Kruskal–Wallis $H(2) = 19.65$; $p < 0.001$). Post-hoc analysis revealed significant differences between Group 1 and Group 3 (Mann–Whitney $U = 581.0$; $p = 0.001$), as well as between Group 2 and Group 3 (Mann–Whitney $U = 667.5$; $p < 0.001$), while no statistically significant difference was found between Groups 1 and 2 ($p > 0.05$).

Results from the generalized linear model (GLM, Gamma, log-link), adjusted for age and sex, confirmed a pronounced and statistically significant increase in C-peptide levels both during active COVID-19 and in the post-COVID period compared to the MetS control group: in Group 1 – approximately a 4.6-fold increase ($\beta = 1.53$; $e^{\beta} = 4.62$; 95% CI: 1.91–7.53; $p < 0.001$), and in Group 2 – more than a 6-fold increase ($\beta = 1.86$; $e^{\beta} = 6.42$; 95% CI: 2.96–9.02; $p < 0.001$). No significant difference was observed between the active and post-COVID phases ($\beta = -0.33$; $p = 0.336$), indicating persistence of increased endogenous secretion after resolution of the acute phase (taking into account the strict selection criteria applied to Group 2).

Intragroup analysis did not reveal statistically significant differences in C-peptide levels according to sex or diabetes status in any of the three groups ($p > 0.05$). In intergroup comparison by diabetes status, diabetics from Group 2 demonstrated higher C-peptide levels compared to diabetics from Group 3 (Mann–Whitney U = 69.0; $p = 0.015$). Among non-diabetics, the highest levels were observed in Group 1, differing significantly from non-diabetics in Group 3 (Mann–Whitney U = 255.0; $p < 0.001$); significant differences were also observed between non-diabetics in Group 2 and Group 3 (Mann–Whitney U = 264.0; $p < 0.001$).

Subgroup analysis within the post-COVID group (Group 2) demonstrated statistically significant differences among subgroups according to the type of newly developed carbohydrate disturbance (Kruskal–Wallis H(3) = 9.80; $p = 0.044$). The lowest values were recorded in individuals with T1DM, who differed significantly from the T2DM subgroup (Mann–Whitney U = 54.0; $p = 0.007$) (Fig. 15).

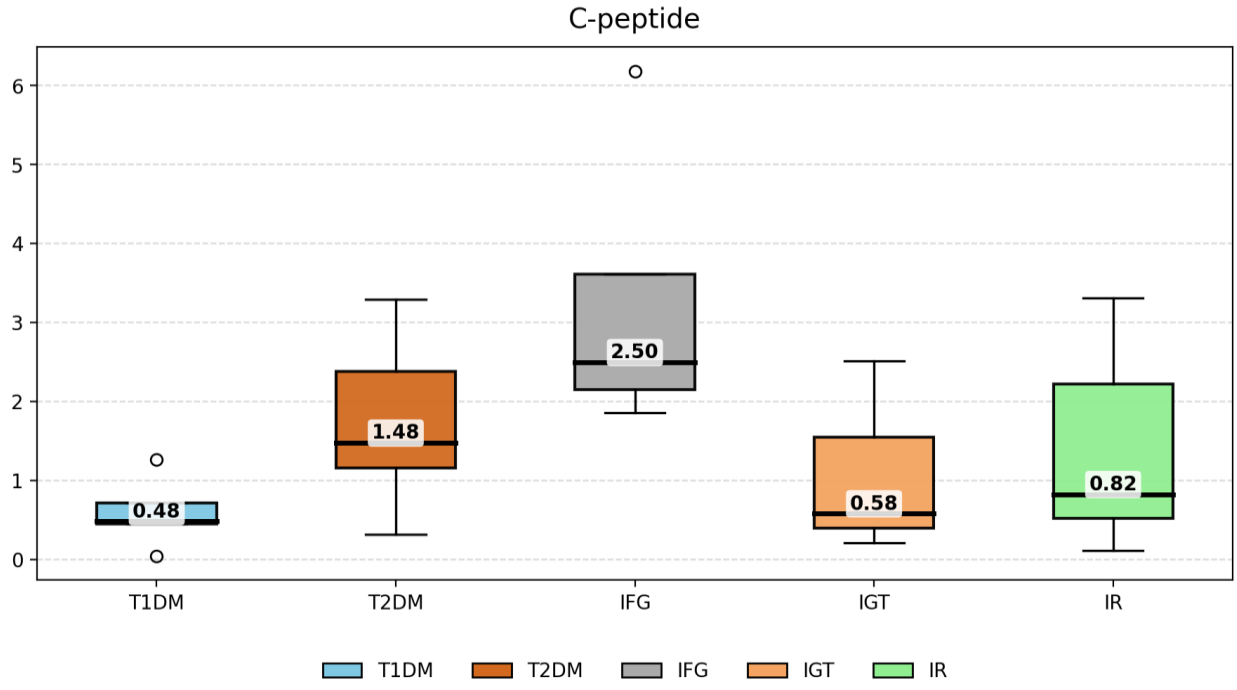

Figure 15. Distribution (Median; IQR) of serum C-peptide levels across the subgroups of Group 2 – T1DM/LADA, T2DM, IFG, IGT, and IR.

Correlation analysis revealed a weak negative correlation between C-peptide and CD8 in Group 1 ($r_s = -0.429$; $p = 0.023$). In all three groups, strong positive correlations were observed between C-peptide and the C-peptide/Glucose ratio (Group 1: $r_s = 0.963$; $p < 0.001$; Group 2: $r_s = 0.931$; $p < 0.001$; Group 3: $r_s = 0.962$; $p < 0.001$), as well as negative correlations with the

Proinsulin/C-peptide ratio (Group 1: $r_s = -0.771$; $p < 0.001$; Group 2: $r_s = -0.827$; $p < 0.001$; Group 3: $r_s = -0.593$; $p = 0.020$). In Group 3, a negative correlation with adiponectin was also observed ($r_s = -0.604$; $p = 0.008$).

Proinsulin. Serum proinsulin levels were assessed in the three groups (Table 13). The highest mean and median values were observed in individuals with active SARS-CoV-2 infection (Group 1), while the lowest were recorded in recovered individuals (Group 2), with COVID-negative individuals with MetS (Group 3) occupying an intermediate position. Intergroup differences did not reach statistical significance (Kruskal–Wallis $H(2) = 3.835$; $p = 0.147$).

Results from the generalized linear model (GLM, Gamma, log-link), adjusted for age and sex, demonstrated a non-significant increase in proinsulin levels both during active infection ($\beta = 0.474$; $p = 0.219$) and in the post-COVID group ($\beta = 0.30$; $p > 0.05$) compared to the MetS control group. No statistically significant difference was observed between the active and post-COVID groups ($\beta = -0.17$; $p > 0.05$). Intragroup analysis did not reveal statistically significant differences according to sex or diabetes status ($p > 0.05$).

Subgroup analysis within the post-COVID group (Group 2) demonstrated a heterogeneous distribution of the parameter (Fig. 16), without statistically significant differences among the individual subgroups (Kruskal–Wallis $H(3) = 3.84$; $p = 0.428$).

Correlation analysis showed that in Group 1, proinsulin correlated positively with HbA1c ($r_s = 0.535$; $p = 0.040$), GLP-1 ($r_s = 0.846$; $p < 0.001$), and leptin ($r_s = 0.626$; $p = 0.001$). In Group 2, a positive correlation was observed with IFN-γ ($r_s = 0.543$; $p = 0.001$). In Group 3, proinsulin correlated positively with insulin ($r_s = 0.860$; $p < 0.001$), GLP-1 ($r_s = 0.886$; $p < 0.001$), and leptin ($r_s = 0.670$; $p = 0.002$), and negatively with the Adiponectin/Leptin ratio ($r_s = -0.806$; $p < 0.001$).

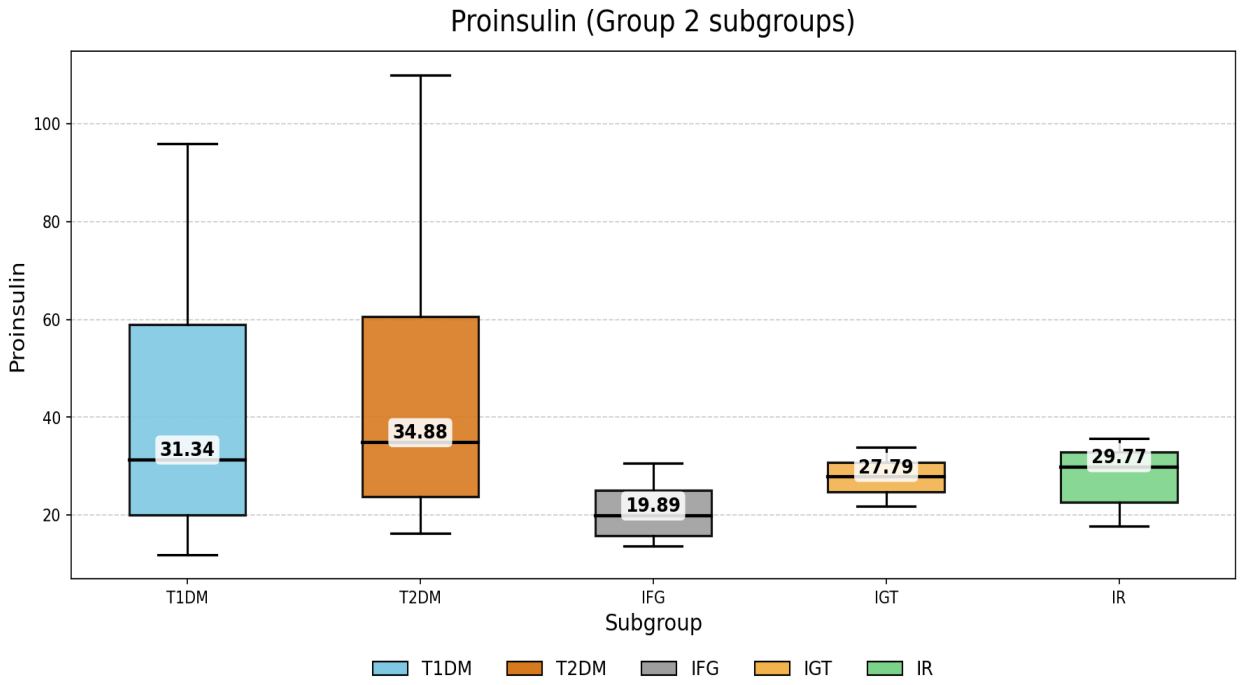

Figure 16. Distribution (Median; IQR) of serum proinsulin levels across the subgroups of Group 2 – T1DM/LADA, T2DM, IFG, IGT, and IR.

5.2. Surrogate Indices of β-Cell Function

Table 14. Descriptive statistics (Mean ± SD; Median (IQR)) of indices reflecting β-cell function and insulin processing in the studied groups

Parameter	Group 1 – Active COVID (n = 32*)	Group 2 – Post-COVID (n = 35*)	Group 3 – COVID(-) with MetS (n = 33*)	Kruskal–Wallis Test
HOMA-B	159.33 ± 138.77 135.10 (149.84)	183.14 ± 175.85 113.41 (209.88)	330.09 ± 441.90 223.27 (204.76)	*H = 19.65* *p < 0.001*
C-peptide/ Glucose ratio	0.89 ± 0.81 0.56 (1.00)	1.35 ± 1.26 1.03 (1.19)	0.45 ± 0.69 0.24 (0.29)	*H = 15.01* *p < 0.001*
Insulin/ Proinsulin ratio	40.11 ± 47.57 26.67 (33.71)	38.67 ± 48.57 33.10 (14.54)	23.33 ± 14.32 24.11 (8.54)	*H = 7.51* *p = 0.023*
Proinsulin/ C-peptide ratio	5.56 ± 6.05 2.61 (1.00)	3.28 ± 5.29 1.05 (1.00)	10.05 ± 8.93 7.35 (1.00)	*H = 18.57* *p < 0.001*

** n – The number of examined individuals may vary between groups due to missing or incomplete laboratory data for some of the analyzed parameters.*

The highest **HOMA-B** values were observed in COVID-negative individuals with MetS, whereas both COVID-related groups demonstrated similar and lower values (Table 14). Intergroup analysis revealed statistically significant differences (Kruskal–Wallis H(2) = 19.65; p < 0.001). Post-hoc analysis demonstrated significant differences between Group 1 and Group 3 (Mann–Whitney U = 223.0; p = 0.007), as well as between Group 2 and Group 3 (Mann–

Whitney U = 240.0; p = 0.023), with no difference between the two COVID-related groups (p > 0.05).

After adjustment for age and sex (GLM, Gamma, log-link), significantly higher HOMA-B values were observed both during active infection (β = 1.74; e^{β} = 5.71; 95% CI: 3.18–10.25; p < 0.001) and in the post-COVID group (β = 1.74; e^{β} = 5.68; 95% CI: 3.84–8.41; p < 0.001) compared to the control group, with no difference between the two phases (β = 0.004; p = 0.989).

A statistically significant intragroup difference between diabetics and non-diabetics was observed only in the post-COVID group (Mann–Whitney U = 32.0; p = 0.001), with non-diabetics demonstrating higher values.

Correlation analysis showed that in recovered individuals, HOMA-B correlated negatively with FPG (r_s = −0.717; p < 0.001), HbA1c (r_s = −0.818; p < 0.001), IL-10 (r_s = −0.438; p = 0.019), and TyG index (r_s = −0.536; p = 0.005).

The **C-peptide/Glucose ratio** also differed significantly between groups (Kruskal–Wallis H(2) = 15.01; p < 0.001). The lowest values were observed in COVID-negative individuals with MetS, whereas the highest were recorded in recovered COVID-19 patients with newly developed carbohydrate disturbances. Individuals with active SARS-CoV-2 infection demonstrated intermediate values (Table 14).

Post-hoc analysis showed significantly higher values in recovered individuals compared to MetS controls (Mann–Whitney U = 595.0; p < 0.001), as well as higher values during active infection compared to the reference group (Mann–Whitney U = 492.0; p = 0.012). No difference was observed between the active and post-COVID groups (p > 0.05).

After adjustment for age and sex (GLM, Gamma, log-link), a significant increase in the ratio was observed both during active infection (β = 1.029; e^{β} = 2.80; 95% CI: 1.32–5.94; p = 0.007) and in the post-COVID group (β = 1.360; e^{β} = 3.90; 95% CI: 2.15–7.07; p < 0.001) compared to the MetS control group, with no difference between the two COVID-related groups (β = −0.331; p = 0.359).

Intragroup analysis revealed a statistically significant difference between diabetics and non-diabetics only during active infection, with diabetics demonstrating lower values (Mann–Whitney U = 29.0; p < 0.001). No differences according to diabetes status were observed in the remaining groups (p > 0.05).

Correlation analysis during active infection showed negative correlations with CD8 (r_s = −0.459; p = 0.019) and TNF-α (r_s = −0.376; p = 0.033). In the post-COVID group, positive correlations were observed with BMI (r_s = 0.423; p = 0.020) and HDL-C (r_s = 0.419; p = 0.037). In the reference group, a negative correlation with adiponectin was observed (r_s = −0.548; p = 0.019). In all three groups, strong positive correlations were observed with C-peptide (Group 1: r_s = 0.963; p < 0.001; Group 2: r_s = 0.931; p < 0.001; Group 3: r_s = 0.962; p < 0.001), and negative correlations with the Proinsulin/C-peptide ratio (Group 1: r_s = −0.740; p < 0.001; Group 2: r_s = −0.840; p < 0.001; Group 3: r_s = −0.682; p = 0.005).

The **Insulin/Proinsulin ratio** demonstrated similar values in patients with active SARS-CoV-2 infection and in recovered individuals with newly developed carbohydrate disturbances, whereas lower values were observed in COVID-negative individuals with MetS (Table 14).

Intergroup analysis revealed statistically significant differences (Kruskal–Wallis H(2) = 7.505; p = 0.023). Pairwise comparisons demonstrated a statistically significant difference only between recovered individuals with newly developed carbohydrate disturbances and MetS controls (Mann–Whitney U = 452.0; p = 0.017). No statistically significant differences were observed between the remaining groups (p > 0.05). After adjustment for age and sex using GLM (Gamma, log-link), no statistically significant intergroup differences were detected (p > 0.05).

Intragroup analysis revealed a statistically significant difference between diabetics and non-diabetics only in the recovered group (Mann–Whitney U = 67.0; p = 0.038). No statistically significant differences were observed in the remaining groups (p > 0.05).

Correlation analysis demonstrated statistically significant associations between the Insulin/Proinsulin ratio and multiple metabolic parameters across all groups, without identifying a specific COVID-associated pattern. In all three groups, significant positive correlations were observed with insulin (Group 1: r_s = 0.756; p < 0.001; Group 2: r_s = 0.521; p = 0.003; Group 3: r_s = 0.637; p = 0.003) and HOMA-IR (Group 1: r_s = 0.712; p < 0.001; Group 2: r_s = 0.418; p = 0.024; Group 3: r_s = 0.577; p = 0.010). Concurrently, negative correlations with QUICKI were observed in all groups (Group 1: r_s = −0.712; p < 0.001; Group 2: r_s = −0.418; p = 0.024; Group 3: r_s = −0.577; p = 0.010).

Additionally, in the active and post-COVID groups, negative correlations were observed with proinsulin (Group 1: r_s = −0.515; p = 0.008; Group 2: r_s = −0.694; p < 0.001), as well as with the Proinsulin/C-peptide ratio (Group 1: r_s = −0.586; p = 0.003; Group 2: r_s = −0.389; p =

0.031). A positive correlation with HOMA-B was observed in the active infection group (r_s = 0.657; $p < 0.001$) and in individuals with MetS (r_s = 0.512; p = 0.025).

Group-specific associations included a negative correlation with IFN-γ in the post-COVID group (r_s = −0.489; p = 0.007), as well as positive correlations in the MetS group with 8-epi-PGF2α (r_s = 0.525; p = 0.044), TyG index (r_s = 0.545; p = 0.016), and the TG/HDL-C ratio (r_s = 0.488; p = 0.034).

The **Proinsulin/C-peptide ratio** demonstrated a clear phase-dependent pattern, with the highest values observed in COVID-negative individuals with MetS, intermediate values in patients with active SARS-CoV-2 infection, and the lowest values in recovered individuals with newly developed carbohydrate disturbances (Table 14).

Intergroup analysis revealed statistically significant differences (Kruskal–Wallis H(2) = 18.57; $p < 0.001$). Post-hoc analysis demonstrated significant differences between Group 1 and Group 2 (Mann–Whitney U = 546.0; p = 0.011), as well as between Group 2 and Group 3 (Mann–Whitney U = 158.0; $p < 0.001$), with no difference between Groups 1 and 3 (Mann–Whitney U = 99.0; p = 0.184).

After adjustment for age and sex, significantly lower values were observed in the post-COVID group compared to controls (β = −1.355; e^{β} = 0.26; 95% CI: 0.11–0.61; p = 0.002). Active infection did not differ from the control group (β = −0.309; p = 0.604). Direct comparison demonstrated higher values during active infection compared to the post-COVID group (β = 1.046; e^{β} = 2.85; 95% CI: 1.06–7.65; p = 0.038).

A statistically significant intragroup difference between diabetics and non-diabetics was observed only in the active infection group (Mann–Whitney U = 120.0; p = 0.024). Additionally, diabetics from the MetS group differed from diabetics in the post-COVID group (Mann–Whitney U = 11.0; p = 0.015).

Correlation analysis showed that in all three groups the Proinsulin/C-peptide ratio correlated negatively with C-peptide (Group 1: r_s = −0.771; $p < 0.001$; Group 2: r_s = −0.827; $p < 0.001$; Group 3: r_s = −0.593; p = 0.020) and with the C-peptide/Glucose ratio (Group 1: r_s = −0.740; $p < 0.001$; Group 2: r_s = −0.840; $p < 0.001$; Group 3: r_s = −0.682; p = 0.005). Negative correlations were also observed with the Insulin/Proinsulin ratio (Group 1: r_s = −0.586; p = 0.003; Group 2: r_s = −0.389; p = 0.031). Additionally, in Group 1 a negative correlation with HDL-C was observed (r_s = −0.556; p = 0.005); in Group 2, a positive correlation with proinsulin

(r_s = 0.591; p = 0.001) and a negative correlation with adiponectin (r_s = −0.433; p = 0.012); and in Group 3, positive correlations with proinsulin (r_s = 0.729; p = 0.002), leptin (r_s = 0.720; p = 0.006), and HOMA-IR (r_s = 0.625; p = 0.013), as well as a negative correlation with QUICKI (r_s = −0.625; p = 0.013).

Subgroup Analysis of β-Cell Function Indices in Group 2 According to the Type of Carbohydrate Disturbance

Subgroup analysis within Group 2 demonstrated statistically significant differences with respect to HOMA-B (Kruskal–Wallis H(3) = 12.693; p = 0.013) and the C-peptide/Glucose ratio (Kruskal–Wallis H(3) = 13.306; p = 0.010), whereas no significant differences were observed for the Insulin/Proinsulin and Proinsulin/C-peptide ratios (p > 0.05) (Table 15).

Table 15. β-Cell Function Indices across the individual subgroups of patients with different types of carbohydrate disturbances within Group 2 (T1DM, T2DM, IFG, IGT, and IR).

β-Cell Function Indices	**T1DM (n = 8*)**	**T2DM (n = 11*)**	**IFG (n = 4*)**	**IGT (n = 3*)**	**IR (n = 9*)**	**K.W. Test**
	Mean ± SD Median (IQR)	**Mean ± SD Median (IQR)**	**Mean ± SD Median (IQR)**	**Mean ± SD Median (IQR)**	**Mean ± SD Median (IQR)**	
HOMA-B	62.52 ± 72.68 20.82 (65.03)	112.10 ± 91.7 77.52 (75.61)	214.62 ± 217.39 113.97 (128.83)	450.62 450.62 (0.0)	298.78 ± 199.79 287.21 (156.53)	*p < 0.05*
C-peptide/ Glucose Ratio	0.36 ± 0.26 0.38 (0.40)	1.31 ± 0.54 1.29 (0.41)	2.86 ± 1.88 2.10 (1.45)	0.69 0.69 (0.0)	1.46 ± 1.46 0.84 (1.62)	*p < 0.05*
Insulin/ Proinsulin Ratio	34.79 ± 14.90 34.61 (11.45)	29.05 ± 10.42 30.10 (12.48)	120.51 ± 145.48 55.43 (83.76)	36.35 ± 10.61 36.35 (7.50)	37.05 ± 17.42 39.34 (11.56)	*NS*
Proinsulin/ C-peptide Ratio	6.45 ± 10.7 1.17 (2.74)	1.83 ± 2.74 0.99 (0.83)	0.36 ± 0.25 0.33 (0.19)	3.84 ± 4.91 3.84 (3.47)	3.83 ± 4.52 1.55 (6.26)	*NS*

*NS – no statistically significant difference between the individual subgroups; p < 0.05 – statistically significant difference between the individual subgroups; * n – the number of examined individuals may vary across subgroups due to missing or incomplete laboratory data for some of the analyzed parameters.*

The lowest HOMA-B values and C-peptide/Glucose ratios were observed in individuals with T1DM. In this subgroup, HOMA-B differed significantly from both T2DM (Mann–Whitney U = 54.0; p = 0.007) and IR (Mann–Whitney U = 1.0; p < 0.001).

Regarding the C-peptide/Glucose ratio, individuals with T1DM differed significantly from those with T2DM (Mann–Whitney U = 57.0; p = 0.002) and from the combined IFG + IGT subgroup (Mann–Whitney U = 0.0; p = 0.004).

The highest HOMA-B values were observed in the IGT and IR subgroups, whereas the highest Insulin/Proinsulin ratio values were recorded in IFG, without statistical significance.

The highest Proinsulin/C-peptide ratio values were registered in T1DM, with no statistically significant intergroup differences ($p > 0.05$).

5.3. Surrogate Indices of Insulin Resistance (IR)

Assessment of insulin sensitivity using **HOMA-IR** demonstrated elevated index values in all three main groups. The highest HOMA-IR values were observed in patients with active SARS-CoV-2 infection, while recovered individuals occupied an intermediate position, and COVID-negative individuals with MetS exhibited the lowest median values (Table 16). Intergroup analysis did not demonstrate statistically significant differences, with the result being borderline significant (Kruskal–Wallis H(2) = 7.55; p = 0.0504).

Table 16. Descriptive statistics (Mean ± SD; Median (IQR)) of IR indices in the studied groups

Parameter	Group 1 – Active COVID (n = 32*)	Group 2 – Post-COVID (n = 35*)	Group 3 – COVID(-) with MetS (n = 33*)	Kruskal–Wallis Test
HOMA-IR	8.56 ± 5.59 8.26 (8.96)	7.41 ± 11.37 4.13 (3.58)	8.4 ± 17.67 3.29 (4.44)	*H = 7.55* *p = 0.05*
QUICKI	0.17 ± 0.03 0.16 (0.03)	0.18 ± 0.03 0.18 (0.02)	0.19 ± 0.04 0.19 (0.04)	*H = 7.55* *p = 0.023*

** n – The number of examined individuals may vary between groups due to missing or incomplete laboratory data for some of the analyzed parameters.*

After adjustment for age and sex (GLM, Gamma, log-link), no statistically significant differences were observed between the groups: during active infection ($\beta = -0.499$; $p = 0.102$), in the post-COVID period ($\beta = -0.322$; $p = 0.200$) compared to the MetS reference group, nor in the direct comparison between the two COVID-related groups ($\beta = -0.178$; $p = 0.685$). Intragroup analysis did not reveal statistically significant differences according to sex or diabetes status ($p > 0.05$).

Correlation analysis demonstrated that HOMA-IR correlated positively with insulin in all three groups (Group 1: $r_s = 0.960$; $p < 0.001$; Group 2: $r_s = 0.697$; $p < 0.001$; Group 3: $r_s = 0.969$; $p < 0.001$), as well as with FPG (Group 1: $r_s = 0.367$; $p = 0.042$; Group 2: $r_s = 0.573$; $p < 0.001$;

Group 3: $r_s = 0.707$; $p < 0.001$) and HOMA-B (Group 1: $r_s = 0.657$; $p < 0.001$; Group 2: $r_s = 0.605$; $p = 0.001$).

In individuals with active SARS-CoV-2 infection, an additional positive correlation was observed with the Insulin/Proinsulin ratio ($r_s = 0.712$; $p < 0.001$). In the post-COVID group, a positive association with HIF-1α was also identified ($r_s = 0.415$; $p = 0.023$).

In the MetS reference group, the correlation profile was broader and included additional positive associations with triglycerides ($r_s = 0.400$; $p = 0.048$), proinsulin ($r_s = 0.840$; $p < 0.001$), leptin ($r_s = 0.808$; $p < 0.001$), GLP-1 ($r_s = 0.852$; $p < 0.001$), the Insulin/Proinsulin ratio ($r_s = 0.577$; $p = 0.010$), the Proinsulin/C-peptide ratio ($r_s = 0.625$; $p = 0.013$), TyG index ($r_s = 0.656$; $p = 0.003$), and METS-IR ($r_s = 0.531$; $p = 0.006$), as well as a negative correlation with the Adiponectin/Leptin ratio ($r_s = −0.796$; $p < 0.001$).

The lowest **QUICKI** values were observed in patients with active SARS-CoV-2 infection, followed by recovered individuals, while COVID-negative individuals with MetS demonstrated the highest values (Table 16). Intergroup analysis revealed statistically significant differences (Kruskal–Wallis $H(2) = 7.55$; $p = 0.023$). Post-hoc analysis showed significantly lower values during active infection compared to recovered individuals (Mann–Whitney $U = 317.0$; $p = 0.033$) and compared to COVID-negative individuals with MetS (Mann–Whitney $U = 244.0$; $p = 0.018$), with no difference between Groups 2 and 3 (Mann–Whitney $U = 310.0$; $p = 0.276$).

After adjustment for age and sex (GLM, Gamma, log-link), no statistically significant differences were observed: during active infection ($\beta = −0.053$; $p = 0.219$), in the post-COVID group ($\beta = −0.038$; $p = 0.292$), or in the direct comparison between the two COVID-related groups ($\beta = −0.016$; $p = 0.70$).

No significant intragroup differences were observed according to sex or diabetes status ($p > 0.05$). After stratification by diabetes status, a statistically significant difference was identified only among non-diabetics between Groups 1 and 3 (Mann–Whitney $U = 60.0$; $p = 0.021$), with patients with active infection demonstrating lower values.

Correlation analysis revealed pronounced associations between QUICKI and parameters of the glucose–insulin axis, as well as other IR indices. In all three groups, a strong negative correlation was observed with insulin (Group 1: $r_s = −0.953$; $p < 0.001$; Group 2: $r_s = −0.697$;

$p < 0.001$; Group 3: $r_s = -0.969$; $p < 0.001$), as well as with the Insulin/Proinsulin ratio (Group 1: $r_s = -0.712$; $p < 0.001$; Group 2: $r_s = -0.418$; $p = 0.024$; Group 3: $r_s = -0.577$; $p = 0.010$).

In individuals with active SARS-CoV-2 infection, an additional negative correlation with HOMA-B was observed ($r_s = -0.708$; $p < 0.001$). In the post-COVID group, QUICKI also correlated negatively with HIF-1α ($r_s = -0.415$; $p = 0.023$), FPG ($r_s = -0.573$; $p = 0.001$), and HOMA-B ($r_s = -0.605$; $p = 0.001$). In the MetS reference group, additional negative correlations were observed with BMI ($r_s = -0.576$; $p = 0.003$), TG ($r_s = -0.400$; $p = 0.048$), FPG ($r_s = -0.707$; $p < 0.001$), the Proinsulin/C-peptide ratio ($r_s = -0.625$; $p = 0.013$), leptin ($r_s = -0.809$; $p < 0.001$), GLP-1 ($r_s = -0.853$; $p < 0.001$), TyG index ($r_s = -0.565$; $p = 0.003$), and METS-IR ($r_s = -0.531$; $p = 0.006$), as well as a positive correlation with the Adiponectin/Leptin ratio ($r_s = 0.796$; $p < 0.001$).

Table 17. Descriptive statistics (Mean ± SD; Median (IQR)) of IR indices in the studied groups

Parameter	Group 4 – Active COVID (n = 69)	Group 2 – Post-COVID (n = 35*)	Group 3 – COVID(-) with MetS (n = 33*)	Kruskal–Wallis Test
TyG index	159.33 ± 138.77 135.10 (149.84)	183.14 ± 175.85 113.41 (209.88)	330.09 ± 441.90 223.27 (204.76)	*H = 59.55* *p < 0.001*
TG/HDL-C ratio	0.89 ± 0.81 0.56 (1.00)	1.35 ± 1.26 1.03 (1.19)	0.45 ± 0.69 0.24 (0.29)	*H = 18.42* *p < 0.001*
METS-IR	-	38.67 ± 48.57 33.10 (14.54)	23.33 ± 14.32 24.11 (8.54)	

** n – The number of examined individuals may vary between groups due to missing or incomplete laboratory data for some of the analyzed parameters.*

Analysis of the non–insulin-based **triglyceride–glucose index** (**TyG index**) revealed pronounced intergroup differences (Kruskal–Wallis $H(2) = 59.55$; $p < 0.001$). The highest TyG index values were observed in individuals with active SARS-CoV-2 infection (Group 4), intermediate values in recovered individuals with newly developed carbohydrate disturbances (Group 2), and the lowest in COVID-negative individuals with MetS (Group 3) (Table 17). Post-hoc analysis demonstrated significant differences between Group 4 and Group 3 (Mann–Whitney $U = 604.0$; $p < 0.001$), as well as between Group 4 and Group 2 (Mann–Whitney $U = 677.0$; $p = 0.015$), with no difference between Groups 2 and 3 ($p = 0.176$).

After adjustment for age and sex (GLM, Gamma, log-link), no statistically significant difference was observed between the post-COVID and the MetS reference group ($\beta = 0.038$; $p = 0.193$). During active infection, a borderline increase compared to the reference group was

noted (β = 0.056; p = 0.060). Direct comparison between the active and post-COVID groups did not demonstrate a significant difference (β = 0.018; p = 0.512).

Intragroup analysis by sex revealed higher values in males in Group 2 (Mann–Whitney U = 142.0; p = 0.033) and Group 4 (Mann–Whitney U = 630.0; p = 0.001). With respect to diabetes status, significant differences were observed in Group 2 (Mann–Whitney U = 168.0; p = 0.005) and Group 3 (Mann–Whitney U = 205.0; p = 0.001), whereas no difference was found in Group 4 (p > 0.05).

Correlation analysis demonstrated that the TyG index correlated positively with fasting glucose and TG in all three groups (glucose: Group 2: $r_s = 0.646$; $p < 0.001$; Group 3: $r_s = 0.754$; $p < 0.001$; Group 4: $r_s = 0.604$; $p < 0.001$; TG: Group 2: $r_s = 0.551$; $p = 0.002$; Group 3: $r_s = 0.917$; $p < 0.001$; Group 4: $r_s = 0.756$; $p < 0.001$), and negatively with HDL-C (Group 2: $r_s = -0.596$; $p = 0.002$; Group 3: $r_s = -0.382$; $p = 0.028$; Group 4: $r_s = -0.571$; $p = 0.011$). Additionally, a positive correlation with the TG/HDL-C ratio was observed in Groups 2 and 3 (Group 2: $r_s = 0.849$; $p < 0.001$; Group 3: $r_s = 0.754$; $p < 0.001$).

In the post-COVID group (Group 2), the TyG index demonstrated the broadest correlation profile, including positive associations with IL-10 ($r_s = 0.481$; $p = 0.008$), IL-17A ($r_s = 0.384$; $p = 0.048$), HCF-D ($r_s = 0.387$; $p = 0.038$), age ($r_s = 0.361$; $p = 0.039$), BMI ($r_s = 0.409$; $p = 0.018$), HbA1c ($r_s = 0.528$; $p = 0.012$), HOMA-IR ($r_s = 0.565$; $p = 0.003$), and METS-IR ($r_s = 0.570$; $p = 0.001$), as well as negative correlations with HOMA-B ($r_s = -0.536$; $p = 0.005$) and QUICKI ($r_s = -0.565$; $p = 0.003$), and a positive association with the Insulin/Proinsulin ratio ($r_s = 0.544$; $p = 0.016$).

In the MetS reference group (Group 3), additional positive correlations were observed with IL-10 ($r_s = 0.346$; $p = 0.041$), HIF-1α ($r_s = 0.489$; $p = 0.005$), and insulin ($r_s = 0.476$; $p = 0.016$). In the active infection group (Group 4), the correlation model was limited to classical lipid–glycemic parameters.

The **TG/HDL-C ratio** also demonstrated a pronounced phase-dependent pattern. The highest values were observed in individuals with active SARS-CoV-2 infection (Group 4), intermediate values in COVID-negative individuals with MetS (Group 3), and the lowest in recovered individuals with newly developed carbohydrate disturbances (Group 2) (Table 17). Intergroup analysis revealed statistically significant differences (Kruskal–Wallis H(2) = 18.42; p < 0.001). Post-hoc analysis demonstrated significant differences between Group 2 and Group 3 (Mann–Whitney U = 284.0; p = 0.01), between Group 2 and Group 4 (Mann–Whitney U =

122.0; p = 0.002), as well as between Group 3 and Group 4 (Mann–Whitney U = 187.0; p = 0.0017).

After adjustment for age and sex (GLM, Gamma, log-link), no statistically significant difference was observed between Group 2 and Group 3 (β = −0.326; p = 0.213), nor between Group 4 and Group 3 (β = 0.360; p = 0.286). Direct comparison between the active and post-COVID groups demonstrated a significantly higher TG/HDL-C ratio during active infection (β = 0.686; e^{β} = 1.99; 95% CI: 1.03–3.84; p = 0.041).

Intragroup comparison by sex revealed a significant difference only in Group 4 (Mann–Whitney U = 66.0; p < 0.001). According to diabetes status, a significant difference was observed in Group 3 (Mann–Whitney U = 191.0; p = 0.007). Additionally, a significant difference was found between diabetics in Group 2 and Group 3 (Mann–Whitney U = 28.0; p = 0.0127). Among non-diabetic individuals, significant differences were observed between Group 2 and Group 4 (Mann–Whitney U = 28.0; p = 0.006) and between Group 3 and Group 4 (Mann–Whitney U = 61.0; p = 0.003).

Correlation analysis demonstrated consistent associations between the TG/HDL-C ratio and classical lipid parameters across all groups, including strong positive correlations with TG (Group 2: r_s = 0.867; p < 0.001; Group 3: r_s = 0.888; p < 0.001; Group 4: r_s = 0.799; p < 0.001) and negative correlations with HDL-C (Group 2: r_s = −0.862; p < 0.001; Group 3: r_s = −0.691; p < 0.001; Group 4: r_s = −0.826; p < 0.001). Additionally, positive correlations with the TyG index were observed in all groups (Group 2: r_s = 0.551; p = 0.002; Group 3: r_s = 0.849; p < 0.001; Group 4: r_s = 0.754; p < 0.001). In Groups 2 and 3, positive correlations were also observed with IL-10 (Group 2: r_s = 0.435; p = 0.021; Group 3: r_s = 0.404; p = 0.016) and HIF-1α (Group 2: r_s = 0.863; p < 0.001; Group 3: r_s = 0.453; p = 0.011).

Specifically in Group 2, additional correlations were observed with IFN-γ (r_s = 0.411; p = 0.037), age (r_s = −0.433; p = 0.021), C-peptide (r_s = −0.505; p = 0.010), proinsulin (r_s = 0.394; p = 0.042), adiponectin (r_s = −0.450; p = 0.018), the Proinsulin/C-peptide ratio (r_s = 0.547; p = 0.006), and METS-IR (r_s = 0.456; p = 0.015), while in Group 4 an additional correlation was found with LDL-C (r_s = 0.567; p = 0.031).

The **METS-IR** index, calculated in recovered and COVID-negative individuals, demonstrated higher mean values in the MetS reference group compared to recovered COVID-19 patients (Table 17), without reaching statistical significance (Mann–Whitney U = 351.0; p = 0.110).

After adjustment for age and sex using GLM (Gamma, log-link), no significant difference between the groups was observed ($\beta = -0.108$; $p = 0.182$).

Significant sex-based differences were observed only in Group 3, where males demonstrated higher values than females (Mann–Whitney U = 79.0; $p = 0.03$). No statistically significant differences were found according to diabetes status in any of the groups ($p > 0.05$).

Correlation analysis demonstrated that in both groups METS-IR correlated positively with HIF-1α (Group 2: $r_s = 0.669$; $p < 0.001$; Group 3: $r_s = 0.490$; $p = 0.005$) and the TG/HDL-C ratio (Group 2: $r_s = 0.457$; $p = 0.015$; Group 3: $r_s = 0.554$; $p = 0.001$). In Group 2, additional positive correlations were observed with IL-7 ($r_s = 0.425$; $p = 0.030$), IL-10 ($r_s = 0.437$; $p = 0.020$), BMI ($r_s = 0.781$; $p < 0.001$), ASAT ($r_s = 0.563$; $p = 0.005$), ALAT ($r_s = 0.637$; $p = 0.001$), uric acid ($r_s = 0.612$; $p = 0.002$), and a negative correlation with HDL-C ($r_s = -0.384$; $p = 0.044$). In Group 3, METS-IR correlated with BMI ($r_s = 0.941$; $p < 0.001$), FPG ($r_s = 0.537$; $p = 0.001$), TG ($r_s = 0.459$; $p = 0.007$), HDL-C ($r_s = -0.515$; $p = 0.002$), insulin ($r_s = 0.500$; $p = 0.011$), leptin ($r_s = 0.563$; $p = 0.012$), HOMA-IR ($r_s = 0.531$; $p = 0.006$), QUICKI ($r_s = -0.531$; $p = 0.006$), and the TyG index ($r_s = 0.569$; $p = 0.001$).

Indices for Assessment of IR in the Subgroups of Group 2

Subgroup analysis within Group 2 revealed differences in the degree of IR depending on the type of newly developed carbohydrate disturbance (Table 18).

For HOMA-IR, a statistically significant difference was observed between the isolated IR subgroup and the combined prediabetes subgroup (IFG + IGT) (Mann–Whitney U = 0.0; $p = 0.0015$), with the highest values observed in individuals with IFG, IGT, and T1DM. No statistically significant differences were found for QUICKI between the subgroups (Kruskal–Wallis $H(3) = 6.84$; $p = 0.145$).

Regarding the TyG index, significant intergroup differences were observed (Kruskal–Wallis $H(3) = 22.13$; $p = 0.0047$), with the T1DM subgroup demonstrating higher values compared to individuals with isolated IR (Mann–Whitney U = 63.0; $p = 0.008$). No statistically significant differences were found between subgroups for the TG/HDL-C ratio (Kruskal–Wallis $H(3) = 5.9039$; $p > 0.05$). Similarly, METS-IR did not demonstrate significant differences across subgroups (Kruskal–Wallis $H(3) = 6.7381$; $p > 0.05$).

In summary, statistically significant differences between subgroups were identified for HOMA-IR and the TyG index, whereas the remaining indices did not demonstrate significant stratification according to the type of carbohydrate disturbance.

Table 18. Indices for Assessment of IR in the Subgroups of Group 2 (T1DM, T2DM, IFG, IGT, and IR)

Parameter	**T1DM (n = 8*)**	**T2DM (n = 11*)**	**IFG (n = 4*)**	**IGT (n = 3*)**	**IR (n = 9*)**	**K.W. Test**
	Mean ± SD Median (IQR)	**Mean ± SD Median (IQR)**	**Mean ± SD Median (IQR)**	**Mean ± SD Median (IQR)**	**Mean ± SD Median (IQR)**	
HOMA-IR	4.99 ± 3.6 4.94 (3.89)	6.41 ± 6.23 3.81 (4.86)	8.3 ± 7.16 4.86 (3.97)	5.24 5.24 (0.0)	3.08 ± 0.82 3.36 (0.75)	*NS**
QUICKI	0.13 ± 0.01 0.13 (0.01)	0.13 ± 0.01 0.14 (0.02)	0.13 ± 0.01 0.13 (0.01)	0.13 0.13 (0.0)	0.14 ± 0.01 0.14 (0.0)	*NS*
TyG index	5.18 ± 0.81 4.92 (1.1)	4.7 ± 0.26 4.65 (0.37)	4.59 ± 0.6 4.32 (0.55)	4.5 4.5 (0.0)	4.27 ± 0.36 4.20 (0.50)	*$p < 0.05$*
TG/HDL-C Ratio	2.62 ± 2.55 1.21 (2.69)	1.87 ± 0.75 1.60 (0.82)	0.67 ± 0.13 0.67 (0.09)	2.29 2.29 (0.0)	2.35 ± 1.40 1.87 (0.91)	*NS*
METS-IR	52.94 ± 29.35 43.25 (6.75)	59.69 ± 11.22 61.19 (15.16)	42.5 ± 1.56 42.5 (1.1)	55.62 55.62 (0.0)	56.16 ± 14.10 58.53 (19.76)	*NS*

NS – no statistically significant difference between subgroups; $p < 0.05$ – statistically significant difference between subgroups; * Post-hoc analysis identified a statistically significant difference between the isolated IR subgroup and the combined prediabetes subgroup (IFG + IGT) (Mann–Whitney U = 0.0; p = 0.0015).

6. Molecules Evaluation of the Role of Adipocytokines and Other Hormonally Active Molecules in the Genesis of COVID-19–Associated Dysglycemia

6.1. Other Hormonally Active Molecules

Table 19. Descriptive statistics (Mean ± SD; Median (IQR)) and intergroup comparisons of serum levels of GLP-1 [pg/mL] and GP-73 [ng/mL]

Parameter	**Group 1 – Active COVID (n = 32*)**	**Group 2 – Post-COVID (n = 35*)**	**Group 3 – COVID(-) with MetS (n = 33*)**	**Kruskal–Wallis Test**
GLP-1	186.71 ± 100.65 194.71 (195.01)	-	145.14 ± 142.56 109.46 (115.69)	-
GP-73	20.78 ± 9.70 19.80 (15.75)	42.39 ± 20.34 44.66 (32.64)	48.91 ± 26.15 42.47 (23.21)	*$H = 28.38$ $p < 0.001$*

** n – The number of examined individuals may vary between groups due to missing or incomplete laboratory data for some of the analyzed parameters.*

GLP-1. When comparing serum GLP-1 levels between patients with active SARS-CoV-2 infection (Group 1) and COVID-negative individuals with MetS (Group 3), no statistically significant difference was observed (Mann–Whitney U = 343.0; p = 0.055), despite a tendency toward higher values during active infection (Table 19).

After adjustment for age and sex using GLM (Gamma, log-link), the difference remained statistically non-significant (β = 0.327; p = 0.376). Intragroup analysis according to sex and diabetes status did not reveal statistically significant differences (p > 0.05).

Correlation analysis demonstrated strong positive associations between GLP-1 and proinsulin both during active infection (r_s = 0.846; p < 0.001) and in individuals with MetS (r_s = 0.886; p < 0.001), as well as positive correlations with leptin in both groups (Group 1: r_s = 0.522; p = 0.005; Group 3: r_s = 0.637; p = 0.003). A negative correlation was observed with the Adiponectin/Leptin ratio (Group 1: r_s = −0.466; p = 0.019; Group 3: r_s = −0.757; p = 0.001). In individuals with MetS, GLP-1 additionally correlated positively with FPG (r_s = 0.570; p = 0.011), insulin (r_s = 0.794; p = 0.001), HOMA-IR (r_s = 0.853; p < 0.001), and negatively with QUICKI (r_s = −0.853; p < 0.001).

Golgi protein – 73 (GP-73). Serum GP-73 levels differed significantly among the three studied groups (Kruskal–Wallis H(2) = 28.38; p < 0.001). The lowest values were observed in individuals with active SARS-CoV-2 infection (Group 1), whereas recovered individuals with newly developed carbohydrate disturbances (Group 2) and COVID-negative individuals with MetS (Group 3) demonstrated significantly higher and comparable levels (Table 19). Post-hoc analysis revealed significantly lower values during active infection compared to both the post-COVID group (Mann–Whitney U = 160.5; p < 0.001) and the MetS reference group (Mann–Whitney U = 45.0; p < 0.001), with no significant difference between Groups 2 and 3 (p = 0.537).

Regression analysis (GLM, Gamma, log-link), adjusted for age and sex, confirmed these findings. During active infection, a 57% reduction in GP-73 levels was observed compared to the reference group (β = −0.84; e^{β} = 0.43; 95% CI: 0.20–0.93; p = 0.032), whereas no significant difference was detected between recovered individuals and the reference group (β = −0.11; p = 0.596). Direct comparison between active and post-COVID phases demonstrated 52% lower GP-73 levels during active infection (β = −0.73; e^{β} = 0.48; 95% CI: 0.28–0.82; p = 0.008).

Intragroup analysis by sex and diabetes status did not reveal statistically significant differences ($p > 0.05$). However, stratification by diabetes status demonstrated significant differences in GP-73 levels. Among diabetic individuals, the highest values were observed in Group 3, being significantly higher compared to Group 1 (Mann–Whitney U = 0.0; $p < 0.001$) and Group 2 (Mann–Whitney U = 55.0; $p = 0.004$). Among non-diabetic individuals, the lowest values were observed in Group 1, differing significantly from both Group 2 (Mann–Whitney U = 29.0; $p = 0.002$) and Group 3 (Mann–Whitney U = 18.0; $p = 0.001$).

Within the subgroups of Group 2 (T1DM, T2DM, IFG, IGT, and isolated IR), no significant differences were observed (Kruskal–Wallis H(3) = 4.7881; $p = 0.310$), despite a tendency toward higher values in T1DM (Fig. 17).

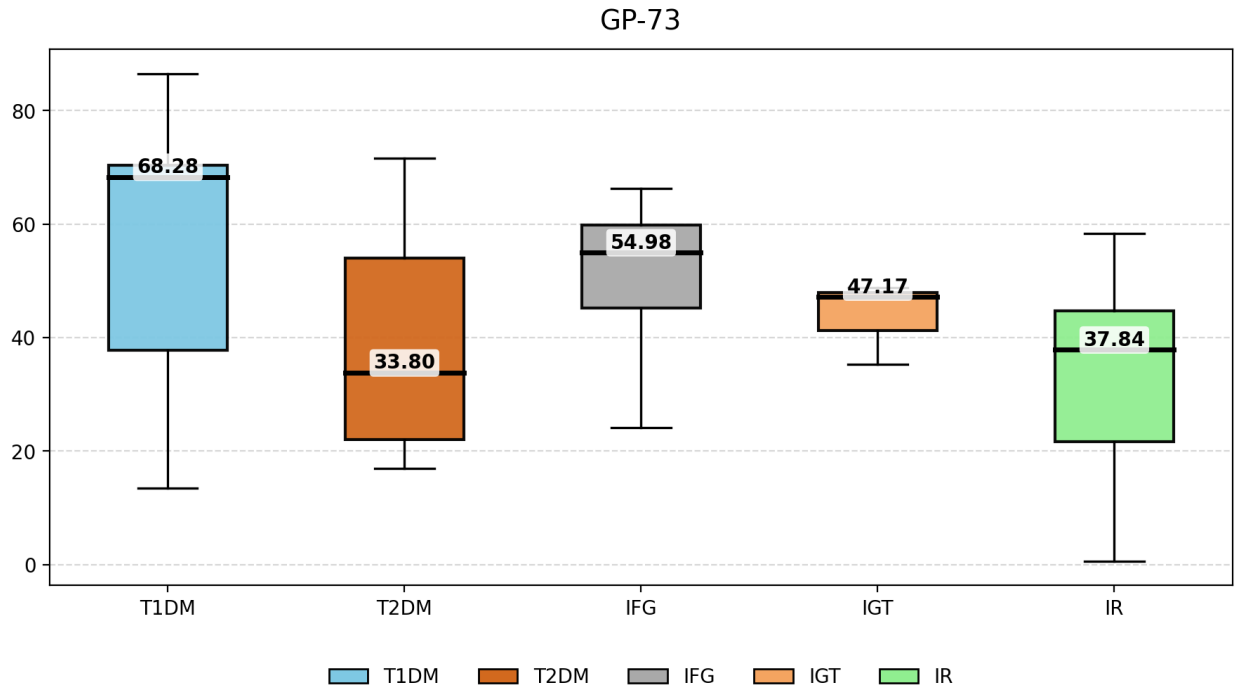

Figure 17. Distribution (Median; IQR) of serum GP-73 levels in the subgroups of Group 2 – T1DM/LADA, T2DM, IFG, IGT, and IR.

Correlation analysis revealed group-specific associations: During active infection, GP-73 correlated positively with IL-10 ($r_s = 0.512$; $p = 0.004$). In recovered individuals with newly developed carbohydrate disturbances, GP-73 correlated negatively with IL-7 ($r_s = -0.398$; $p = 0.032$) and IFN-γ ($r_s = -0.623$; $p = 0.001$). In individuals with MetS, GP-73 correlated positively with IFN-γ ($r_s = 0.499$; $p = 0.006$), HIF-1α ($r_s = 0.514$; $p = 0.024$), and glucagon ($r_s = 0.599$; $p = 0.011$).

6.2. Adipocytokines and Adipokine Balance

Leptin. Serum leptin levels were elevated in all three studied groups, with the lowest levels observed in individuals with active SARS-CoV-2 infection (Group 1), intermediate levels in recovered individuals with newly developed carbohydrate disturbances (Group 2), and the highest levels in COVID-negative individuals with MetS (Group 3) (Table 20).

Table 20. Descriptive statistics (Mean ± SD; Median (IQR)) and intergroup comparisons of serum levels of Leptin [pg/mL], Adiponectin [μU/mL], and the Adiponectin/Leptin ratio

Parameter	Group 1 – Active COVID (n = 32*)	Group 2 – Post-COVID (n = 35*)	Group 3 – COVID(-) with MetS (n = 33*)	Kruskal–Wallis Test
Leptin	20.25 ± 26.30 8.09 (31.18)	32.14 ± 25.69 22.81 (38.32)	52.02 ± 34.59 43.86 (70.39)	*H = 15.75* *p < 0.001*
Adiponectin	23.53 ± 3.92 25.90 (4.58)	25.03 ± 1.84 25.72 (1.67)	25.87 ± 0.60 25.94 (0.75)	*H = 4.07* *p = 0.131*
Adiponectin/ Leptin ratio	5.81 ± 8.35 2.42 (7.66)	2.24 ± 3.69 1.13 (1.91)	0.89 ± 0.79 0.60 (1.24)	*H = 10.48* *p = 0.005*

** n – The number of examined individuals may vary between groups due to missing or incomplete laboratory data for some of the analyzed parameters.*

Intergroup analysis revealed statistically significant differences (Kruskal–Wallis H(2) = 15.746; $p < 0.001$). Post-hoc analysis demonstrated significant differences between Group 1 and Group 2 (Mann–Whitney U = 281.0; $p = 0.010$), as well as between Group 1 and Group 3 (Mann–Whitney U = 93.5; $p < 0.001$), with no significant difference between Groups 2 and 3 ($p > 0.05$).

GLM analysis (Gamma, log-link), adjusted for age and sex, did not demonstrate a statistically significant difference between active infection and MetS ($\beta = -0.76$; $p = 0.071$), nor between post-COVID and MetS ($\beta = -0.17$; $p = 0.596$). Direct comparison between the active and post-COVID groups showed a tendency toward lower levels during active infection ($\beta = -0.60$; $p = 0.091$), without reaching statistical significance.

After stratification by diabetes status, the lowest leptin levels were observed in non-diabetic individuals with active infection, who differed significantly from non-diabetics in Group 2 (Mann–Whitney U = 39.0; $p = 0.014$) and Group 3 (Mann–Whitney U = 19.0; $p = 0.001$). Among individuals with diabetes, no statistically significant differences were observed between groups ($p > 0.05$).

Subgroup analysis within Group 2 (Fig. 18) demonstrated the highest median leptin levels in individuals with T2DM and in those with normoglycemia and IR, and the lowest in individuals

with T1DM, without reaching statistical significance between subgroups (Kruskal–Wallis H(3) = 4.9016; p = 0.297).

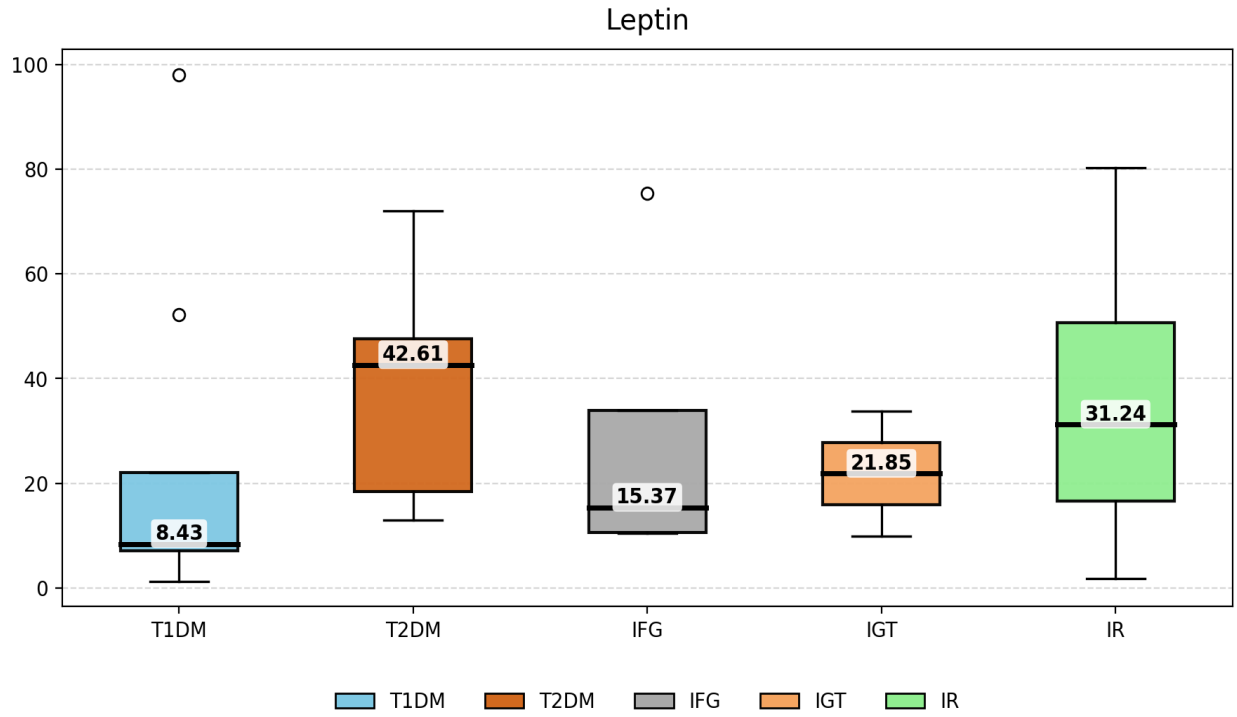

Figure 18. Distribution (Median; IQR) of serum leptin levels in the subgroups of Group 2 – T1DM/LADA, T2DM, IFG, IGT, and IR.

Correlation analysis demonstrated a positive association between leptin and BMI in Group 1 (r_s = 0.401; p = 0.021) and Group 2 (r_s = 0.680; p = 0.001). In Group 3, leptin correlated positively with FPG (r_s = 0.512; p = 0.025), insulin (r_s = 0.745; p = 0.001), HOMA-IR (r_s = 0.809; p < 0.001), and METS-IR (r_s = 0.563; p = 0.012), and negatively with QUICKI (r_s = −0.809; p < 0.001). In Groups 1 and 3, positive correlations were observed with proinsulin (Group 1: r_s = 0.626; p = 0.001; Group 3: r_s = 0.670; p = 0.002) and GLP-1 (Group 1: r_s = 0.522; p = 0.005; Group 3: r_s = 0.637; p = 0.003). In all three groups, a strong negative correlation was observed with the Adiponectin/Leptin ratio (Group 1: r_s = −0.985; p < 0.001; Group 2: r_s = −0.996; p < 0.001; Group 3: r_s = −0.837; p < 0.001).

Adiponectin. Serum adiponectin levels were within the reference range and did not differ significantly between the studied groups (Kruskal–Wallis H(2) = 4.065; p = 0.131) (Table 20). GLM analysis (Gamma, log-link), adjusted for age and sex, likewise did not demonstrate significant differences: active COVID vs MetS (β = −0.08; p = 0.090), post-COVID vs MetS (β = −0.01; p = 0.720), and active COVID vs post-COVID (β = −0.06; p = 0.086).

Intragroup analysis by sex also revealed no statistically significant differences ($p > 0.05$). After stratification by diabetes status, a significant difference was observed only in the MetS group, with lower adiponectin levels in diabetic compared to non-diabetic individuals (Mann–Whitney U = 14.0; $p = 0.020$). When comparing corresponding subgroups across groups, the only significant difference was found between non-diabetic individuals with active infection and non-diabetic individuals with MetS (Mann–Whitney U = 33.0; $p = 0.009$).

Subgroup analysis within the post-COVID group (Group 2) did not reveal significant differences according to the type of carbohydrate disturbance (Kruskal–Wallis H(2) = 3.3006; $p = 0.509$) (Fig. 19).

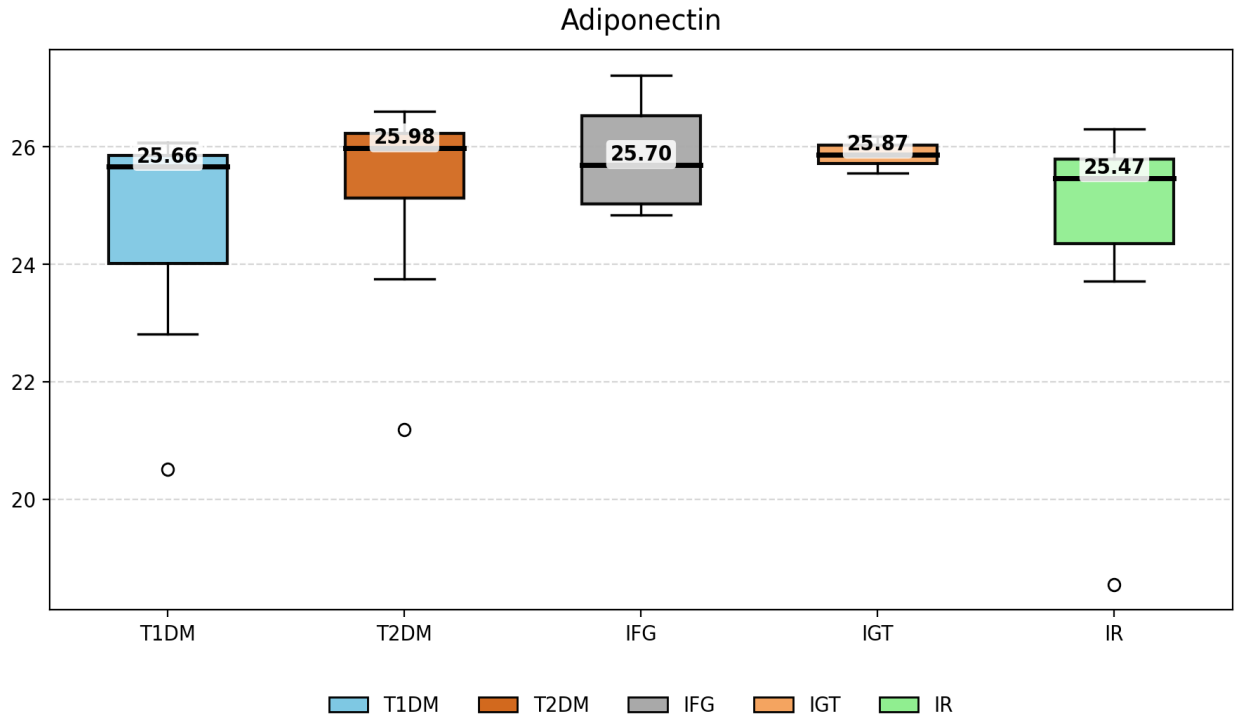

Figure 19. Distribution (Median; IQR) of serum adiponectin levels in the subgroups of Group 2 – T1DM/LADA, T2DM, IFG, IGT, and IR.

Correlation analysis demonstrated that in Group 2 adiponectin levels showed positive correlations with HDL-C ($r_s = 0.483$; $p = 0.011$) and glucagon ($r_s = 0.398$; $p = 0.020$), and a negative correlation with the Proinsulin/C-peptide ratio ($r_s = −0.443$; $p = 0.012$). In Group 3, adiponectin correlated negatively with HIF-1α ($r_s = −0.460$; $p = 0.041$), C-peptide ($r_s = −0.604$; $p = 0.008$), and the C-peptide/Glucose ratio ($r_s = −0.548$; $p = 0.019$).

Adiponectin/Leptin Ratio. The Adiponectin/Leptin ratio demonstrated the highest values during active COVID, intermediate values in the post-COVID group, and the lowest in the MetS reference group (Table 20).

Intergroup analysis revealed statistically significant differences (Kruskal–Wallis H(2) = 10.475; p = 0.005). Pairwise comparisons showed a significant difference only between Groups 1 and 3 (Mann–Whitney U = 330.0; p = 0.003), with no significant differences between Groups 1 and 2 or between Groups 2 and 3 (p > 0.05).

After adjustment for age and sex (GLM; Gamma, log-link), the ratio remained significantly higher both during active infection (β = 1.24; e^{β} = 3.47; 95% CI: 1.57–7.67; p = 0.002) and in the post-COVID group compared to the MetS reference group (β = 0.69; e^{β} = 1.99; 95% CI: 1.20–3.30; p = 0.008), with no significant difference between active and post-COVID phases (β = 0.56; p = 0.209). Female sex was an independent predictor of a lower ratio (β = −1.40; e^{β} = 0.25; 95% CI: 0.13–0.48; p < 0.001), whereas age did not show an independent association.

Regarding COVID-19 severity in Group 1, no statistically significant differences in the Adiponectin/Leptin ratio were observed across the four severity grades (Kruskal–Wallis H(3) = 6.03; p = 0.110). However, additional analysis demonstrated that patients with severe infection (n = 16, 50%) exhibited significantly higher ratio values compared to all other severity categories combined (Mann–Whitney U = 111.0; p = 0.029).

Intragroup comparisons by sex and diabetes status in Group 1 did not reveal significant differences (p > 0.05). In Group 2, however, males demonstrated significantly higher values compared to females (Mann–Whitney U = 42.0; p = 0.029), with no significant differences according to diabetes status (p > 0.05).

The subgroup profile within Group 2 showed the highest median values in T1DM and the lowest in T2DM, while the IFG, IGT, and IR/hyperinsulinemia subgroups demonstrated similar and overlapping distributions (Fig. 20).

Correlation analysis demonstrated a very strong negative correlation with serum leptin in all three groups (Group 1: r_s = −0.985; p < 0.001; Group 2: r_s = −0.996; p < 0.001; Group 3: r_s = −0.837; p < 0.001). In Group 1, the Adiponectin/Leptin ratio correlated negatively with proinsulin (r_s = −0.601; p = 0.002) and GLP-1 (r_s = −0.466; p = 0.012).

In Group 2, a negative correlation with BMI (r_s = −0.434; p = 0.012) and a positive correlation with HbA1c (r_s = 0.473; p = 0.026) were observed.

In Group 3, the ratio correlated negatively with BMI ($r_s = -0.709$; $p = 0.026$), FPG ($r_s = -0.549$; $p = 0.022$), insulin ($r_s = -0.739$; $p = 0.002$), proinsulin ($r_s = -0.806$; $p < 0.001$), HOMA-IR ($r_s = -0.796$; $p < 0.001$), the Proinsulin/C-peptide ratio ($r_s = -0.650$; $p = 0.022$), and METS-IR ($r_s = -0.596$; $p = 0.012$), and positively with QUICKI ($r_s = 0.796$; $p < 0.001$).

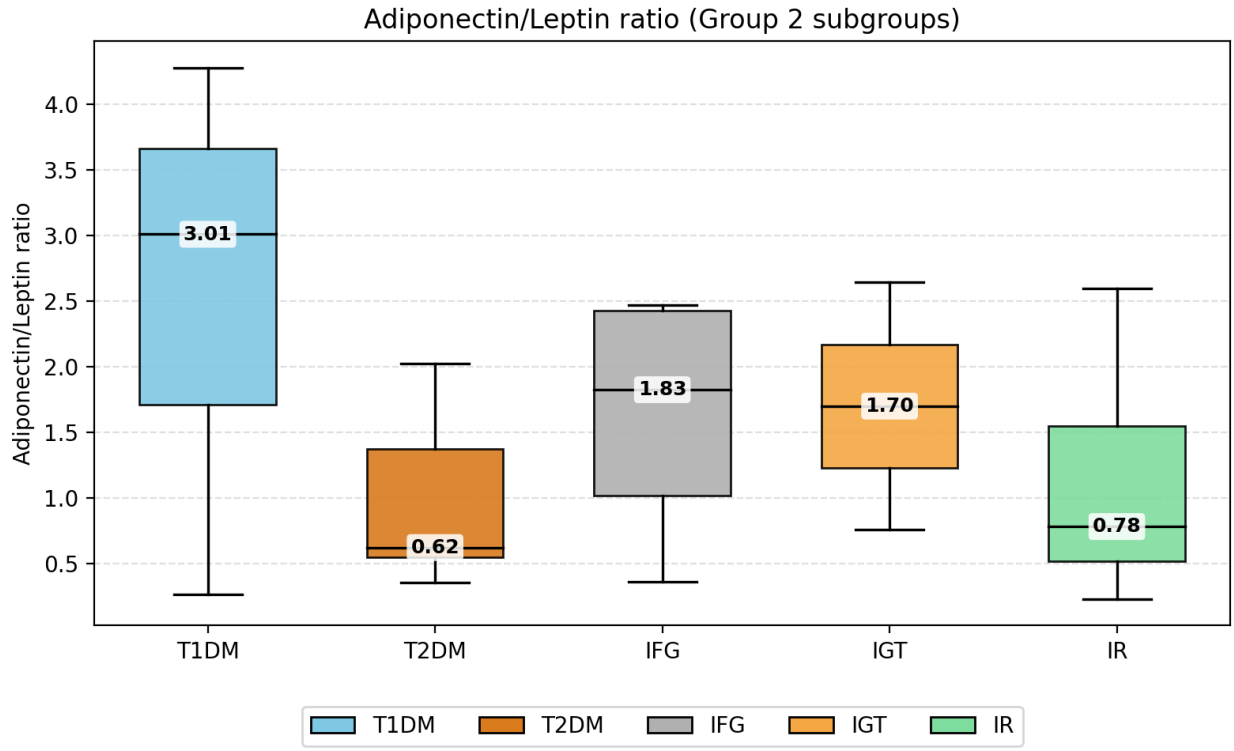

Figure 20. Distribution (Median; IQR) of the serum Adiponectin/Leptin ratio in the subgroups of Group 2 – T1DM/LADA, T2DM, IFG, IGT, and IR.

7. Analysis of the Risk Effect of the Investigated Parameters on the Probability of Developing DM in the Context of COVID-19 (ROC Analysis)

The ROC analysis identified a complex profile of non-modifiable, clinical, biochemical, and immunological parameters associated with an increased risk of developing DM in the context of SARS-CoV-2 infection—both during the active phase of the disease and in the post-COVID period (Table 21).

Parameters demonstrating excellent diagnostic performance (AUC > 0.80) included HCF-D (AUC = 0.868), IL-7 (AUC = 0.824), and fasting plasma glucose (AUC = 0.814).

Parameters with good discriminative ability (AUC 0.70–0.80) were IFN-γ (0.768), leptin (0.767), C-peptide (0.750), the Adiponectin/Leptin ratio (0.748), HOMA-IR (0.706), and CD4 (0.701), as well as 8-epi-PGF2α (0.788) and glucagon (0.797, borderline toward excellent performance).

Table 21. Summary Results of the ROC Analysis for Determination of Threshold (Cut-off) Values Associated with Increased Risk of Developing Diabetes Mellitus in the Context of SARS-CoV-2 Exposure

Parameter	Cut-off value	AUC (95% CI)	p - value	Se (%)	Sp (%)	PPV (%)	NPV (%)
Age [years]	≥ 54.5	0.625 (0.516 –0.735)	0.043	53.8	75.8	81.4	45.9
IL-7 [ng/mL]	≤ 39.905	0.824 (0.724 – 0.925)	<0.001	80.0	71.9	72.7	79.3
IL-17A [ng/mL]	≤ 26.624	0.695 (0.565 –0.826)	0.008	46.7	84.4	73.7	62.8
IFN-γ [ng/mL]	≤ 7.293	0.768 (0.653 –0.884)	<0.001	45.2	100.0	100.0	65.3
TNF-α [ng/mL]	≥ 57.25	0.662 (0.529 –0.796)	0.027	45.2	100.0	100.0	65.3
CD4 [ng/mL]	≥ 10.452	0.701 (0.573 –0.829)	0.006	36.7	93.9	84.6	62.0
CD8 [ng/mL]	≤ 21.437	0.630 (0.502 –0.759)	0.040	62.3	62.5	60.6	64.2
HCF-D [ng/mL]	≤ 1436.79	0.868 (0.777 –0.960)	<0.001	66.7	96.7	95.5	74.4
HIF-1α (pg/mL)]	≥ 200.36	0.646 (0.510 –0.782)	0.048	83.9	38.7	98.0	44.9
8-epi- PGF2α [pg/mL]	≤ 58.523	0.788 (0.639 –0.937)	0.003	57.9	94.1	91.7	66.7
Plasma Glucose [mmol/L]	≥ 5.85	0.814 (0.702 –0.926)	<0.001	83.3	75.8	75.8	83.3
C-peptide [ng/mL]	≥ 0.4685	0.750 (0.614 –0.886)	0.002	71.0	80.0	80.0	69.0
Glucagon [pg/mL]	≤ 6802.55	0.797 (0.669 –0.925)	<0.001	75.0	85.7	87.5	72.0
GP-73 [ng/mL]	≤ 37.434	0.672 (0.521 –0.823)	0.044	66.7	73.7	80.0	58.3
Leptin [ng/mL]	≤ 10.283	0.767 (0.636 –0.897)	0.002	46.7	100.0	100.0	54.3
HOMA-IR	≥ 3.324	0.706 (0.561 – 0.851)	0.010	85.7	52.0	66.7	76.5
HOMA-B	≤ 149.69	0.304 (0.160 –0.448)	0.015	63.0	76.0	73.9	65.5
C-peptide /Glucose ratio	≥ 0.0985	0.670 (0.520 –0.820)	0.034	57.1	84.0	80.0	63.6
Adiponectin/ Leptin ratio	≥ 0.722	0.748 (0.606 –0.890)	0.005	72.7	70.6	80.8	60.0

determined threshold (cut-off) value; Se – sensitivity; Sp – specificity; PPV – positive predictive value; NPV – negative predictive value.

Parameters showing moderate or borderline discrimination (AUC 0.60–0.70) included age (0.625), CD8 (0.630), HIF-1α (0.646), TNF-α (0.662), GP-73 (0.672), the C-peptide/Glucose ratio (0.670), and IL-17A (0.695), indicating a more limited independent predictive capacity.

Only HOMA-B demonstrated discrimination below the level of random classification (AUC < 0.50; AUC = 0.304). This low value reflects an inverse direction of association—lower HOMA-B values are associated with a higher risk. Upon inversion of direction, the index would demonstrate good discriminative capacity; therefore, an AUC < 0.50 does not indicate lack of clinical relevance, but rather an inverse association with the outcome.

8. Assessment of Quality of Life in Individuals Recovered from COVID-19 Using a Validated Questionnaire (SF-36)

Among participants in Group 2 (n = 35), the results of the survey conducted using the standardized SF-36 questionnaire demonstrate substantial impairment in quality of life across the physical, emotional, and social domains.

Nearly half of the participants rated their overall health as good, whereas approximately one third reported a deterioration in health status compared to the period prior to the infection.

Mild to moderate limitations in daily activities were frequently reported, with severe physical limitations observed in 20–42% of individuals, predominantly in activities requiring greater physical exertion.

Limitations in work capacity and usual activities were reported by approximately 60% of respondents, and around 70% indicated a negative impact of emotional status on daily functioning.

Data regarding psycho-emotional status reveal a high prevalence of fatigue and depressive symptoms—approximately 20% reported persistent fatigue, more than 50% reported depressive experiences, and 62% self-assessed as exhausted for a substantial portion of the time.

Social interactions were moderately or markedly limited in approximately 35–40% of individuals. Only 40% described themselves as happy, and merely 8.5% rated their health as excellent.

DISCUSSION

1. General Clinical and Metabolic Characteristics of the Studied Population

1.1. General Clinical Characteristics

The higher mean age among individuals with active SARS-CoV-2 infection is consistent with published data indicating that advanced age is an independent risk factor for severe disease course and hospitalization in COVID-19 [343]. The similar age profile between individuals recovered from COVID-19 with newly developed carbohydrate metabolism disorders and the reference group with MetS minimizes the likelihood of age acting as a confounding factor in the analysis of post-COVID metabolic alterations.

The predominance of female participants in most groups likely reflects the generally higher participation of women in clinical studies, whereas the relatively higher proportion of males in the active infection group aligns with data indicating a more severe clinical course of COVID-19 in men. The increased prevalence of a family history of DM among recovered individuals and those with MetS supports the presence of pre-existing metabolic risk, upon which SARS-CoV-2 infection may act as a triggering or modifying factor.

1.2. Metabolic Characteristics of the Studied Population

The obtained results are consistent with the established role of obesity and metabolic imbalance in the development of carbohydrate metabolism disorders during both the active and post-COVID phases of SARS-CoV-2 infection. The observed differences between the study groups delineate distinct metabolic profiles across the various phases of infection.

The higher prevalence of obesity, particularly morbid obesity, among non-infected individuals with MetS (Group 3) reflects the well-established pathophysiological model of chronic IR associated with a pronounced adiposity-driven inflammatory background. This is consistent with evidence that advanced obesity represents a central determinant of MetS and progression to T2DM [14].

In contrast, among individuals recovered from COVID-19 with newly developed carbohydrate metabolism disorders (Group 2), a lower mean BMI and a smaller proportion of morbid obesity were observed. These findings support the hypothesis that, in this population, SARS-CoV-2 infection may act as a trigger for the manifestation of glucose abnormalities in the presence of subclinical metabolic vulnerability. The substantial presence of newly developed T1DM

(including LADA) in this group raises the hypothesis of possible involvement of virus-induced autoimmune and inflammatory mechanisms described in COVID-19 [35, 197].

The absence of a statistically significant difference in mean BMI between Groups 2 and 3 underscores the limited diagnostic value of BMI as an isolated marker of metabolic risk and supports the need for a comprehensive assessment incorporating hormonal, inflammatory, and functional parameters. In this context, the significantly higher BMI among diabetic individuals in Group 3 compared with those in Group 2 may reflect differences in the duration and mechanism of β-cell dysfunction—chronic in MetS versus potentially more acute and inflammation-mediated in post-COVID conditions.

Among patients with active SARS-CoV-2 infection (Groups 1 and 4), the high prevalence of DM, including a considerable proportion of newly diagnosed cases during hospitalization, supports the concept of acute infection-induced disruption of glucose homeostasis. These observations are consistent with data indicating that SARS-CoV-2 may induce transient or persistent hyperglycemia through the combined effects of systemic inflammation, hypoxia, cytokine-mediated IR, and direct β-cell injury [197, 343].

The lipid profile further reflects the dynamics of metabolic dysregulation. The most pronounced lipid abnormalities were observed in individuals with active infection (Group 4), characterized by marked hypertriglyceridemia and significantly reduced HDL-C levels. This profile corresponds to the virus-induced dyslipidemia described in COVID-19, which is associated with infection severity and systemic inflammatory response [256].

In the post-COVID group (Group 2), lipid disturbances were moderately expressed, suggesting partial restoration of lipid homeostasis following the acute phase, yet with persistent metabolic risk—particularly among individuals with IR and hyperinsulinemia. In contrast, non-infected individuals with MetS (Group 3) demonstrated a typical atherogenic lipid profile, reflecting chronic metabolic dysregulation independent of viral infection.

The highest mean uric acid levels were observed in the MetS group, further supporting the association between IR, adiposity-related inflammation, and purine metabolism as a potential additional mechanism contributing to increased cardiometabolic risk.

In summary, the results are consistent with the concept that SARS-CoV-2 infection may act as a multifactorial metabolic stressor capable of accelerating or triggering carbohydrate and lipid disturbances in predisposed individuals. The observed intergroup differences suggest

variability in the underlying mechanisms depending on the phase of infection and the pre-existing metabolic status.

2. Assessment of Major Lipid Profile Parameters and Other Key Metabolic Indicators, as well as Liver Function Status, Across Different Phases of Infection

2.1. Major Lipid and Other Metabolic Parameters

The current findings delineate distinct patterns of lipid disturbances across the different phases of infection. Active SARS-CoV-2 infection is associated with the most pronounced abnormalities, whereas the post-COVID state in individuals with newly developed carbohydrate metabolism disorders demonstrates a lipid profile comparable to that of COVID-negative individuals with MetS. The most consistent finding is the significant reduction in total cholesterol during active infection, which remains evident after adjustment for age and sex using generalized linear models. These findings are consistent with the concept of inflammatory hypocholesterolemia as part of the acute systemic response in COVID-19 [173, 428].

The observed higher TG levels and markedly reduced HDL-C levels during the active phase are in line with the described inflammation-induced dyslipidemic phenotype, associated with cytokine-mediated increased hepatic VLDL production and impaired lipid transport [202, 428]. The attenuation of some of these differences after adjustment for demographic factors suggests that age, sex, and underlying metabolic risk modulate the expression of dyslipidemia and that the acute infectious process does not necessarily lead to a classical atherogenic lipid profile. The absence of significant differences in LDL-C between groups further supports the notion that LDL-C does not emerge as a leading marker of acute metabolic alterations in COVID-19.

Regarding uric acid, significantly lower levels during active infection, persisting after adjustment for age and sex, likely reflect increased oxidative and inflammatory stress, in which uric acid functions as a circulating antioxidant and becomes “consumed” during the acute process [22, 149]. Additionally, alterations in renal urate excretion, reduced nutritional intake, and systemic inflammation have been described as mechanisms of transient hypouricemia in acute infections, including COVID-19 [79, 130]. In contrast, similar uric acid levels in post-COVID patients and individuals with MetS are consistent with the well-established association between IR and hyperuricemia in chronic metabolic dysregulation [186].

In summary, the present findings support the understanding that SARS-CoV-2 infection acts as an acute metabolic "modifier," leading to transient, phase-dependent changes in lipid and purine metabolism, whereas in the post-infectious phase the metabolic profile appears to be determined predominantly by underlying cardiometabolic risk.

The observed correlation patterns emphasize the central role of age, obesity, and IR as key determinants of metabolic dysregulation, irrespective of COVID-19 status. The consistent positive correlation between age and HIF-1α across all groups is consistent with the hypothesis of cellular hypoxia as a shared pathophysiological mechanism, which intensifies with advancing age and contributes to metabolic and vascular dysfunction [291]. Strong associations between BMI and major IR indices, as well as with adipokine imbalance (reduced Adiponectin/Leptin ratio), are in line with the established role of obesity as an integral factor in the pathogenesis of IR and related cardiometabolic risk [139, 155, 330].

The observed correlations between TG, their derived indices (TyG, TG/HDL-C ratio), and HDL-C reflect a classical atherogenic lipid profile in chronic metabolic dysfunction [147, 269], whereas during active SARS-CoV-2 infection these relationships are likely modified by acute inflammatory and systemic stress [202, 428]. The association between uric acid and METS-IR, as well as with hepatic transaminases in recovered patients, may reflect persistent metabolic–hepatic imbalance in the post-COVID period [186, 258], while the association with age during active infection likely reflects transient inflammation-related changes and altered renal homeostasis [424].

In conclusion, the present results are consistent with the concept that SARS-CoV-2 infection is associated with transient, phase-specific alterations in lipid and purine metabolism. In the post-infectious phase, the metabolic profile appears to be driven predominantly by underlying cardiometabolic risk.

2.2. Hepatobiliary Function

The current results are consistent with data indicating that hepatic involvement is a frequent feature of SARS-CoV-2 infection, with the most pronounced abnormalities observed during the acute phase of the disease. Elevated ASAT levels in patients with active COVID-19, compared with recovered individuals and COVID-negative subjects with MetS, are in agreement with published findings suggesting that ASAT is a more sensitive marker of infection severity and systemic inflammation than ALAT [65, 121, 253].

The absence of significant differences in ALAT levels between the active and post-COVID periods is compatible with the possibility of persistent hepatocellular involvement, likely related to metabolic stress and low-grade inflammation [124, 252].

The high and variable GGT levels observed in actively infected patients may be interpreted as reflecting a cholestatic component of liver injury and support the concept of combined hepatocellular and cholangiocellular involvement in COVID-19 [253, 361, 440].

The identified correlations between liver enzymes and inflammatory mediators, including IL-17A and LDH, further support the hypothesis that the systemic immune-inflammatory response contributes to the pathogenesis of hepatic dysfunction during active infection and in the post-COVID period [121, 272, 452].

3. Evaluation of Inflammatory Status, the Role of Pro- and Anti-Inflammatory Cytokines, and Other Markers of Immune Inflammation

3.1. Inflammatory Status and Clinical Severity

The present findings indicate that severe and critical forms predominated in the hospitalized cohorts, which is consistent with a pronounced systemic inflammatory response and multi-organ stress. The higher CRP and LDH levels in the baseline cohort (Group 4) compared with Group 1 likely reflect differences in clinical severity and/or the pandemic period (including distinct viral variants and therapeutic approaches). LDH emerges as a potentially sensitive indirect marker of tissue injury and hypoxic-inflammatory stress. The presence of a significant, albeit weak, correlation between LDH and clinical severity in Group 4 further supports its role as a dynamic biochemical indicator associated with disease severity.

Although fibrinogen did not demonstrate a direct association with severity, it showed a consistent correlation with CRP in both active infection groups, in line with its recognition as an inflammation-mediated hemostatic marker reflecting immunocoagulatory activation in COVID-19.

Elevated D-dimer levels in both cohorts, in the absence of a significant intergroup difference in median values, are consistent with activation of the coagulation system in hospitalized patients. The observed correlations between D-dimer and LDH, as well as GP-73 in Group 1, suggest a potential interaction between inflammation, cellular injury, and metabolic dysregulation even in the acute stage of COVID-19.

The relationship between DM and clinical course differed between the two groups: in Group 1, DM was primarily associated with prolonged hospital stay, whereas in Group 4, DM was associated with more severe disease and unfavorable outcomes. These findings are consistent with the concept of an aggravated metabolic background in patients with underlying dysglycemia.

3.2. Pro- and Anti-Inflammatory Cytokines

Analysis of proinflammatory cytokines indicates that SARS-CoV-2 infection is associated with marked alterations in the cytokine profile, differing between the acute and post-COVID phases. Elevated TNF-α levels observed both during active infection and in recovered individuals with newly developed carbohydrate metabolism disorders are consistent with persistent low-grade inflammatory activation beyond the acute "cytokine response" phase [91, 219, 324]. The statistically significant increase in TNF-α in the post-COVID group supports the hypothesis that this cytokine may contribute to the maintenance of a chronic inflammatory milieu, potentially linked to the development of IR and β-cell dysfunction [181, 402].

IL-17A demonstrated a distinct profile, characterized by reduced levels in both the acute and post-acute phases, suggesting suppression of Th17-mediated immune pathways at the time of assessment and impaired restoration of adaptive immune responses following recovery [364]. Decreased IFN-γ levels in the post-COVID period, irrespective of diabetic status, are compatible with reduced Th1-mediated antiviral activity, potentially reflecting ongoing immune dysregulation and contributing to metabolic risk [47, 78, 136]. Collectively, these findings support the hypothesis that the cytokine profile may remain altered after the acute phase of COVID-19, transitioning toward a state of low-grade immune activation with potential immunometabolic implications [280, 325, 412].

In addition to proinflammatory mediators, analysis of anti-inflammatory and immunoregulatory cytokines provides further insight into immune regulation in COVID-19. Reduced IL-7 levels during both active infection and the post-COVID period, compared with COVID-negative individuals with MetS, suggest disruption of IL-7–mediated mechanisms of T-cell homeostasis [21, 76, 246]. Given the critical role of IL-7 in maintaining survival and functional capacity of $CD4^+$ and $CD8^+$ lymphocytes, these data support the concept of persistent T-cell dysregulation following SARS-CoV-2 infection, potentially contributing to ongoing inflammatory activity and impaired immune regulation in the post-COVID phase [123, 280].

Relatively higher IL-7 levels in COVID-negative individuals with MetS are consistent with the concept of chronic low-grade immune activation in metabolic disorders, whereas suppression of IL-7 in COVID-related groups underscores the dominant effect of viral infection on its regulation [89, 127, 325]. Observed correlations between IL-7, markers of T-cell immunity, antioxidant defense, and IR indices further support its involvement in the immunometabolic continuum linking inflammation and disturbances in glucose homeostasis after COVID-19 [351, 381].

Regarding IL-10, the results did not demonstrate clear intergroup differences, despite a trend toward higher levels during the active phase of infection. This suggests a variable anti-inflammatory response that may be insufficient to fully counterbalance hyperinflammatory processes in some patients [68, 135, 177]. The relatively low absolute IL-10 levels across all study groups, including during active infection, are consistent with data indicating compromised anti-inflammatory regulation in individuals with MetS and IR [125, 351].

Correlations between IL-10 and parameters of glycemic control, β-cell function, and IR indices in the post-COVID group support the hypothesis that IL-10–mediated regulation is linked to immunometabolic alterations following SARS-CoV-2 infection [268, 394]. In this context, IL-10 does not emerge as an isolated protective factor, but rather as part of a broader immunoregulatory network whose alterations may be associated with persistent immunometabolic imbalance.

Within the post-COVID group (Group 2), differences in cytokine profile were observed between subgroups according to the type of carbohydrate metabolism disorder. Higher TNF-α levels and lower IFN-γ and IL-17A levels in individuals with newly diagnosed DM are consistent with a more pronounced immunometabolic imbalance compared with subgroups with prediabetes and isolated IR.

In summary, the combination of increased proinflammatory activation (TNF-α), reduced Th1/Th17-mediated markers (IFN-γ, IL-17A), and alterations in key immunoregulatory cytokines (IL-7 and IL-10) delineates a complex immune profile following SARS-CoV-2 infection. These changes likely contribute to immunometabolic mechanisms associated with post-COVID metabolic disturbances, including IR and β-cell dysfunction, and are consistent with the concept of COVID-19 as a potential trigger of long-term immunometabolic consequences [280, 325, 412].

3.3. Markers of Cell-Mediated Immune Response and the Complement System

The results of the present study indicate that SARS-CoV-2 infection is associated with pronounced, phase-dependent alterations in the cell-mediated immune response and the complement system. Elevated CD4 levels observed both during active infection and in the post-COVID period are consistent with persistent Th-cell activation following clinical recovery, in line with reports of sustained T-cell immune activation in COVID-19 [99, 182, 336]. These findings may reflect disturbances in immune homeostasis and could be linked to the maintenance of low-grade inflammatory activity.

In contrast to CD4, reduced CD8 levels during active infection and the tendency toward partial recovery in the post-COVID period suggest diminished cytotoxic T-cell activity. Such an imbalance between Th- and Tc-cell responses has been described in COVID-19 and is associated with impaired antiviral control and prolonged immune dysfunction [142, 208, 457]. The observed associations between CD8 and parameters of β-cell function support a possible link between cytotoxic T-cell immunity and β-cell involvement during SARS-CoV-2 infection, analogous to mechanisms described in other virus-induced forms of diabetes [47, 136].

Of particular significance is the observed profile of HCF-D, demonstrating marked and persistent suppression of the alternative complement pathway in the post-COVID period. In contrast to the chronically elevated complement activity observed in MetS among COVID-negative controls, SARS-CoV-2 infection was associated with reduced complement activity, most pronounced after recovery [75, 169, 336]. This finding may be interpreted as a potential compensatory regulatory mechanism or functional exhaustion of the alternative pathway following the acute phase, as described in other studies [102, 196, 367].

Taken together, these data indicate that cell-mediated immunity and the complement system are closely associated with immunometabolic alterations following SARS-CoV-2 infection. The imbalance between Th- and Tc-cell activity, combined with reduced complement activity, is consistent with an immune-dysregulated environment that may contribute to β-cell dysfunction and the development of carbohydrate metabolism disorders after SARS-CoV-2 infection [280, 325, 412].

4. Markers of Oxidative Stress, Antioxidant Defense, and Virus-Induced Cellular Hypoxia

The results delineate a pattern in which the observed changes are consistent with a persistent oxidative imbalance in the post-COVID period, while the antioxidant response (NFE2L2) does not demonstrate a distinct group-related dynamic but exhibits considerable variability and

dependence on the type of carbohydrate metabolism disorder. This interpretation is consistent with evidence supporting the role of oxidative stress and impaired redox homeostasis in the pathogenesis of COVID-19 and its post-infectious sequelae [39, 140, 294, 305, 412].

The elevation of 8-epi-PGF2α in the post-COVID group, as well as its observed association with fasting glucose levels, suggests a potential link between oxidative stress and disturbances in glycaemic control following infection, with 8-epi-PGF2α being recognized as a reliable in vivo marker of lipid peroxidation and systemic oxidative stress [316, 334]. The highest levels observed in individuals with metabolic syndrome are consistent with evidence indicating that chronic metabolic stress sustains a pro-oxidant environment [396], while COVID-19 may act as an additional aggravating factor in metabolically vulnerable individuals [412].

With regard to cellular hypoxia, elevated HIF-1α levels during the acute phase are consistent with pronounced hypoxic stress during infection and with its role as a key regulator of the cellular response to hypoxia in COVID-19 [69, 112, 429]. The observed decrease in HIF-1α levels in the post-COVID group, together with significant associations with HbA1c, glucose, glucagon, and indices of insulin resistance, suggests the involvement of hypoxia-related signalling in post-infectious metabolic alterations. Similar relationships between HIF-1α, inflammation, and metabolic dysregulation have also been reported by other investigators [156, 394].

Taken together, these findings support the concept of a mismatch between increased pro-oxidant burden and a relatively heterogeneous antioxidant response in the context of altered hypoxia-related signalling. This imbalance may create a metabolic milieu associated with insulin resistance and β-cell dysfunction and may contribute to the development of newly emerging disturbances in glucose metabolism [282, 412].

5. Assessment of Glucose Homeostasis in the Acute Phase of COVID-19 and in the Asymptomatic Post-COVID Period Through Analysis of Pancreatic α- and β-Cell Function, Insulin Secretion, and Insulin Sensitivity

5.1. Major Parameters of Glucose Homeostasis

The present findings suggest that disturbances in glucose homeostasis exhibit distinct profiles in the acute and post-COVID phases, with the second group comprising individuals with already manifested newly developed carbohydrate metabolism disorders following infection. Elevated fasting plasma glucose levels in this group, as well as their independent increase

compared with the MetS control group after adjustment for age and sex, suggest established and clinically significant metabolic dysregulation rather than a transient post-infectious effect. These observations are consistent with published data reporting an increased risk of newly diagnosed diabetes and persistent abnormalities in glucose metabolism following SARS-CoV-2 infection [442].

In contrast, during active infection, elevated glycemic values may be interpreted within the context of an acute stress and inflammatory response. Data from dynamic monitoring in the baseline cohort with active COVID-19 demonstrate that both mean glycemia and glycemic variability correlate with infection severity and IR indices, in line with evidence indicating an adverse impact of hyperglycemia on clinical outcomes in hospitalized COVID-19 patients [460].

The fact that all individuals in the second group had newly developed carbohydrate metabolism disorders explains the higher HbA1c levels and its observed associations with parameters of β-cell function and IR. This supports the hypothesis that, following SARS-CoV-2 infection, a subset of patients may develop a relatively stable metabolic phenotype characterized by the combined contribution of IR and β-cell dysfunction.

The recorded incidence of newly diagnosed DM during the acute phase further supports the possibility that viral infection may act as a trigger for the manifestation or acceleration of underlying metabolic abnormalities in predisposed individuals.

In summary, the data support the concept that, in some patients, SARS-CoV-2 infection may serve as a trigger for the manifestation or acceleration of underlying metabolic disorders, whereas during the acute phase, glycemic disturbances more likely reflect the intensity of the systemic inflammatory and stress response.

5.2. Analysis of Pancreatic α- and β-Cell Function

The present findings indicate that SARS-CoV-2 infection is associated with complex alterations in islet cell function, with β-cell abnormalities playing a leading role in the observed metabolic dysregulation. Suppressed glucagon secretion in both the acute and post-COVID phases, in contrast to the higher levels observed in classical MetS, suggests a potentially specific impairment of α-cell regulation in the context of viral infection, likely related to immune-inflammatory and hypoxic mechanisms. The absence of a substantial difference

between the active and post-COVID phases implies that these alterations are not confined solely to the acute period.

At the level of β-cells, a marked dissociation between insulin, C-peptide, and proinsulin was observed, characterized by persistently elevated C-peptide levels alongside relatively lower basal insulinemia in both active infection and the post-COVID group compared with the MetS control group. This profile suggests that the increased C-peptide reflects enhanced endogenous insulin secretion, likely in the setting of a compensatory β-cell response. The relatively lower insulin levels may also be related to differences in insulin clearance or peripheral sensitivity, rather than reflecting isolated IR alone. Such mechanisms are consistent with data on the role of hepatic steatosis and systemic inflammation in regulating insulin metabolism [451].

The absence of significant and persistent post-infectious hyperproinsulinemia suggests a functional and dynamic β-cell stress response rather than a sustained defect in proinsulin processing, as such alterations have been described predominantly during the acute phase of infection [48]. Within the selected post-COVID group with newly developed disturbances, heterogeneity was observed. The lowest C-peptide levels in individuals with T1DM are consistent with more pronounced β-cell depletion in insulinopenic forms, whereas in the remaining subgroups a profile of increased endogenous secretion was preserved. The dissociation between proinsulin and C-peptide in insulinopenic forms of newly diagnosed diabetes aligns with described mechanisms of early β-cell exhaustion and impaired hormonal processing [280].

The identified correlations between β-cell parameters and markers of inflammation, oxidative stress, and cellular hypoxia (IFN-γ, CD8, NFE2L2, HIF-1α) further support the multifactorial nature of the observed changes. The data point toward an interaction between immune activation, oxidative stress, and hypoxic signaling in maintaining impaired islet cell regulation. In this context, β-cell dysfunction emerges as a key element in the pathophysiological model of post-COVID metabolic dysregulation and a potential mediator linking immunometabolic stress to disturbed glucose homeostasis [297].

In summary, the results outline a profile of modified α-cell regulation and persistently increased endogenous β-cell activity in a selected population with newly developed disturbances following SARS-CoV-2 infection, without evidence of a dominant and sustained defect in proinsulin processing. These findings support a dynamic and multifactorial mechanism of islet cell dysfunction.

5.3. Surrogate Indices of β-Cell Function

Analysis of surrogate indices of β-cell function reveals distinct, phase-dependent patterns of β-cell adaptation in active SARS-CoV-2 infection, post-COVID metabolic disturbances, and classical MetS. Elevated HOMA-B values and increased C-peptide/Glucose ratios in the COVID-related groups, confirmed after adjustment for age and sex, suggest preserved or compensatorily activated β-cell secretory capacity in the setting of increased IR, without a substantial difference between the acute and post-COVID phases.

In contrast, COVID-negative individuals with MetS demonstrate a profile consistent with chronic β-cell burden, characterized by a lower Insulin/Proinsulin ratio and a higher Proinsulin/C-peptide ratio, findings compatible with more pronounced impairment in insulin processing during prolonged metabolic dysregulation [339].

The low Proinsulin/C-peptide values in the post-COVID group, together with the absence of significant hyperproinsulinemia, suggest a lack of persistent disproportionate hyperproinsulinemia and relatively preserved insulin processing after resolution of acute infectious stress. Correlation patterns—particularly the negative associations of HOMA-B with glucose, HbA1c, and TyG index in the post-COVID group, as well as the distinct association profile observed in MetS—further emphasize the differing pathophysiological contexts across populations.

Taken together, these results support the concept that disturbances in glucose homeostasis in COVID-19 are predominantly driven by IR and heterogeneous β-cell adaptation rather than by universal and sustained primary β-cell failure [280]. The expression of β-cell dysfunction appears to be phenotype-dependent.

5.4. Surrogate Indices of IR

The analysis of IR using multiple surrogate indices demonstrates that IR represents the leading metabolic defect in the course of SARS-CoV-2 infection, with its manifestation and severity clearly phase-dependent. The most unfavorable profile is observed during the acute phase of infection, whereas in the post-COVID period there is a tendency toward partial recovery of insulin sensitivity, although without full normalization compared with COVID-negative individuals with MetS.

Insulin-based indices show differential informativeness in capturing these changes. Although HOMA-IR does not reveal statistically significant between-group differences after adjustment

for age and sex, QUICKI demonstrates a more pronounced gradient, with the lowest values in active SARS-CoV-2 infection and significant differences compared with the other groups. This suggests that during acute infection, dynamic IR and accompanying hormonal fluctuations may not be fully reflected by static fasting-based indices alone [261, 280].

Non–insulin-based indices exhibit clearer discriminatory capacity in the context of COVID-19. Elevated TyG index and TG/HDL-C ratio values in individuals with active infection, along with a gradient toward lower values in the post-COVID phase, support the role of acute inflammatory–metabolic stress in the transient exacerbation of atherogenic IR [155, 347]. The absence of substantial differences between post-COVID individuals with newly developed disturbances and COVID-negative individuals with MetS suggests that part of these alterations are transient and overlap with pre-existing metabolic risk.

METS-IR demonstrates similar values between the post-COVID group and the MetS reference group, indicating greater sensitivity to chronic metabolic burden rather than to acute infection-induced changes. This may explain the lack of statistically significant escalation of METS-IR in the post-COVID period despite the presence of newly developed disturbances in glucose metabolism [43].

Subgroup analysis within the post-COVID cohort shows that the degree of IR varies according to the type of disturbance in glucose metabolism, with statistically significant stratification observed for HOMA-IR and TyG index. These findings support the concept of a post-COVID metabolic phenotype in which IR plays a central role, yet with variable clinical expression and differing severity across subtypes.

Finally, the correlations between IR indices and markers of inflammation, immune activation, and hypoxic stress (including HIF-1α, IFN-γ, IL-10, and IL-17A) reinforce the multifactorial nature of the observed changes. These data suggest that post-infectious IR is not an isolated metabolic defect but rather the result of interaction between persistent immune activation, hypoxia-induced cellular stress, and underlying metabolic vulnerability.

Taken together, the findings outline a pathophysiological model in which IR forms the dominant metabolic background, while β-cell dysfunction or failed adaptation determines progression toward clinically significant dysglycemia.

6. Assessment of the Role of Adipocytokines and Other Hormonally Active Molecules in the Genesis of COVID-19–Associated Dysglycemia

6.1. Hormonally Active Molecules

The absence of a statistically significant difference in serum GLP-1 levels between patients with active SARS-CoV-2 infection and COVID-negative individuals with MetS, including after adjustment for age and sex, indicates that incretin secretion is not substantially suppressed during the acute phase of infection. The observed trend toward higher GLP-1 levels in active COVID-19 may reflect a compensatory incretin response under conditions of acute inflammatory and metabolic stress, without evidence of primary incretin deficiency.

The strong positive correlations with proinsulin and leptin, as well as the negative association with the adiponectin/leptin ratio in both groups, suggest secondary modulation of GLP-1 in parallel with β-cell stress and adipocyte dysfunction. Additional associations with glucose, insulin, and IR indices in individuals with MetS further support the interpretation that GLP-1 more likely reflects the degree of metabolic imbalance rather than representing a central pathogenetic mechanism of COVID-19–associated dysglycemia [45, 49, 327].

In contrast, GP-73 exhibits a clearly phase-dependent profile, characterized by a significant reduction during active SARS-CoV-2 infection and restoration to levels comparable to those observed in COVID-negative individuals with MetS during the post-COVID period. This pattern, confirmed after multivariable adjustment, suggests dynamic regulation of the protein in the context of the acute systemic inflammatory response.

Its suppression in the acute phase likely reflects a transient alteration in hepatic metabolic function, whereas the absence of a difference between post-COVID patients with newly developed disturbances in glucose metabolism and individuals with MetS supports the role of GP-73 as a marker of chronic hepatometabolic stress rather than of acute infection-induced changes. The identified associations with cytokines, HIF-1α, and glucagon further underscore its interaction with immune-inflammatory and metabolic pathways [84, 170, 417].

Taken together, the data indicate that both the incretin axis and GP-73 function predominantly as adaptive or secondary components within a broader network of metabolic and inflammatory regulation in COVID-19, rather than as primary driving mechanisms of post-infectious dysglycemia.

6.2. Adipocytokines and Adipokine Balance

The gradual increase in serum leptin levels from active SARS-CoV-2 infection to the post-COVID period and MetS delineates a phase-dependent dynamic of adipocyte dysfunction and

the development of leptin resistance. The relatively lower levels observed during active infection are consistent with transient dysregulation of leptin secretion or signaling under conditions of acute inflammatory stress, whereas the elevated levels following recovery and in MetS are typical of chronic metabolic and immunoinflammatory stress [115, 333, 408]. The identified correlations with proinsulin, GLP-1, and IR indices underscore the role of leptin as a linking factor between adipocyte dysfunction, β-cell stress, and impaired glucose homeostasis.

The absence of significant between-group differences in absolute adiponectin levels indicates that, in the studied population, SARS-CoV-2 infection is not associated with marked adiponectin deficiency, in contrast to findings reported in severely and critically ill patients [333]. Preserved adiponectin levels in both the acute and post-COVID phases suggest that in mild to moderate infection the anti-inflammatory adiponectin response remains relatively intact. The observed associations with markers of β-cell function and with HIF-1α further support the pleiotropic role of adiponectin in regulating metabolic adaptation and cellular responses under chronic immunometabolic stress [383, 435].

The significantly higher Adiponectin/Leptin ratio in active and post-COVID infection compared with MetS highlights its sensitivity as an integrative marker of adipocyte function and insulin sensitivity. Elevated values in COVID-associated conditions, in the absence of substantial adiponectin reduction, primarily reflect dynamic changes in leptin secretion and in the balance between pro- and anti-inflammatory adipokines [103, 333]. Strong correlations with proinsulin, GLP-1, and IR indices indicate that disruption of adipokine balance is closely linked to β-cell dysfunction and compensatory metabolic mechanisms in both SARS-CoV-2 infection and classical MetS.

7. **Risk Factors for Diabetes Mellitus in the Context of COVID-19**

ROC analysis delineates a multifactorial predictive model associated with increased vulnerability to the development of DM in the context of SARS-CoV-2 infection, encompassing immunological, metabolic, and hormonal parameters. Markers with excellent discriminatory capacity—HCF-D, IL-7, and fasting glucose—highlight the combined contribution of impaired glucose homeostasis and immune dysregulation as a key risk profile.

The good predictive performance of IFN-γ, 8-epi-PGF2α, and glucagon suggests involvement of T-cell activation, oxidative stress, and the counterregulatory hormonal axis in the process of metabolic decompensation. In parallel, metabolic indices (HOMA-IR, C-peptide, and the

Adiponectin/Leptin ratio) confirm the central role of IR and β-cell adaptation in the progression toward clinically overt dysglycemia. The inverse association observed for HOMA-B, reflected by an AUC < 0.50, indicates that lower β-cell functional capacity is associated with higher risk, consistent with exhaustion of compensatory secretory reserve.

Taken together, these findings suggest that the risk of developing diabetes following SARS-CoV-2 infection is determined by the interplay between persistent immune activation, oxidative stress, adipocyte dysfunction, and impaired β-cell adaptation, rather than by an isolated metabolic defect.

8. **Quality of Life in Individuals with Newly Developed Disturbances in Glucose Metabolism after SARS-CoV-2 Infection**

The observed impairment in quality of life among individuals who recovered from SARS-CoV-2 infection and subsequently developed new disturbances in glucose metabolism reflects the multifaceted impact of COVID-19 on physical, psycho-emotional, and social functioning. Persistent fatigue, reduced work capacity, and increased prevalence of depressive symptoms are consistent with the clinical spectrum of post-COVID syndrome and suggest ongoing immunometabolic and inflammatory stress following resolution of the acute infection.

The concordance between subjective complaints and objectively documented metabolic abnormalities supports the concept that reduced quality of life is not solely attributable to residual infectious symptoms but is also associated with alterations in glucose homeostasis, insulin sensitivity, and adipocyte function. These findings emphasize that post-COVID metabolic disturbances have not only biochemical implications but also functional and social consequences.

In this context, the results substantiate the need for a comprehensive, multidisciplinary approach, including endocrinological follow-up, psycho-emotional support, and and the implementation of individualized metabolic management strategies in patients with post-COVID dysglycemia.

CONCLUSIONS

1. Immune dysregulation in COVID-19 is characterized by complex disturbances within the immunoregulatory axis, involving both proinflammatory and regulatory cytokines, thereby extending beyond the classical concept of a “cytokine storm.”

2. The identified imbalance in the IL-7/IL-10 axis, characterized by elevated IL-7 levels and an inadequate compensatory IL-10 response, indicates persistent impairment of immune homeostasis, sustaining a chronic inflammatory–metabolic milieu during both the acute and post-COVID phases.
3. The proinflammatory cytokines TNF-α and IL-17A are associated with IR, whereas suppression of IFN-γ following recovery suggests post-COVID Th1 dysfunction and an altered immune balance.
4. The observed associations between cytokine profiles, glucose homeostasis, β-cell function, and IR support an immune-mediated mechanism of metabolic dysregulation and reinforce the concept of COVID-19 as an immunometabolic trigger for pancreatic involvement.
5. Among individuals with newly developed disturbances in glucose metabolism after SARS-CoV-2 infection, a heterogeneous immunoinflammatory profile emerges, varying according to the clinical metabolic phenotype, suggesting the presence of distinct yet interconnected pathogenetic pathways.
6. The cell-mediated immune response plays a significant role in pancreatic involvement, with $CD4^+$- and $CD8^+$-related mechanisms contributing differentially to regulatory processes and to α- and β-cell dysfunction.
7. Oxidative stress and virus-induced cellular hypoxia, mediated via HIF-1α, emerge as key mechanisms linking inflammation, metabolic stress, and β-cell dysfunction in both the acute and post-COVID phases.
8. IR represents the dominant metabolic defect in COVID-19 and may persist following recovery. The combined use of multiple surrogate indices provides a more comprehensive assessment of metabolic disturbances.
9. Adipocyte dysfunction and alterations in incretin and hepatometabolic regulation contribute to the maintenance of a prolonged immunometabolic continuum following SARS-CoV-2 infection.
10. ROC analysis identifies a complex profile of clinical, metabolic, and immunological parameters associated with increased risk of developing DM in the context of SARS-CoV-2 infection—both during active disease and in the post-COVID period—highlighting its relevance for early risk stratification in clinical practice.

CONTRIBUTIONS

I. Scientific and Theoretical Contributions

1. A comprehensive clinical and laboratory investigation was conducted in a Bulgarian cohort, expanding current knowledge regarding the relationship between SARS-CoV-2 infection, pancreatic β-cell function, and disturbances in glucose homeostasis during both the acute and post-COVID phases.
2. Dynamic alterations in immune homeostasis during and after SARS-CoV-2 infection were systematically analyzed, together with their impact on β-cell function and key glucoregulatory mechanisms, further supporting the concept of COVID-19 as an immunometabolic disease.
3. An association between SARS-CoV-2 infection and the development of a broad spectrum of disturbances in glucose metabolism was demonstrated, including newly diagnosed T1DM (including LADA), T2DM, and prediabetic states.
4. Phenotype-specific immunopathogenetic mechanisms involved in β-cell injury across different forms of newly diagnosed diabetes following COVID-19 were identified, with a leading role attributed to cell-mediated immune responses.
5. The central role of IR as the dominant metabolic defect in COVID-19 was established, with evidence suggesting its persistence in the post-COVID period, irrespective of pre-existing diabetic status.
6. The involvement of oxidative stress, virus-induced cellular hypoxia, adipocyte dysfunction, and incretin dysregulation was demonstrated as interconnected mechanisms contributing to a sustained immunometabolic continuum following SARS-CoV-2 infection.

II. Scientific and Applied Contributions

1. The frequency of newly diagnosed diabetes among patients hospitalized for COVID-19 was determined, and phase-specific and clinical-context differences were analyzed.
2. The combined use of insulin-based and non–insulin-based surrogate indices for the assessment of β-cell function and IR in acute and post-COVID settings was validated.
3. Clinical, biochemical, and immunological parameters associated with increased risk of diabetes development in the context of SARS-CoV-2 infection were identified.
4. For the first time in Bulgaria, quality of life was assessed in individuals with newly developed disturbances in glucose metabolism following SARS-CoV-2 infection, demonstrating significant impairment in physical and psycho-emotional domains.

STUDY LIMITATIONS

The present study has several limitations that should be considered when interpreting the results. The absence of a control group consisting of metabolically healthy individuals necessitated the use of a reference group with MetS, which limits the possibility of direct comparison with a metabolically and immunologically intact population. In this COVID-negative group, prior asymptomatic SARS-CoV-2 infection cannot be completely excluded due to the lack of serological data in a subset of participants.

The inability to determine BMI in patients with active SARS-CoV-2 infection restricted its inclusion as a covariate in certain statistical models. Furthermore, the relatively small sample size in some subgroups and the single time-point assessment of selected immunological and metabolic markers limit statistical power and preclude definitive conclusions regarding causal relationships.

Future longitudinal, prospective studies with larger sample sizes and the inclusion of healthy control groups are warranted to more precisely elucidate the immunometabolic mechanisms underlying the development of DM in the context of SARS-CoV-2 infection.

LIST OF PUBLICATIONS RELATED TO THE DISSERTATION

1. Tsvetkova V, Todorova M, Todorova K, Atanasova M, Gencheva I, Atherogenic insulin resistance indices and immune disturbances in COVID–19. Journal of Biomedical and Clinical Research 2025 (18): 293-306. ISNN 1133-6917, https://doi.org/10.3897/jbcr.e173237
2. Tsvetkova VT, Todorova MS, Todorova KN. Link Between Immune Dysregulation in COVID-19 and Beta-Cell Dysfunction. J Endocrinol Metab. 2025;15(4):161-180. ISNN 1923-2861, doi:10.14740/jem1547
3. Tsvetkova V., Todorova K., Hyperglycemia and COVID-19 – two sides of one coin, Archiv euromedica 2023;13(4): 1–12; ISNN 2193-3863, DOI 10.35630/2023/13/4.801
4. Tsvetkova V, Todorova K. Biomolecular Mechanisms of Pancreatic Beta-Cell Injury in COVID-19. Nauka Endokrinologia. 2022,(2):45–56; ISNN 1313-0897
5. Tsvetkova V, Todorova K. Metabolic Syndrome and COVID-19. MedInfo. 2022, (5):32–39; ISNN 1314-0345

CONFERENCE PARTICIPATION RELATED TO THE DISSERTATION

1. Tsvetkova V. Changes in Beta-Cell Function in COVID-19. Pleven Endocrinology Days, 13–15 May 2022, Pleven, Bulgaria.
2. Tsvetkova V., Todorova K. E-poster: “Changes in Beta-Cell Function in COVID-19.” National Congress of Endocrinology, organized by the Bulgarian Society of Endocrinology, 12–14 October 2023, Plovdiv, Bulgaria.
3. Tsvetkova V., Todorova K., Todorova M. “Can COVID-19 Cause Diabetes Mellitus?” Scientific presentation at the XV National Interdisciplinary Congress of the Bulgarian Diabetes Association with international participation, 6–9 June 2024, Pamporovo, Bulgaria.
4. Tsvetkova V. Insulin Resistance and COVID-19. Pleven Endocrinology Days, 14–15 June 2024, Pleven, Bulgaria.